AFWL-TR-
68-46

EXPONENTIALLY DECAYING PRESSURE PULSE MOVING WITH SUPERSEISMIC VELOCITY ON THE SURFACE OF A HALF SPACE OF VON MISES ELASTO-PLASTIC MATERIAL

Hans H. Bleich Alva Matthews

Paul Weidlinger, Consulting Engineer
New York, New York 10017

Contract F29601-67-C-0091

TECHNICAL REPORT NO. AFWL-TR-68-46

August 1968

AIR FORCE WEAPONS LABORATORY
Research and Technology Division
Air Force Systems Command
Kirtland Air Force Base
New Mexico

AFWL-TR-68-46

EXPONENTIALLY DECAYING PRESSURE PULSE MOVING WITH SUPERSEISMIC VELOCITY ON THE SURFACE OF A HALF SPACE OF VON MISES ELASTO-PLASTIC MATERIAL

Hans H. Bleich Alva Matthews

Paul Weidlinger, Consulting Engineer

New York, New York 10017

Contract F29601-67-C-0091

TECHNICAL REPORT NO. AFWL-TR-68-46

FOREWORD

This report was prepared by Paul Weidlinger, Consulting Engineer, New York, N. Y. under Contract F29601-67-C-0091. The research was performed under Program Element 6.16.46.01.41, Project 5710, Subtask RSS2144, and was funded by the Defense Atomic Support Agency (DASA).

Inclusive dates of research were October 1967 to May 1968. The report was submitted 18 June 1968 by the AFWL Project Officer, Dr. Henry F. Cooper, Jr. (WLDC).

This report has been reviewed and is approved.

Henry F. Cooper Jr.

DR. HENRY F. COOPER, JR.
Project Officer

Robert E. Crawford

ROBERT E. CRAWFORD
Lt Col USAF
Chief, Civil Engineering Branch

George C Darby Jr

GEORGE C. DARBY JR
Colonel USAF
Chief, Development Division

ABSTRACT

(Distribution Limitation Statement 2)

An approximate solution is given for the effect of an exponentially decaying pressure pulse traveling with super-seismic velocity on the surface of a half-space. The half-space is an elastic-plastic material of the von Mises type. The effect of a step wave for this geometry and medium was treated previously. For that case, the peak pressures do not decrease with increase in depth, while such a decrease is obtained for a decaying surface load. The prime purpose of this investigation is to determine the magnitude of this attenuation. The approximate solutions obtained are valid for a limited distance behind the wave front, and are tabulated for different sets of parameters pertaining to the material and velocity. The tabulated results show that the peak pressures in the case of the decaying surface load do decrease with depth, but that the decrease is less than one might intuitively expect. On the other hand the attenuation is in general larger than that encountered in the similar problem of an elasto-plastic material of the Coulomb type.

This page intentionally left blank.

CONTENTS

LIST OF ILLUSTRATIONS

LIST OF TABLES

LIST OF SYMBOLS

a_i , b_i , c_i	Coefficients of Taylor series expansion.
c_P , c_S , $\bar{c}$	Velocity of propagation of elastic P-waves, S-waves, and inelastic shock fronts, respectively.
f_i , g_i	Arbitrary functions of x or y.
G	Shear modulus.
J_1 , J_2	Invariants, Eqs. (51) and (2).
k	Material parameter related to yield stress in shear.
$M = \frac{V}{c_P}$, $M_S = \frac{V}{c_S}$	
n	Ratio defined by Eq. (11).
N_1 ,..., N_{10}	Functions defined by Eqs. (82).
$p(x - Vt)$	Surface pressure.
p_o	Initial value of the surface pressure.
t	Time.
u, v, $\dot{u}$, $\dot{v}$	Particle displacements and velocities in x and y directions, respectively.
$\dot{u}_N$, $\dot{u}_T$	Particle velocities normal and tangential, respectively to fronts of discontinuity.
V	Velocity of surface pressure.
x, y	Cartesian coordinates.
$\Delta\sigma$, $\Delta\dot{u}$, $\Delta\tau$	Increments of σ, $\dot{u}$, τ, etc., at a front.

ε_i	Strain rates.
$\xi = x - Vt$	Coordinate.
θ	Angle between direction of principal stress σ_1 and x-axis.
μ	Decay constant of surface pressure, Eq. (46).
ν	Poisson's ratio.
ρ	Mass density of medium.
σ_i , τ	Normal and shear stresses, respectively.
σ_1 , σ_2 , σ_3	Principal stresses.
σ_N , τ_N , σ_T	Stresses, respectively in the plane, and perpendicular to the plane of a shock front.
ϕ	Position angle of element, Fig. 8.
ϕ_P , ϕ_S , $\bar{\phi}$	Position angle of elastic P- and S- and inelastic shock fronts, respectively.
Φ, Ψ, $\bar{\Psi}$, $\bar{\bar{\Psi}}$	Potential functions.

This page intentionally left blank.

SECTION I

INTRODUCTION

In a preceding analysis, Refs. [1] and [2]*, the effect of a step pressure, Fig. 1, progressing with a superseismic velocity V on the surface of a half-space has been studied for an elastic-plastic material subject to the von Mises yield condition

$$J_2 - k^2 = 0 \tag{1}$$

where k is the yield stress in shear and J_2 is the invariant

$$J_2 = \frac{1}{2} s_{ij} s_{ij} \tag{2}$$

The present report considers the more general problem of a decaying pressure pul p(x - Vt), Fig. 2, moving with a superseismic, constant velocity V. The problem under study here is more realistic than the one treated in Refs. [1] and [2], but it is also considerably more complex. Because of the complexity only an approximate solution will be derived, which is valid for a limited distance from the moving front.

---

* [1] Bleich, H.H. and Matthews, A.T., "Step Load Moving with Superseismic Velocity on the Surface of an Elastic-Plastic Half-Space", Int. J. Solids and Structures, 3, 819-852, 1967. (Also Office of Naval Research, Tech. Rpt. 38, Contract Nonr-266(86), December 1965.)

[2] Matthews, A.T. and Bleich, H.H., "Stresses in an Elastic-Plastic Half-Space Due to a Superseismic Step Load", TBL, Ballistics Research Laboratory, Aberdeen, Md., Tech. Rpt. 4, Contract DA-30-069-AMC-8(R), March 1966.

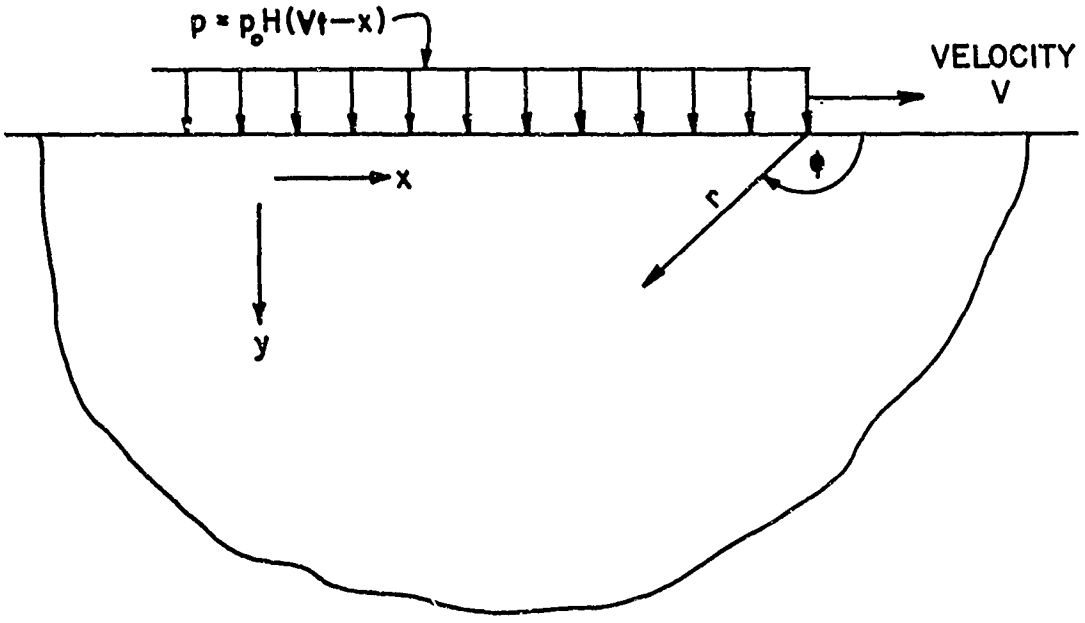

FIG. 1

Step Pressure moving over Half-Space

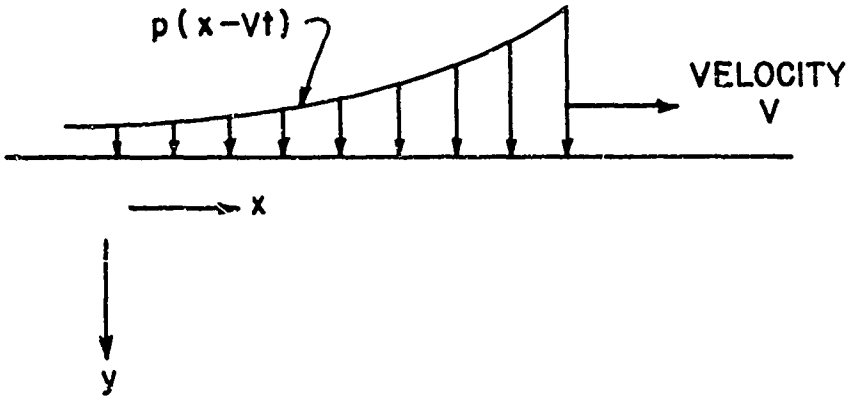

FIG. 2

Decaying Pressure moving over Half-Space

The approximation employed is somewhat similar to the one utilized and discussed in Ref. [3]* for a material subject to a different yield condition.

Because the velocity V of the load is constant, the resulting stress and velocity fields remain unchanged if considered in a coordinate system moving with velocity V. In other words, Refs. [1], [2] and [3] and the present paper consider steady-state solutions, which may be used as approximations to actual situations when the velocity V varies gradually.

It was found in Refs. [1] and [2] that the response to the step pressure changes in character depending on the range in which the values of Poisson ratio ν, of the velocity ratio V/c_p, and of the intensity of the surface step load p_o are situated. As introduction to the problem with a decay of pressure, some aspects of the results of the analysis for the step pressure are restated in the following.

Defining the location of a field point by the polar coordinates ϕ and r, Fig. 1, where the origin of the coordinate system lies at and moves with the front of the surface load, it was found that the stresses and velocities are functions of the angle ϕ only. For a step pressure there is

---

* [3] Bleich, H.H. and Matthews, A.T., "Exponentially Decaying Pressure Pulse Moving with Superseismic Velocity on the Surface of a Half-Space of Granular Material", Tech. Rpt. AFWL-TR-67-21, Contract AF29(601)-7082, July 1967.

therefore no dependence of stresses or velocities on the radius r, so that there is no attenuation with depth. It was found, further, that for sufficiently large values of the surface load, $p_o > p_L$, the solution has the character of Fig. 3, where the value of p_L depends on the parameters ν and V/c_p .

The configuration shown in Fig. 3 shows two discontinuities, a P-front and an S-front, moving with the velocities of elastic P- and S-waves

$$c_P^2 = \frac{2(1-\nu)}{1-2\nu}\,\frac{G}{\rho} \tag{3}$$

$$c_S^2 = \frac{G}{\rho} \tag{4}$$

respectively. The locations of the fronts are defined by the related angles

$$\phi_P = \pi - \sin^{-1}\left[\frac{1}{V}\sqrt{\frac{2(1-\nu)G}{(1-2\nu)\rho}}\right] \tag{5}$$

$$\phi_S = \pi - \sin^{-1}\left[\frac{1}{V}\sqrt{\frac{G}{\rho}}\right] \tag{6}$$

The changes in stress and velocity at these fronts are entirely elastic. There are four "neutral" regions of uniform stress (and uniform velocity), i.e., regions where the yield condition, Eq. (1), is just satisfied, but no yield occurs at the particular instant. There are two plastic regions, ϕ_1 to ϕ_2 , and from ϕ_3 to ϕ_4 , where plastic deformations occur at the particular instant, and where the stresses

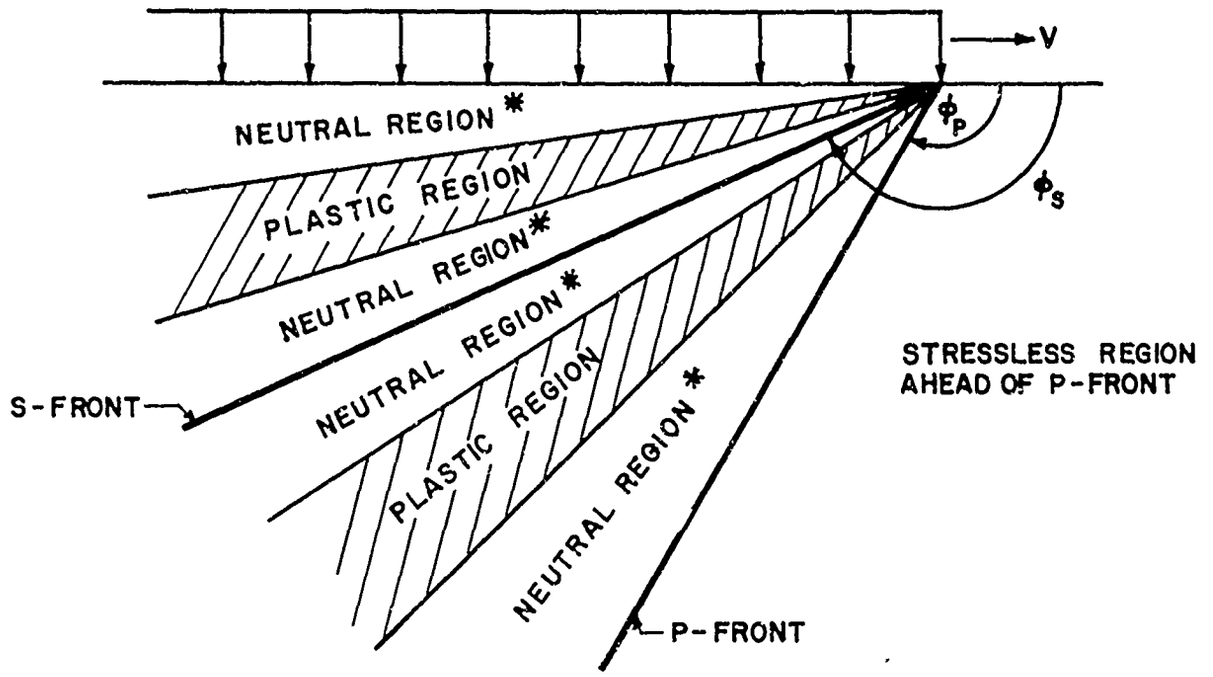

* NEUTRAL REGIONS OF UNIFORM STRESS SATISFYING EQ.1

CONFIGURATION FOR STEP PRESSURES $p_o > p_L$

FIG.3

(and velocities) vary as functions of the location ϕ. One of the plastic regions is always located between the P- and S-fronts, and one between the S-front and the surface.

If the surface load lies below the limit p_L, but above another value $p_E < p_L$, so that

$$p_E < p_o < p_L \tag{7}$$

only one of the two plastic regions occurs, which one occurs depends on the parameters ν and V/c_p. If these parameters lie in Range I or II of Fig. 4, the configurations of Fig. 5 or 6 apply, respectively. In these cases two of the neutral regions shown in Fig. 3 coalesce and become a region of uniform stress below yield as noted in Figs. 5 and 6. The demarkation line between Ranges I and II in Fig. 4 is given by the relation

$$V/c_p = \frac{(1-2\nu)^2}{(1-\nu)(1-3\nu)} \tag{8}$$

If, finally, $p_o \leq p_E$, the solution becomes entirely elastic, Fig. 7.

One detail obtained in Ref. [1] for the step pressure is crucial for the present purpose. If p_o is not only larger, but very much larger than p_L, it was found that one of the two plastic regions in Fig. 3 is of much greater importance than the other. This means that the energy dissipated and the changes in stress and velocity in the "important" region

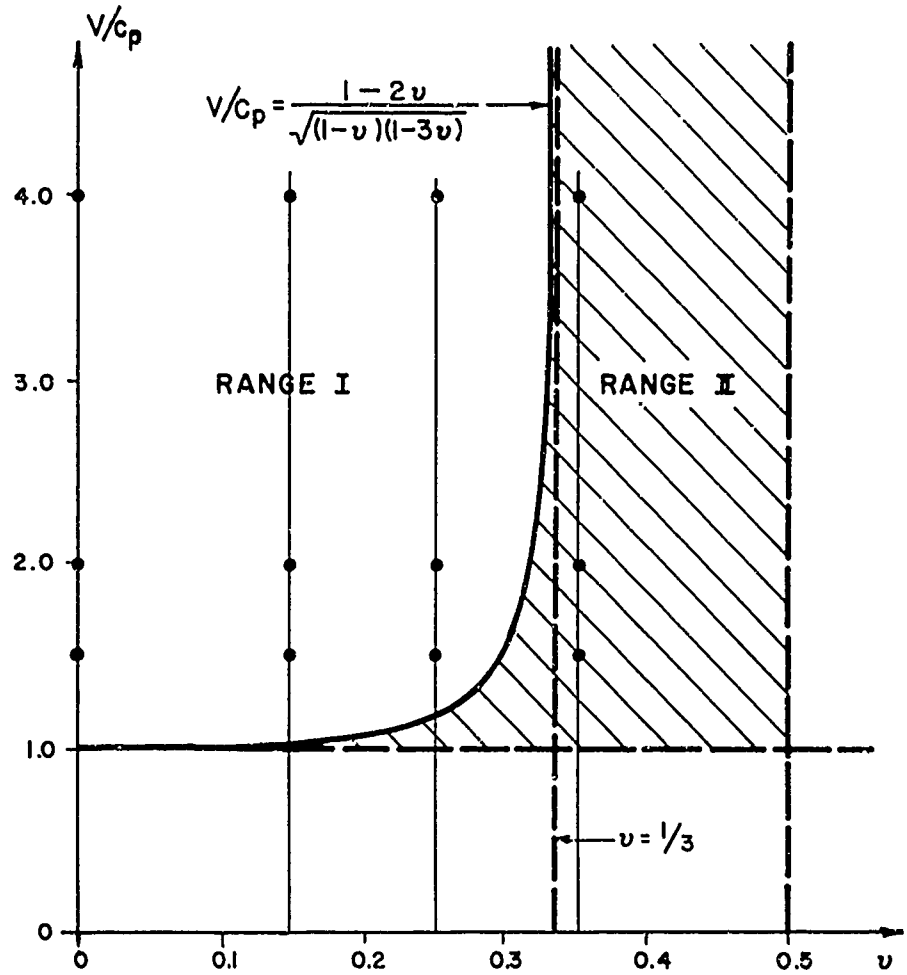

- PARAMETERS FOR WHICH TABLES ARE GIVEN IN SECTION IV.

FIG. 4

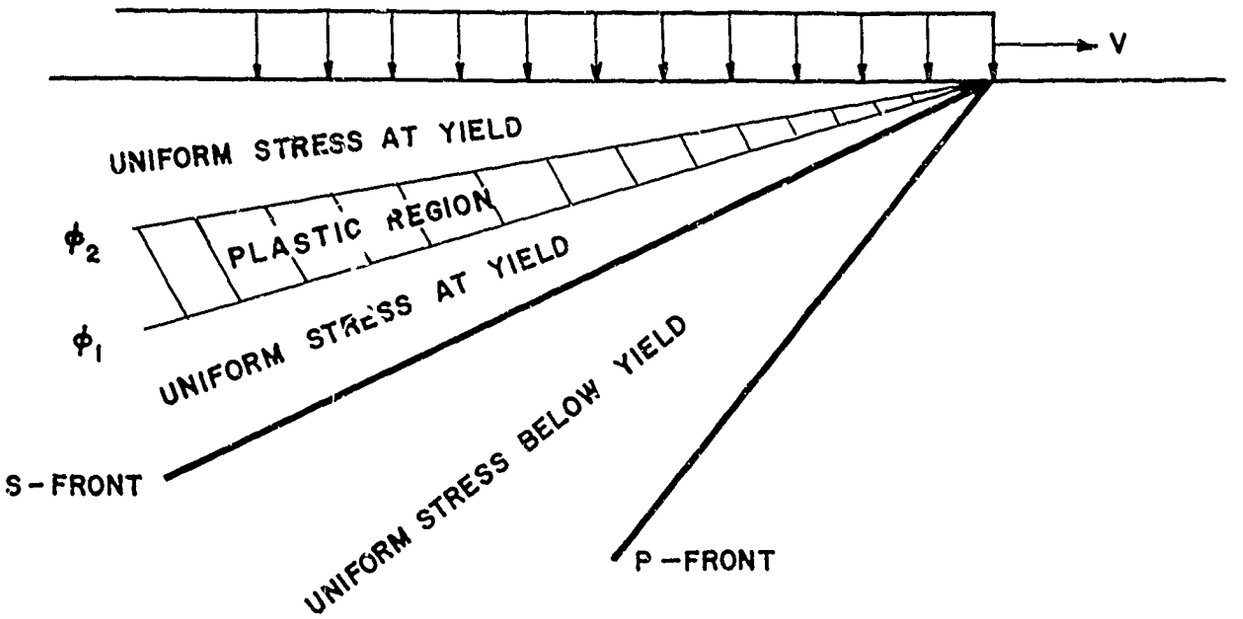

RANGE I SOLUTIONS, $p_E < p_0 < p_L$

FIG. 5

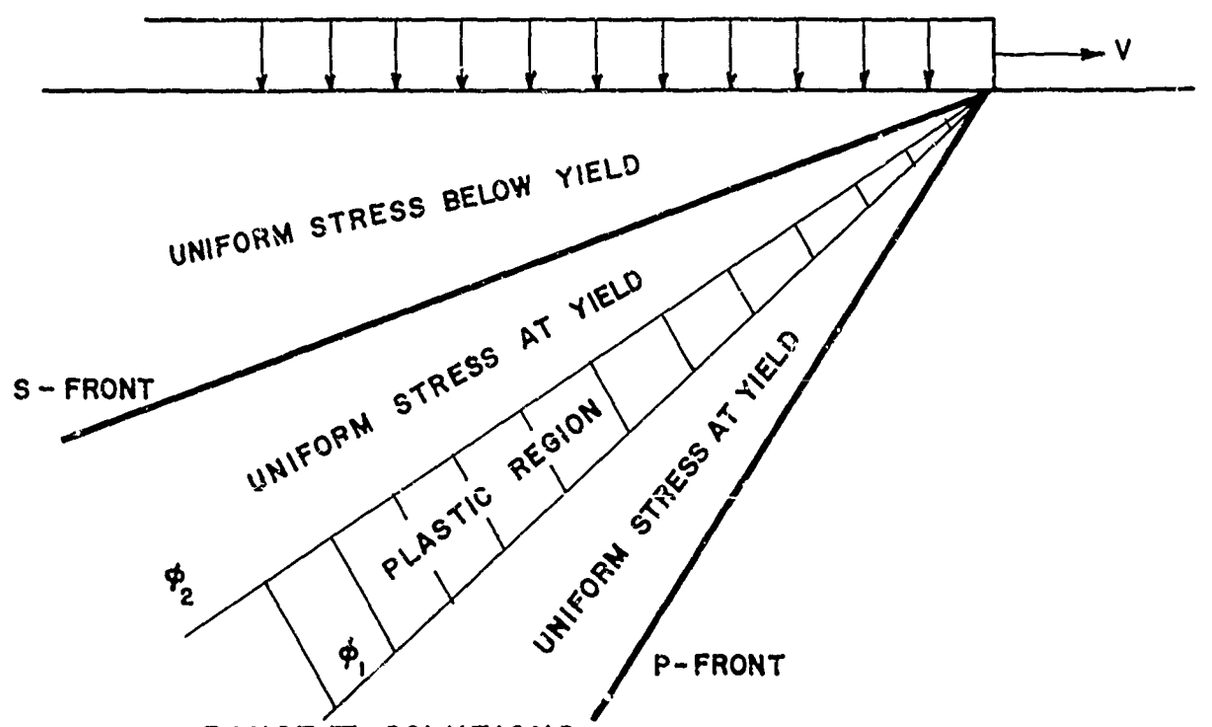

RANGE II SOLUTIONS, $p_E < p_0 < p_L$

FIG. 6

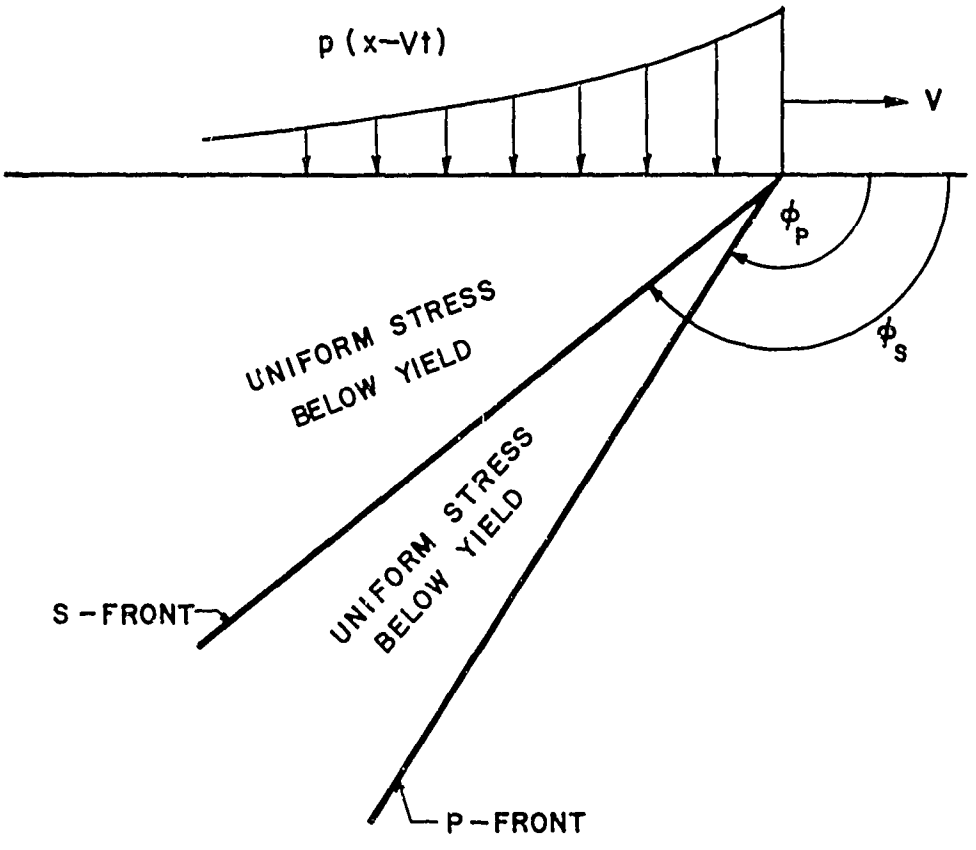

CONFIGURATION OF ELASTIC SOLUTIONS

FIG. 7

are very much larger than in the other plastic region. In the "important" region the bulk of energy dissipation and of the changes in stress and velocity occur for values of ϕ very close to a critical angle $\bar{\phi}$ for which the basic differential equations are capable of a singular, discontinuous solution. The critical angle is connected with the fact, that in the von Mises material considered, plastic shock fronts may exist, having a velocity

$$\bar{c}^2 = \frac{2(1+\nu)}{3(1-2\nu)} \frac{G}{\rho} \tag{9}$$

As discussed in Ref. [1], at such shock fronts the state of stress ahead and behind the front must be at yield, but - in addition - the major principal stress must be at a right angle to the front and the other two principal stresses must be equal. It is shown in Ref. [1] that at such a plastic shock front all three principal stresses change by the same amount $\overline{\Delta\sigma}$, while the component of the velocity normal to the front changes as required by conservation of momentum.

In the present steady-state problem the angle $\bar{\phi}$ may be obtained from the value for $\bar{c}$,

$$\bar{\phi} = \sin^{-1}\left[\frac{1}{V}\sqrt{\frac{2(1+\nu)}{3(1-2\nu)}\frac{G}{\rho}}\right] \tag{10}$$

The location of this front depends on the value of Poisson's ratio ν. If $\nu > 1/8$ the critical angle $\bar{\phi}$ lies between ϕ_p and ϕ_s.

While in the actual problem the above stated conditions for a discontinuity are not exactly satisfied and no shock front occurs, the conditions are nearly satisfied when $p_o >> p_L$. As a result, very rapid changes were found in Ref. [1] in an extremely narrow range of the angle ϕ near $\bar{\phi}$ when p_o exceeds about 5. (See the tables in Ref. [2].)

The fact that for large values of p_o the plastic effects are nearly a "shock front" at $\phi = \bar{\phi}$, suggests that approximate solutions could be obtained by compressing (approximately) all plastic effects into a discontinuity in normal pressure and velocity at $\bar{\phi}$, and treating the material elsewhere (approximately) as entirely elastic, even if the yield condition is slightly violated. For the case of a step pressure $p_o > p_L$, this approximate solution for $\nu > 1/8$ would have the configuration shown in Fig. 8. In addition to the elastic discontinuities at ϕ_S and ϕ_P , there is an assumed discontinuity at $\bar{\phi}$, consisting of a change of all three principal stresses by an amount $\overline{\Delta\sigma}$ and an appropriate change of normal velocity. In the region between these fronts the stresses and velocities are uniform, but the yield condition in one or two of the regions will be violated. Such violation is considered acceptable provided it is not too severe.

In view of the fact that correct solutions for the step pressure are available, there is no need to consider this case further, but the equivalent approximations can be made, and will be made below for the case of a decaying surface load.

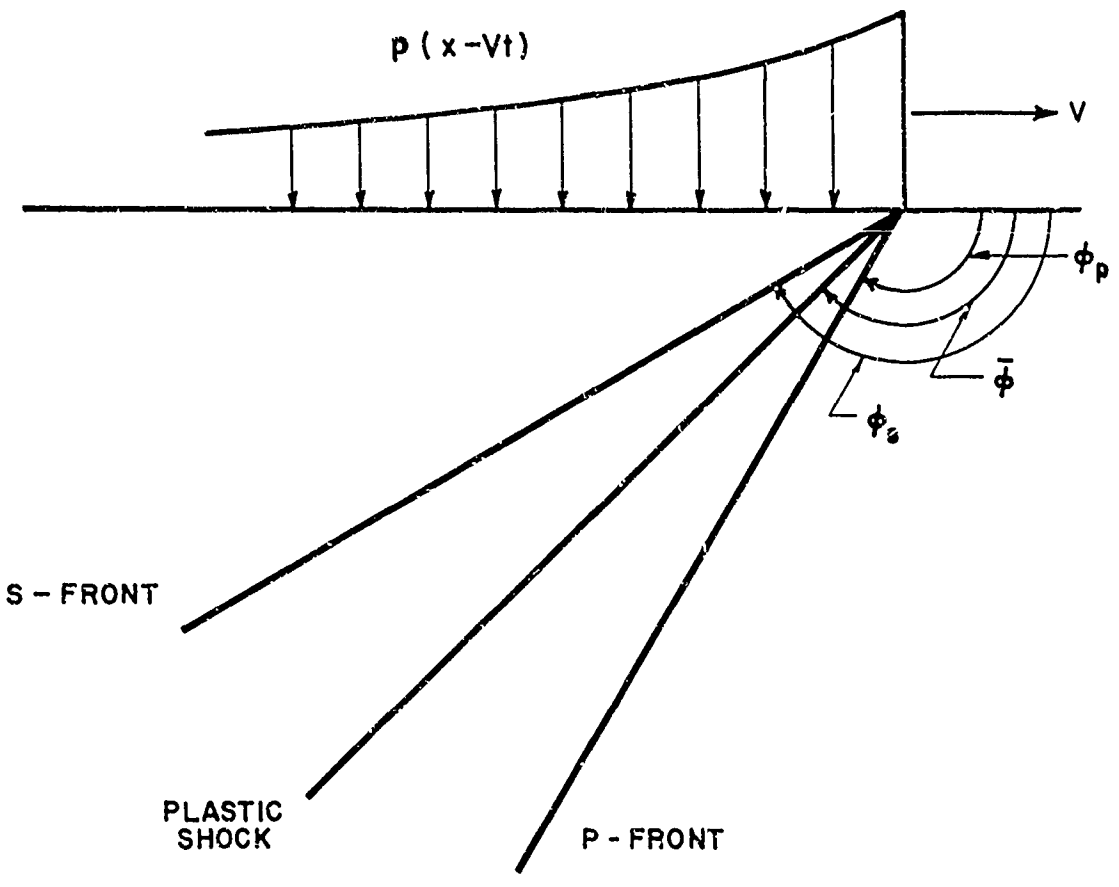

CONFIGURATION FOR APPROXIMATE SOLUTION
($\nu = 1/8$)

FIG. 8

Assuming the discontinuities stated above, at ϕ_p , ϕ_s and $\bar{\phi}$, it will be assumed that the elastic differential equations apply in each of the three wedge shaped regions shown in Fig. 8. Solving the boundary value problem posed by the prescribed surface load and by momentum or continuity considerations, approximate solutions are obtained. After finding the solutions the degree of violation of the yield condition can be checked by computing the ratio,

$$n = \frac{|\sqrt{J_2}|}{k} \tag{11}$$

starting near the leading edge of the load. If the solution in this location and within some distance $\bar{r}$ from the wave front is acceptable, the hyperbolic nature of the problem permits one to accept the solution in the range $r < \bar{r}$, even if serious violations of the yield condition occur elsewhere for $r > \bar{r}$. A further restraint on the range of validity, $\bar{r}$, is the fact that the compressive stress at the shock front $\phi = \bar{\phi}$ must inherently increase and the solution can only be accepted within a radius $\bar{r}$ where this requirement holds.

In the numerical solution obtained later the ratios n indicating compliance or violation of the yield condition are stated for each point where stresses are given. For engineering purposes values up to n = 1.2 were considered, but a reader may elect not to use the full range of the solution given if smaller values of n appear appropriate. It is found that the range of applicability shrinks as V/c_p becomes smaller and approaches unity.

The formulation of the problem given below applies only for values $\nu \geq 1/8$. Therefore the tables given contain only values $V/c_p \geq 1.5$ and $\nu > 1/8$.

SECTION II

FORMULATION OF THE APPROXIMATE ANALYSIS

Based on the reasoning outlined in Section I, approximate solutions for the case of the decaying shock wave, Fig. 2, will be formulated. Only the case $\nu > 1/8$ is considered so that $\phi_s > \bar{\phi}$. In accordance with the discussion in the Introduction, it is assumed (approximately) that plastic deformations occur in any element only at the time of passing of the plastic shock front indicated in Fig. 8, while stress changes thereafter are elastic. The applicable elastic relations between stress rates and strain rates for the present case of plain strain are

$$\dot{\varepsilon}_x \equiv \frac{\partial \dot{u}}{\partial x} = \frac{1}{E}\left[\dot{\sigma}_x - \nu\dot{\sigma}_y - \nu\dot{\sigma}_z\right] = \left(\frac{1-\nu^2}{E}\right)\left[\dot{\sigma}_x - \frac{\nu}{1-\nu}\,\dot{\sigma}_y\right] \tag{12}$$

$$\dot{\varepsilon}_y \equiv \frac{\partial \dot{v}}{\partial y} = \frac{1}{E}\left[-\nu\dot{\sigma}_x + \dot{\sigma}_y - \nu\dot{\sigma}_z\right] = \left(\frac{1-\nu^2}{E}\right)\left[-\frac{\nu}{1-\nu}\,\dot{\sigma}_x + \dot{\sigma}_y\right] \tag{13}$$

$$\dot{\varepsilon}_z \equiv 0 = \frac{1}{E}\left[-\nu\dot{\sigma}_x - \nu\dot{\sigma}_y + \dot{\sigma}_z\right] \tag{14}$$

$$\dot{\varepsilon}_{xy} \equiv \frac{1}{2}\left[\frac{\partial \dot{u}}{\partial y} + \frac{\partial \dot{v}}{\partial x}\right] = \frac{1}{2G}\,\dot{\tau} \tag{15}$$

where σ_x , σ_y , σ_z , τ are the stresses, while u, v, are the displacements in the x and y directions, respectively. In addition, the equation of motion

$$\frac{\partial \sigma_x}{\partial x} + \frac{\partial \tau}{\partial y} = \rho\,\frac{\partial \dot{u}}{\partial t} \tag{16}$$

$$\frac{\partial \tau}{\partial x} + \frac{\partial \sigma_y}{\partial y} = \rho \frac{\partial \dot{v}}{\partial t} \tag{17}$$

must be satisfied. Equations (12, 13, 15) may be integrated with respect to time, requiring the addition of arbitrary functions $f_i(x,y)$ of x and y,

$$\frac{\partial u}{\partial x} = \frac{1-\nu^2}{E} \left[\sigma_x - \frac{\nu}{1-\nu} \sigma_y\right] + f_1(x,y) \tag{18}$$

$$\frac{\partial v}{\partial y} = \frac{1-\nu^2}{E} \left[-\frac{\nu}{1-\nu} \sigma_x + \sigma_y\right] + f_2(x,y) \tag{19}$$

$$\frac{1}{2} \left[\frac{\partial u}{\partial y} + \frac{\partial v}{\partial x}\right] = \frac{1}{2G} \tau + f_3(x,y) \tag{20}$$

while Eq. (14) after integration may be written

$$\sigma_z = \nu(\sigma_x + \sigma_y) + f_o(x,y) \tag{21}$$

The last equation is the only relation containing σ_z , and simply defines this quantity. It is noted that the arbitrary functions f_1 , f_2 and f_3 are not entirely "arbitrary", but are related by a compatibility relation, as may be seen by eliminating u and v from Eqs. (18), (19) and (20).

The solution to the differential equations (16-20) may be expressed in terms of potentials Φ and Ψ which satisfy the wave equations

$$\Phi_{xx} + \Phi_{yy} = \frac{1}{c_p^2} \Phi_{tt} \tag{22}$$

$$\Psi_{xx} + \Psi_{yy} = \frac{1}{c_s^2} \Psi_{tt} \tag{23}$$

Subscripts on potentials indicate derivatives. In terms of these potentials and of two arbitrary functions g_1 and g_2 of x and y, the displacements become

$$u = \Phi_x - \Psi_y + g_1(x,y) \tag{24}$$

$$v = \Phi_y + \Psi_x + g_2(x,y) \tag{25}$$

while the velocities $\dot{u}$ and $\dot{v}$ are

$$\dot{u} = \dot{\Phi}_x - \dot{\Psi}_y \tag{26}$$

$$\dot{v} = \dot{\Phi}_y + \dot{\Psi}_x \tag{27}$$

The stresses are

$$\sigma_x = 2G \left[\frac{1-\nu}{1-2\nu} \Phi_{xx} + \frac{\nu}{1-2\nu} \Phi_{yy} - \Psi_{xy}\right] \tag{28}$$

$$\sigma_y = 2G \left[\frac{\nu}{1-2\nu} \Phi_{xx} + \frac{1-\nu}{1-2\nu} \Phi_{yy} + \Psi_{xy}\right] \tag{29}$$

$$\tau = 2G \left[\Phi_{xy} + \frac{1}{2} (\Psi_{xx} - \Psi_{yy})\right] \tag{30}$$

with σ_z given by Eq. (21).

Substitution of Eqs. (24-25) and (28-30) into Eqs. (18-20) furnishes relations between the three "arbitrary" functions f_1, f_2 and f_3, and the two functions g_1 and g_2, i.e.,

$$f_1 = \frac{\partial g_1}{\partial x} \quad , \quad f_2 = \frac{\partial g_2}{\partial y} \quad , \quad f_3 = \frac{1}{2} \left(\frac{\partial g_1}{\partial y} + \frac{\partial g_2}{\partial x}\right) \tag{31}$$

These three relations and the Eqs. (28-30) satisfy compatibility indentically, leaving the two functions $g_1(x,y)$ and $g_2(x,y)$ as arbitrary functions in lieu of the related functions f_1 , f_2 and f_3 .

It is now noted that the velocities $\dot{u}$ and $\dot{v}$, and the stresses σ_x , σ_y and τ in terms of the potentials Φ and Ψ have exactly the same form as in an elastic plane problem and these quantities will therefore have the same values as in an entirely elastic problem with the same boundary conditions. The plastic deformations at the shock front lead, however, to different expressions for u, v and σ_z because the functions g_1 , g_2 and f_o now occur. As will be seen later, these three arbitrary functions follow from conditions at the P-front and at the plastic front.

Due to the fact that the steady-state problem is considered, the surface pressure is solely a function of

$$\xi = x - Vt \tag{32}$$

and the solutions are only functions of ξ and y. The wave equations for the potentials then become

$$\left.\begin{aligned} \Phi_{yy} &= (M^2 - 1)\, \Phi_{\xi\xi} \\ \Psi_{yy} &= (M_S^2 - 1)\, \Psi_{\xi\xi} \end{aligned}\right\} \tag{33}$$

where

$$M = \frac{V}{c_p} \quad ; \quad M_S = \frac{V}{c_S} \tag{34}$$

Noting that the open functions f_o , g_1 and g_2 , which are not functions of t, can in the steady-state not depend on x either, the expressions for displacements and stresses become

$$u = \Phi_\xi - \Psi_y + g_1(y) \tag{35}$$

$$v = \Phi_y + \Psi_\xi + g_2(y) \tag{36}$$

$$\sigma_x = G[2(1 + \frac{\nu M^2}{1-2\nu}) \Phi_{\xi\xi} - 2\Psi_{\xi y}] \tag{37}$$

$$\sigma_y = G[(M_S^2 - 2) \Phi_{\xi\xi} + 2\Psi_{\xi y}] \tag{38}$$

$$\tau = G[2\Phi_{\xi y} - (M_S^2 - 2) \Psi_{\xi\xi}] \tag{39}$$

$$\sigma_z = \nu(\sigma_x + \sigma_y) + f_o(y) \tag{40}$$

To formulate the boundary conditions, expressions will be required for the normal and tangential velocities $\dot{u}_N$, $\dot{u}_T$ and the normal, tangential and shear stresses σ_N , σ_T , τ_N for planes inclined at any angle ϕ (see Fig. 1)

$$\frac{\dot{u}_N}{V} = \sin \phi \, \Phi_{\xi\xi} - \cos \phi \, \Phi_{\xi y} - \cos \phi \, \Psi_{\xi\xi} - \sin \phi \, \Psi_{\xi y} \tag{41}$$

$$\frac{\dot{u}_T}{V} = - \cos \phi \, \Phi_{\xi\xi} - \sin \phi \, \Phi_{\xi y} - \sin \phi \, \Psi_{\xi\xi} + \cos \phi \, \Psi_{\xi y} \tag{42}$$

$$\frac{\sigma_N}{G} = [M_S^2 (1 - \frac{1-2\nu}{1-\nu} \sin^2\phi) - 2 \cos 2\phi] \Phi_{\xi\xi} -$$

$$- 2 \sin 2\phi \, \Phi_{\xi y} + 2 \cos 2\phi \, \Psi_{\xi y} + (M_S^2 - 2) \sin 2\phi \, \Psi_{\xi\xi} \tag{43}$$

$$\frac{\sigma_T}{G} = [M_S^2 \left(1 - \frac{1-2\nu}{1-\nu} \cos^2\phi\right) + 2 \cos 2\phi] \, \Phi_{\xi\xi} +$$

$$+ 2 \sin 2\phi \, \Phi_{\xi y} - 2 \cos 2\phi \, \Psi_{\xi y} - (M_S^2 - 2) \sin 2\phi \, \Psi_{\xi\xi} \quad (44)$$

$$\frac{\tau_N}{G} = (M^2 - 2) \sin 2\phi \, \Phi_{\xi\xi} + 2 \cos 2\phi \, \Phi_{\xi y} +$$

$$+ 2 \sin 2\phi \, \Psi_{\xi y} - (M_S^2 - 2) \cos 2\phi \, \Psi_{\xi\xi} \quad (45)$$

To state the boundary conditions of the problem properly, and to be able to make statements on the character of the solutions, the differential equations for Φ and Ψ must be discussed. While both differential equations are hyperbolic, the characteristics for Φ are steeper than the boundary $\bar{\phi}$ defining the plastic front, $\phi_p < \bar{\phi}$. The solution for Φ in the region of interest, $\bar{\phi} < \phi < \pi$, Fig. 8, is therefore defined by statements on the boundaries $\phi = \bar{\phi}$ and $\phi = \pi$. Φ will be a continuous function if the prescribed conditions at the boundaries are continuous. This being the case, it will be possible to use for Φ an expansion in a Taylor series in ξ and y for a region near the origin $\xi = y = 0$.

On the other hand, the characteristic directions for the differential equation on Ψ are flatter than the boundary, $\phi_S > \bar{\phi}$. The differential equation does therefore not apply at $\phi = \phi_S$, and the solutions $\bar{\Psi}$ for $\phi > \phi_S$, and $\bar{\bar{\Psi}}$ for $\bar{\phi} < \phi < \phi_S$ are not fully defined by prescriptions on $\phi = \pi$ and $\phi = \bar{\phi}$. The two functions $\bar{\Psi}$ and $\bar{\bar{\Psi}}$ must, however, lead to

values of stress and velocities which satisfy momentum considerations at $\phi = \phi_s$, which furnish additional conditions for their determination. While at least some of the derivatives of $\bar{\Psi}$ and $\bar{\bar{\Psi}}$ at $\phi = \bar{\phi}_s$ will not be continuous, each of these potentials in its region will be continuous, and each of the potentials $\bar{\Psi}$ and $\bar{\bar{\Psi}}$ can again be expanded in a Taylor series.

The functions Φ, $\bar{\Psi}$ and $\bar{\bar{\Psi}}$ are therefore subject to the conditions listed below. On the surface the normal and tangential stresses are prescribed. Thus, for an exponentially decaying surface load, the stresses are

<u>at $y = 0$, $\xi < 0$</u>

$$\frac{\sigma_y}{k} = -\frac{p_o}{k} e^{\mu\xi} \qquad (\mu > 0) \tag{46}$$

$$\frac{\tau}{k} = 0 \tag{47}$$

At the plastic front $\phi = \bar{\phi}$ conservation of momentum requires

<u>at $\phi = \bar{\phi}$</u>

$$\frac{\Delta J_1}{k} = \frac{3\rho\bar{c}}{k} \Delta\dot{u}_N \tag{48}$$

$$\frac{\Delta\tau}{k} = 0 \tag{49}$$

$$\Delta\sigma_N = \Delta\sigma_T = \Delta\sigma_z = \overline{\Delta\sigma} = \frac{1}{3} \Delta J_1 \tag{50}$$

where J_1 is the invariant

$$J_1 = \sigma_x + \sigma_y + \sigma_z \tag{51}$$

and where the symbol Δ indicates the jump in stress, or velocity at a front of discontinuity and where $\bar{c}$ and $\bar{\phi}$ are given by Eqs. (9) and (10), respectively. Moreover, energy considerations require that the signs of $\overline{\Delta\sigma}$ and of the total normal stress σ_N at $\bar{\phi}$ are equal.

Due to the fact that different expressions $\bar{\Psi}$ and $\bar{\bar{\Psi}}$ for the solution of the second of Eqs. (33) will be used, it is necessary to consider conditions at the location $\phi = \phi_S$. Momentum considerations require that discontinuities in the shear stress τ_N and the tangential component of the velocity $\dot{u}_T$ are proportional

<u>at $\phi = \phi_S$</u>

$$\Delta\tau_N = \rho\, c_S\, \Delta\dot{u}_T \tag{52}$$

while all the normal and tangential stresses and the normal velocity at $\phi = \phi_S$ must be continuous

<u>at $\phi = \phi_S$</u>

$$\Delta\sigma_N = 0 \tag{53}$$

$$\Delta\sigma_T = 0 \tag{54}$$

$$\Delta\sigma_z = 0 \tag{55}$$

$$\Delta\dot{u}_N = 0 \tag{56}$$

In the assumed approximate solution, the plastic shock propagates into a region which has been previously stressed by the passage of the P-front. In this region, $\phi_P < \phi < \bar{\phi}$, the stresses are uniform and just at the yield limit. Their values are:

for $\phi_P < \phi < \bar{\phi}$

$$\frac{\sigma_x}{k} = \frac{-\sqrt{3}\,(1-\nu)}{1-2\nu}\,[1 - 2\sin^2\phi_S \cot^2\phi_P] \tag{57}$$

$$\frac{\sigma_y}{k} = \frac{-\sqrt{3}\,(1-\nu)}{1-2\nu}\cos 2\phi_S \tag{58}$$

$$\frac{\tau_{xy}}{k} = \frac{2\sqrt{3}\,(1-\nu)}{1-2\nu}\sin^2\phi_S \cot\phi_P \tag{59}$$

$$\frac{\sigma_z}{k} = \frac{-\sqrt{3}}{2}\sin 2\phi_P \tag{60}$$

The above equations complete the available conditions for the determination of the potentials Φ, $\bar{\Psi}$ and $\bar{\Psi}$. After the potentials are obtained the arbitrary function $f_o(y)$ appearing in Eq. (40) can be obtained from Eq. (50). The arbitrary functions $g_1(y)$ and $g_2(y)$ in Eqs. (35) and (36) are defined by the fact that displacements at the plastic front may be computed from the velocities in the region between ϕ_P and $\bar{\phi}$, using the relations:

for $\phi_P < \phi < \bar{\phi}$

$$u = -\frac{\dot{u}}{V}\,(\xi + y \cot\phi_P) \tag{61}$$

$$v = -\frac{\dot{v}}{V}\,(\xi + y \cot\phi_P) \tag{62}$$

SECTION III

SOLUTION OF THE DIFFERENTIAL EQUATIONS BY TAYLOR SERIES

The differential equations for the potentials to be solved are

$$\Phi_{yy} - (M^2 - 1)\,\Phi_{\xi\xi} = 0 \tag{63}$$

$$\left.\begin{aligned} \bar{\Psi}_{yy} - (M_S^2 - 1)\,\bar{\Psi}_{\xi\xi} &= 0 \\ \bar{\bar{\Psi}}_{yy} - (M_S^2 - 1)\,\bar{\bar{\Psi}}_{\xi\xi} &= 0 \end{aligned}\right\} \tag{64}$$

The boundary conditions, Eqs. (46-47) on the surface give

<u>at $y = 0,\ \xi < 0$</u>

$$(M_S^2 - 2)\,\Phi_{\xi\xi} + 2\bar{\Psi}_{\xi y} = -\frac{p_o}{G}\,e^{\mu\xi} \tag{65}$$

$$2\Phi_{\xi y} - (M_S^2 - 2)\,\bar{\Psi}_{\xi\xi} = 0 \tag{66}$$

While the conditions, Eqs. (48-50) at the plastic front give three equations

<u>at $y = \xi \tan \bar{\phi}$</u>

$$\frac{G}{k}\left\{(M^2 - 1)\,\Phi_{\xi\xi} + \cot\bar{\phi}\,[\Psi_{\xi y} + \bar{\Psi}_{\xi\xi}] + \bar{\Psi}_{\xi y}\right\} =$$

$$= -\frac{\sqrt{3}}{2} + \frac{1}{2}\sqrt{\frac{1-\nu}{1+\nu}}\cos(\bar{\phi} - \phi_p) \tag{67}$$

$$\frac{G}{k}\left\{(M^2 - 2)\sin 2\bar{\phi}\,\Phi_{\xi\xi} + 2\cos 2\bar{\phi}\,\Phi_{\xi y} + 2\sin 2\bar{\phi}\,\bar{\Psi}_{\xi y} - \right.$$

$$\left. - (M_S^2 - 2)\cos 2\bar{\phi}\,\bar{\Psi}_{\xi\xi}\right\} = 0 \qquad (68)$$

$$\frac{G}{k}\left\{(M^2 - 2)\cos 2\bar{\phi}\,\Phi_{\xi\xi} - 2\sin 2\bar{\phi}\,\Phi_{\xi y} + 2\cos 2\bar{\phi}\,\bar{\Psi}_{\xi y} + \right.$$

$$\left. + (M_S^2 - 2)\sin 2\bar{\phi}\,\bar{\Psi}_{\xi\xi}\right\} = -\frac{\sqrt{3}}{2}\cos 2(\bar{\phi} - \phi_p) \qquad (69)$$

Finally, the five conditions, Eqs. (52-56) at the S-front lead to only one condition on $\bar{\Psi}$ and $\bar{\bar{\Psi}}$

<u>at $y = \xi \tan \phi_S$</u>

$$(\bar{\Psi}_{\xi\xi} - \bar{\bar{\Psi}}_{\xi\xi}) + \tan \phi_S(\bar{\Psi}_{\xi y} - \bar{\bar{\Psi}}_{\xi y}) = 0 \qquad (70)$$

The surface load is expanded in a series in ξ

$$p_o\, e^{\mu\xi} = p_o \sum_{m=0}^{\infty} \frac{1}{m!}\,\mu^m\,\xi^m \qquad (71)$$

applicable for $\xi < 0$, while the potentials Φ, $\bar{\Psi}$ and $\bar{\bar{\Psi}}$ are expanded in double series

$$\frac{G}{k}\begin{bmatrix}\Phi\\ \bar{\Psi}\\ \bar{\bar{\Psi}}\end{bmatrix} = \sum_{i,j}\begin{bmatrix}a_{i,\ell}\\ b_{i,\ell}\\ c_{i,\ell}\end{bmatrix}\xi^i\, y^{\ell} \qquad (72)$$

The differential equations and the conditions, Eqs. (46-56) are homogeneous, i.e., they contain consistently only second derivatives of Φ, $\bar{\Psi}$ and $\bar{\bar{\Psi}}$ with respect to ξ and y.

Substitution of Eqs. (72) into Eqs. (63), (64) and (66-70) results therefore in linear equations for the values $a_{i,\ell}$, $b_{i,\ell}$, $c_{i,\ell}$ which couple only those terms with indices $m = i+\ell-2$. The potentials can therefore be conveniently written as a series of polynomials. Each set of polynomials of class m can be determined independently from the polynomials for a different value of m.

$$\frac{G\Phi}{k} = \sum_{m=0}^{\infty} \Phi^{(m)} \qquad \Phi^{(m)} = \sum_{i=0}^{m+2} a_i^{(m)} \xi^i y^{m+2-i} \tag{73}$$

$$\frac{G\bar{\Psi}}{k} = \sum_{m=0}^{\infty} \bar{\Psi}^{(m)} \qquad \bar{\Psi}^{(m)} = \sum_{i=0}^{m+2} b_i^{(m)} \xi^i y^{m+2-i} \tag{74}$$

$$\frac{G\bar{\bar{\Psi}}}{k} = \sum_{m=0}^{\infty} \bar{\bar{\Psi}}^{(m)} \qquad \bar{\bar{\Psi}}^{(m)} = \sum_{i=0}^{m+2} c_i^{(m)} \xi^i y^{m+2-i} \tag{75}$$

The case m = 0 corresponds to the step load and, while quite simple, is treated differently, see Appendix I. For each value $m \geq 1$ there are (3m + 9) unknown coefficients $a_i^{(m)}$, $b_i^{(m)}$, $c_i^{(m)}$. Substituting the second derivatives of Eqs. (73-75) into the conditions on the boundaries of the regions, Eqs. (65-70), yields six equations for each value $m \geq 1$:*

$$(M_S^2 - 2)(m + 2)(m + 1)\, a_{m+2} + 2(m + 1)\, c_{m+1} = - \frac{p_o\, \mu^m}{k\, m!} \tag{76}$$

$$2(m + 1)\, a_{m+1} - (M_S^2 - 2)(m + 2)(m + 1)\, c_{m+2} = 0 \tag{77}$$

$$\sum_{j=1}^{m+2} (b_j - c_j)\, j\, (\tan \phi_S)^{m+2-j} = 0 \tag{78}$$

---

* The superscripts used in Eqs. (73-75) have been omitted for simplicity.

$$(m + 1)(m + 2)[(M^2 - 1)\, a_{m+2} + \cot \bar{\phi}\, b_{m+2}] +$$

$$+ (m + 1)(\tan \bar{\phi})^m [\cot \bar{\phi}\, a_1 + b_1] +$$

$$+ \sum_{j=2}^{m+1} (m + 3 - j)(\tan \bar{\phi})^{j-1} \{[(m + 2 - j)(M^2 - 1) +$$

$$+ (j - 1) \cot^2 \bar{\phi}]\, a_{m+3-j} + [(m + 2 - j) \cot \bar{\phi} +$$

$$+ (j - 1) \cot \bar{\phi}]\, b_{m+3-j}\} = 0 \qquad (79)$$

$$(m + 2)(m + 1)[N_5 a_{m+2} + N_8 b_{m+2}] + (m + 1)(\tan \bar{\phi})^m [N_6 a_1 + N_7 b_1] +$$

$$+ \sum_{j=2}^{m+1} (m + 3 - j)(\tan \bar{\phi})^{j-1} \{[(m + 2 - j)\, N_5 +$$

$$+ (j - 1) \cot \bar{\phi}\, N_6]\, a_{m+3-j} + [(m + 2 - j)\, N_8 +$$

$$+ (j - 1) \cot \bar{\phi}\, N_7]\, b_{m+3-j}\} = 0 \qquad (80)$$

$$(m + 2)(m + 1)[N_9 a_{m+2} + N_{10} b_{m+2}] + (m + 1)(\tan \bar{\phi})^m [N_7 a_1 - N_6 b_1] +$$

$$+ \sum_{j=2}^{m+1} (m + 3 - j)(\tan \bar{\phi})^{j-1} \{[(m + 2 - j)\, N_9 +$$

$$+ (j - 1)\, N_7 \cot \bar{\phi}]\, a_{m+3-j} + [(m + 2 - j)\, N_{10} -$$

$$- (j - 1)\, N_6 \cot \bar{\phi}]\, b_{m+3-j}\} = 0 \qquad (81)$$

where

$$
\left.
\begin{aligned}
N_1 &= M_S^2 - 2 + \sin^2\bar{\phi}\,(4 - 2M^2 - M_S^2) \\
N_2 &= -\left(\frac{M_S^2 - 4}{2}\right)\sin 2\bar{\phi} \\
N_3 &= 2 + (M_S^2 - 4)\sin^2\bar{\phi} \\
N_4 &= \left(\frac{3M_S^2 - 4}{2}\right)\sin 2\bar{\phi} \\
N_5 &= (M^2 - 2)\sin 2\bar{\phi} \\
N_6 &= 2\cos 2\bar{\phi} \\
N_7 &= 2\sin 2\bar{\phi} \\
N_8 &= -(M_S^2 - 2)\cos 2\bar{\phi} \\
N_9 &= 2\left[\cos 2\bar{\phi} + (M_S^2 - M^2)\left(\frac{1 + 2\alpha\sqrt{3}}{2 + \alpha\sqrt{3}}\right) - \frac{1}{2}M_S^2 + M^2\sin^2\bar{\phi}\right] \\
N_{10} &= -(M_S^2 - 2)\sin 2\bar{\phi}
\end{aligned}
\right\} \quad (82)
$$

Substituting Eqs. (73-75) into the wave equations, Eqs. (63-64), and equating coefficients of like powers of ξ and y, yields $(3m + 3)$ recurrence equations

$$
\left.
\begin{aligned}
a_{m-2q+2} &= (M^2 - 1)^q \, a_{m+2} \prod_{\ell=1}^{q} P_{m,\ell} \\
a_{m-2q+1} &= (M^2 - 1)^q \, a_{m+1} \, \delta_{2q-2,m} \prod_{\ell=1}^{q} \bar{P}_{m,\ell} \\
b_{m-2q+2} &= (M_S^2 - 1)^q \, b_{m+2} \prod_{\ell=1}^{q} P_{m,\ell} \\
b_{m-2q+1} &= (M_S^2 - 1)^q \, b_{m+1} \, \delta_{2q-2,m} \prod_{\ell=1}^{q} \bar{P}_{m,\ell} \\
c_{m-2q+2} &= (M_S^2 - 1)^q \, c_{m+2} \prod_{\ell=1}^{q} P_{m,\ell} \\
c_{m-2q+1} &= (M_S^2 - 1)^q \, c_{m+1} \, \delta_{2q-2,m} \prod_{\ell=1}^{q} \bar{P}_{m,\ell}
\end{aligned}
\right\} \qquad (83)
$$

where

$$
\left.
\begin{aligned}
P_{m,\ell} &= \frac{(m + 3 - 2\ell)(m + 4 - 2\ell)}{2\ell(2\ell - 1)} \\
\bar{P}_{m,\ell} &= \frac{(m + 2 - 2\ell)(m + 3 - 2\ell)}{2\ell(2\ell + 1)} \\
\delta_{2q-2,m} &= \begin{cases} 1 & \text{if } 2q - 2 \neq m \\ 0 & \text{if } 2q - 2 = m \end{cases} \\
1 \leq q &\leq \frac{2m + 3 + (-1)^m}{4}
\end{aligned}
\right\} \qquad (84)
$$

Equations (76-81) and Eqs. (83) give the required number of $(3m + 9)$ equations for the $(3m + 9)$ unknown coefficients a_i, b_i and c_i.

Substitution of Eqs. (83) into Eqs. (76) to (81) reduces the system to a set of six linear, nonhomogeneous, simultaneous equations, involving only the unknowns a_{m+2} , a_{m+1} , b_{m+2} , b_{m+1} , c_{m+2} . c_{m+1} . After solving for these values, the stresses, velocities and displacements for each of the m components of the surface load may be computed at any location (ξ,y) behind the front at $\bar{\phi}$.

SECTION IV

NUMERICAL RESULTS AND DISCUSSION

Numerical results from the relations derived in the previous section were obtained on a digital computer, truncating the series solution by retaining terms up to and including m = 7. Retention of terms m > 7 would have required the use of double precision, in spite of the fact that the computer employed carries 14 digits. The stresses found are presented in Tables II to XXVIII and in the accompanying figures, for all combinations of the velocity ratios V/c_p = 1.5, 2.0, 4.0 and of Poisson's ratio ν = 0.15, 0.25, 0.35, and for three peak values of surface loading. The values of p_o/k are selected to permit interpolation and extrapolation.

The approximation employed restricts the applicability of the approximate solutions to distances from the front of the applied load where the ratio n, Eq. (11), exceeds unity only moderately. To check this matter, the Tables indicate the value n for all points where stresses are listed. Truncation of the series further limits the validity of the results to points where $|\mu\xi| < 1.7$ and only such points are listed. Finally, the range of applicability of the present solution is limited by the fact that the approximate results can only be accepted as a reasonable approximation in the

range where the shock is compressive. The tables have been restricted in range such that this requirement is never seriously violated.

For each set of values ν and V/c_p considered, results for three levels of the load p_o/k are given. For values of p_o/k below the minimum considered, the elastic solution presented in Appendix II may be used, because this will generally result only in a very slight violation of the yield condition. For values p_o/k between the lowest and highest values given in the tables, interpolation between the three values given can be used without serious error, except at point (1^*). For values p_o/k which exceed the highest value, $\max(p_o/k)$ considered, the principal stresses at all points, except at point (1^*) can be obtained by using the results σ_i for the respective highest value of p_o/k, and adding the increment

$$\sigma_i^{(in)} = \max(p_o/k) - p_o/k \tag{85}$$

to each value σ_i in the table applicable for the value $\max(p_o/k)$. The increment $\sigma_i^{(in)}$ is inherently negative, i.e., compressive. Stresses at point (1^*) are always those shown in the tables for all values p_o/k above the minimum considered.

1. Discussion of typical results

The results for $V/c_p = 2.0$, $\nu = 0.25$ for the three loads $p_o/k = 4.0$, 6.0 and 10.0 are discussed as typical.

The principal stresses σ_1/k, σ_2/k, σ_3/k, the angle θ between the direction of σ_1 and the ξ-axis, and the values of n indicating violation of the yield condition are tabulated at fourteen points on a rectangular grid in the ξ-y plane. The results for these cases are given in Tables XIV - XVI. In every table point 1 has three sets of stresses because the stress field there has a directional singularity, i.e., the values depend on the direction of approach ϕ, and the results differ depending on whether $\phi_P < \phi < \bar{\phi}$, $\bar{\phi} < \phi < \phi_S$ or $\phi_S < \phi < \pi$. The three sets of values at point 1 immediately behind the front of the applied load are equal to those due to a step load without decay. In each of these three tables the yield violation at point 1 is the same, n = 1.056. The yield violations for a step wave, for a range of the parameters V/c_f, ν and p_o/k are shown in Fig. 9. For each combination of V/c_p and ν there is a limiting load, above which the degree of violation, n, remains constant. This is due to the fact that the effect of any higher value of p_o/k results only in a jump in the stress invariant J_1 at $\phi = \bar{\phi}$, a matter which does not affect the von Mises yield condition.

In order to judge the seriousness of the yield violation at point 1, n = 1.056, Table I gives the exact values of the stresses σ_i/k and of the angle θ, for a load of $p_o/k = 4.41$, as obtained in Ref. [1].

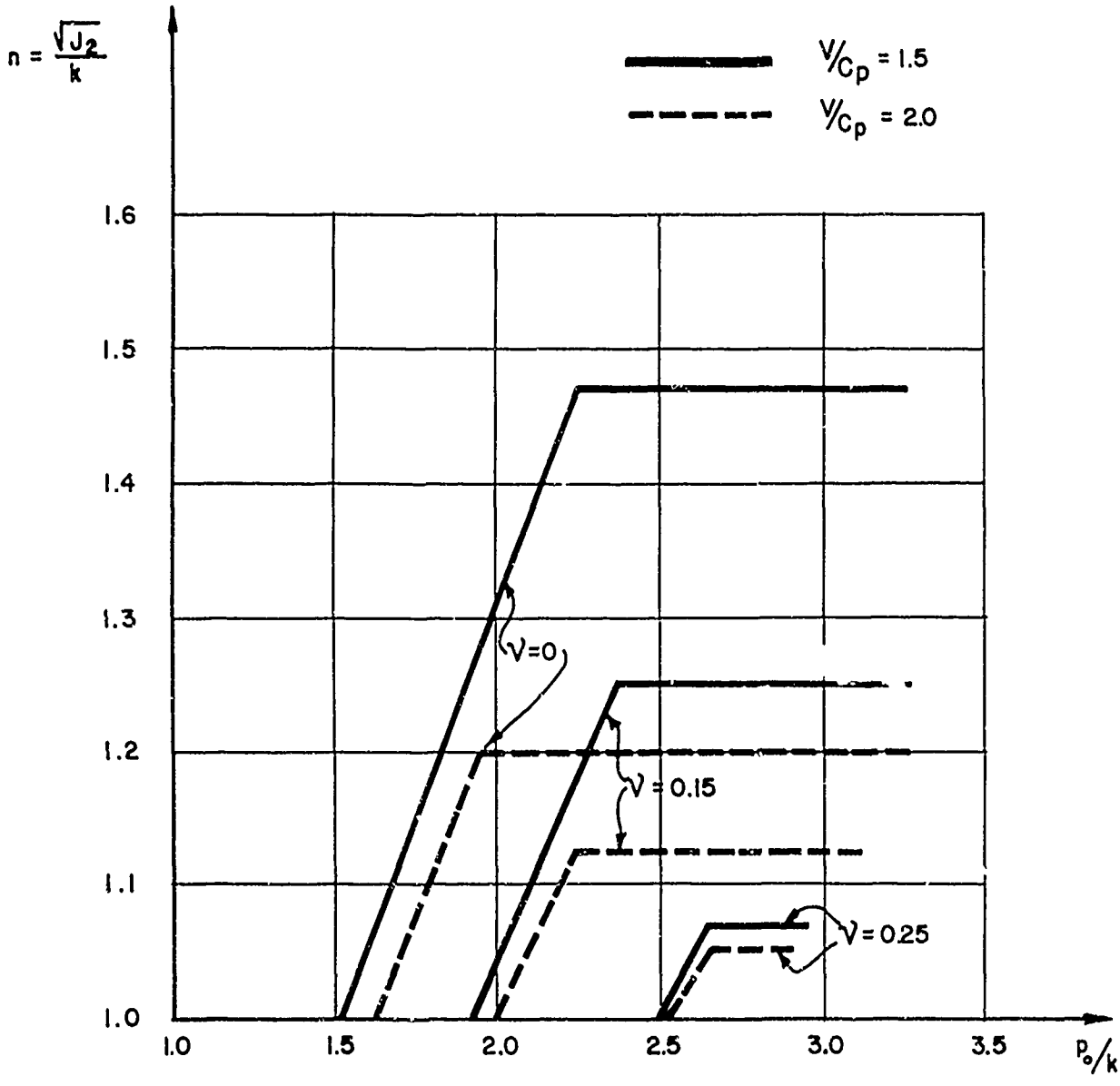

YIELD VIOLATION AT THE SURFACE FOR A STEP WAVE

FIG. 9

TABLE Ia $\nu = 0.25$, $V/c_p = 2.0$, $p_o = 4.41k$
(Exact Stresses)

Location	$-\sigma_1/k$	$-\sigma_2/k$	$-\sigma_3/k$	θ
$\phi_p < \phi < \phi_1$	2.598	0.866	0.866	60.00°
$\phi_2 < \phi < \phi_s$	4.20	2.47	2.47	67.46°
$\phi_s < \phi < \phi_3$	4.20	2.47	2.47	78.98°
$\phi_3 < \phi < \pi$	4.41	2.63	2.73	90.00°

The comparable stresses in the approximate solution for $p_o = 4.41k$ are

TABLE Ib $\nu = 0.25$, $V/c_p = 2.0$, $p_o = 4.41k$
(Approximate Stresses)

Location	$-\sigma_1/k$	$-\sigma_2/k$	$-\sigma_3/k$	θ
$\phi_p < \phi < \bar{\phi}$	2.598	0.866	0.866	60.00°
$\bar{\phi} < \phi < \phi_s$	4.345	2.613	2.613	60.00°
$\phi_s < \varphi < \phi$	4.41	2.549	2.549	90.00°

The differences in the principal stresses in the two tables are not large, the maximum being 7%. While the values θ listed in Table Ia agree with those in Table Ib, it is noted that in the exact case the value θ varies between $\phi_1 < \phi < \phi_2$ from 60.00° to 67.46° and between $\phi_3 < \phi < \phi_4$ from 78.98° to 90.00°. In the approximate

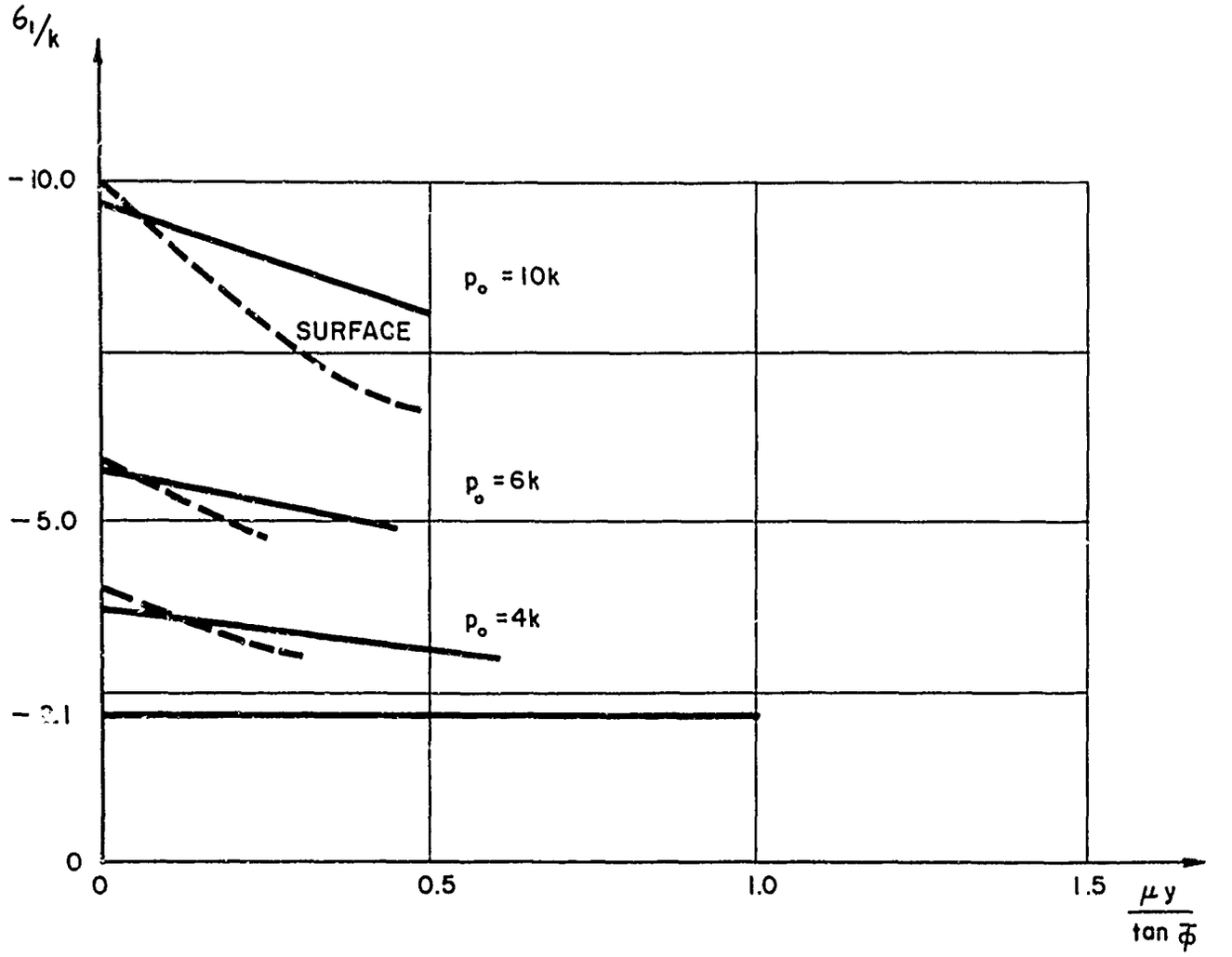

PRINCIPAL STRESS σ_1/k AT $\bar{\phi}$
FOR $\nu = 0.15$ $v/c_p = 1.50$

FIG. 10

TABLE II

RESULTS FOR $\nu = 0.150$ $V/c_p = 1.5$ $p_o = 4.0k$

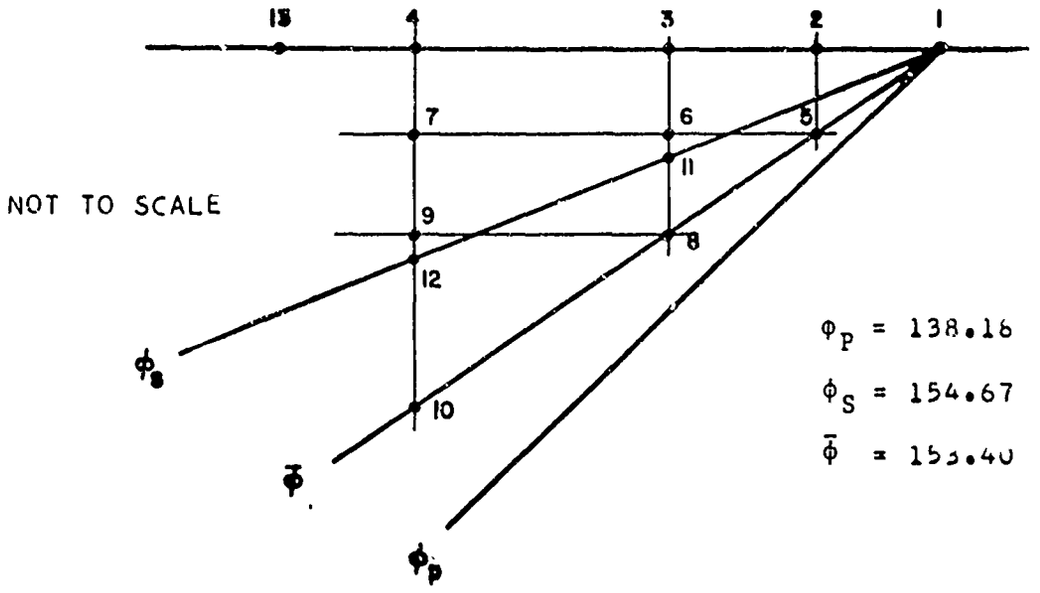

Pt.	$\mu\xi$	μy	σ_1/k	σ_2/k	σ_3/k	θ^o	n
1*	0.000	0.000	-2.103	-0.371	-0.371	48.189	1.000
1**	0.000	0.000	-3.720	-1.987	-1.987	48.189	1.000
1***	0.000	0.000	-4.000	-1.707	-1.987	90.000	1.250
2	-0.099	0.000	-3.619	-1.613	-1.916	90.000	1.081
3	-0.199	0.000	-3.275	-1.522	-1.851	90.000	0.951
4	-0.299	0.000	-2.964	-1.434	-1.791	90.000	0.850
5	-0.099	0.050	-3.578	-1.846	-1.846	48.189	1.000
6	-0.199	0.050	-3.509	-1.460	-1.778	89.645	1.102
7	-0.299	0.050	-3.173	-1.379	-1.715	89.748	0.954
8	-0.199	0.100	-3.443	-1.710	-1.710	48.195	1.000
9	-0.299	0.100	-3.404	-1.313	-1.645	89.311	1.123
10	-0.299	0.150	-3.313	-1.580	-1.580	48.195	1.000
11****	-0.199	0.094	-3.737	-1.395	-1.718	89.200	1.269
12****	-0.299	0.141	-3.615	-1.249	-1.591	88.846	1.278
13	-1.500	0.000	-0.896	-0.576	-1.351	90.000	0.390

* For $\phi_p < \phi < \bar{\phi}$

** For $\bar{\phi} < \phi < \phi_S$

*** For $\phi_S < \phi \leq \pi$

**** At ϕ_S^+

$\Delta\tau = 1.357$ k

TABLE III

RESULTS FOR $\nu = 0.150$, $V/c_p = 1.5$, $p_o = 6.0k$

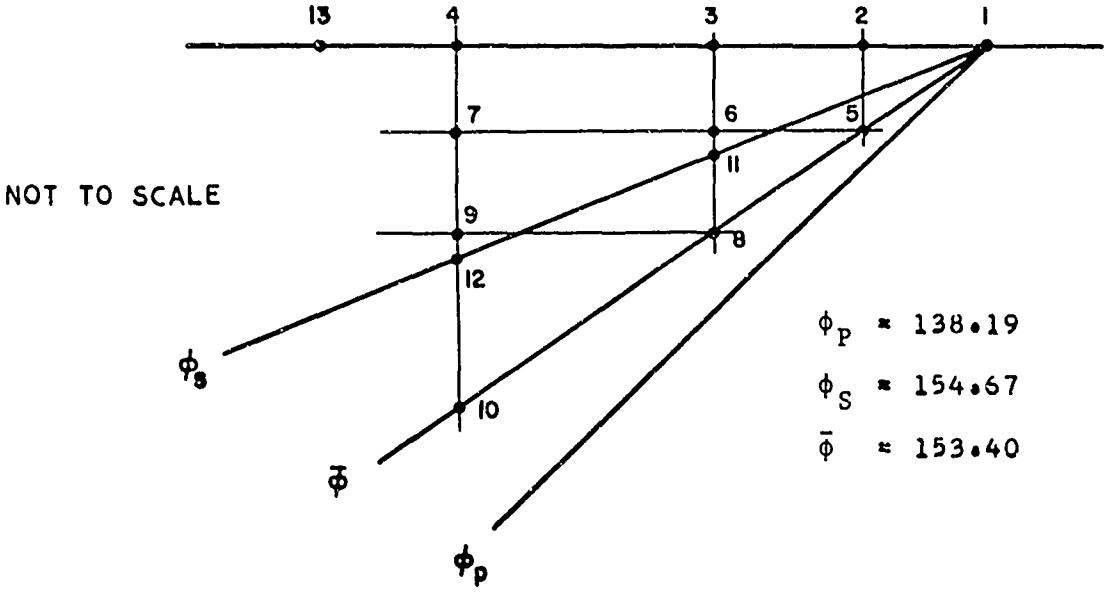

Pt.	$\mu\xi$	μy	σ_1/k	σ_2/k	σ_3/k	θ°	n
1*	0.000	0.000	-2.103	-0.371	-0.371	48.189	1.000
1**	0.000	0.000	-5.720	-3.987	-3.987	48.189	1.000
1***	0.000	0.000	-6.000	-3.707	-3.987	90.000	1.250
2	-0.059	0.000	-5.651	-3.622	-3.922	90.000	1.094
3	-0.119	0.000	-5.321	-3.538	-3.860	90.000	0.950
4	-0.179	0.000	-5.012	-3.456	-3.802	90.000	0.817
5	-0.059	0.030	-5.591	-3.859	-3.859	48.189	1.000
6	-0.119	0.030	-5.547	-3.479	-3.796	89.630	1.113
7	-0.179	0.030	-5.223	-3.401	-3.735	89.668	0.970
8	-0.119	0.060	-5.456	-3.733	-3.733	48.199	1.000
9	-0.179	0.060	-5.447	-3.340	-3.671	89.278	1.132
10	-0.179	0.090	-5.344	-3.611	-3.611	48.198	1.000
11****	-0.119	0.056	-5.759	-3.421	-3.741	89.262	1.267
12****	-0.179	0.085	-5.644	-3.284	-3.622	88.923	1.276
13	-1.500	0.000	-2.010	-1.335	-3.033	90.000	0.855

* For $\phi_p < \phi < \bar{\phi}$

** For $\bar{\phi} < \phi < \phi_S$

*** For $\phi_S < \phi \leq \pi$

**** At ϕ_S^+

$\Delta\tau = 1.357k$

TABLE IV

RESULTS FOR $\nu = 0.150$, $V/c_p = 1.5$, $p_o = 10.0k$

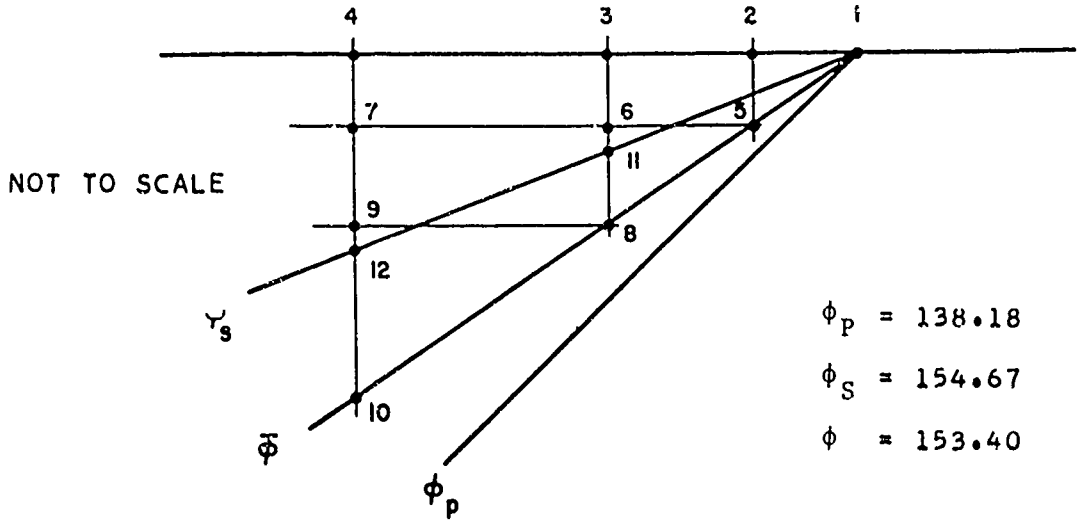

Pt.	$\mu\xi$	μy	σ_1/k	σ_2/k	σ_3/k	θ^o	n
1*	0.000	0.000	-2.103	-0.371	-0.371	48.189	1.000
1**	0.000	0.000	-9.720	-7.987	-7.987	48.189	1.000
1***	0.000	0.000	-10.000	-7.707	-7.987	90.000	1.250
2	-0.039	0.000	-9.608	-7.612	-7.914	90.000	1.075
3	-0.080	0.000	-9.231	-7.518	-7.844	90.000	0.909
4	-0.119	0.000	-8.869	-7.425	-7.776	90.000	0.753
5	-0.039	0.020	-9.576	-7.844	-7.844	48.189	1.000
6	-0.080	0.020	-9.490	-7.451	-7.772	89.552	1.096
7	-0.119	0.020	-9.118	-7.361	-7.703	89.550	0.931
8	-0.080	0.040	-9.436	-7.702	-7.702	48.205	1.001
9	-0.119	0.040	-9.375	-7.292	-7.632	89.126	1.117
10	-0.119	0.060	-9.298	-7.564	-7.564	48.205	1.000
11****	-0.080	0.037	-9.729	-7.387	-7.711	89.173	1.269
12****	-0.119	0.056	-9.599	-7.230	-7.576	88.787	1.279

* For $\phi_p < \phi < \bar{\phi}$

** For $\bar{\phi} < \phi < \phi_S$

*** For $\phi_S < \phi \leq \pi$

**** At ϕ_S^+

$\Delta\tau = 1.357k$

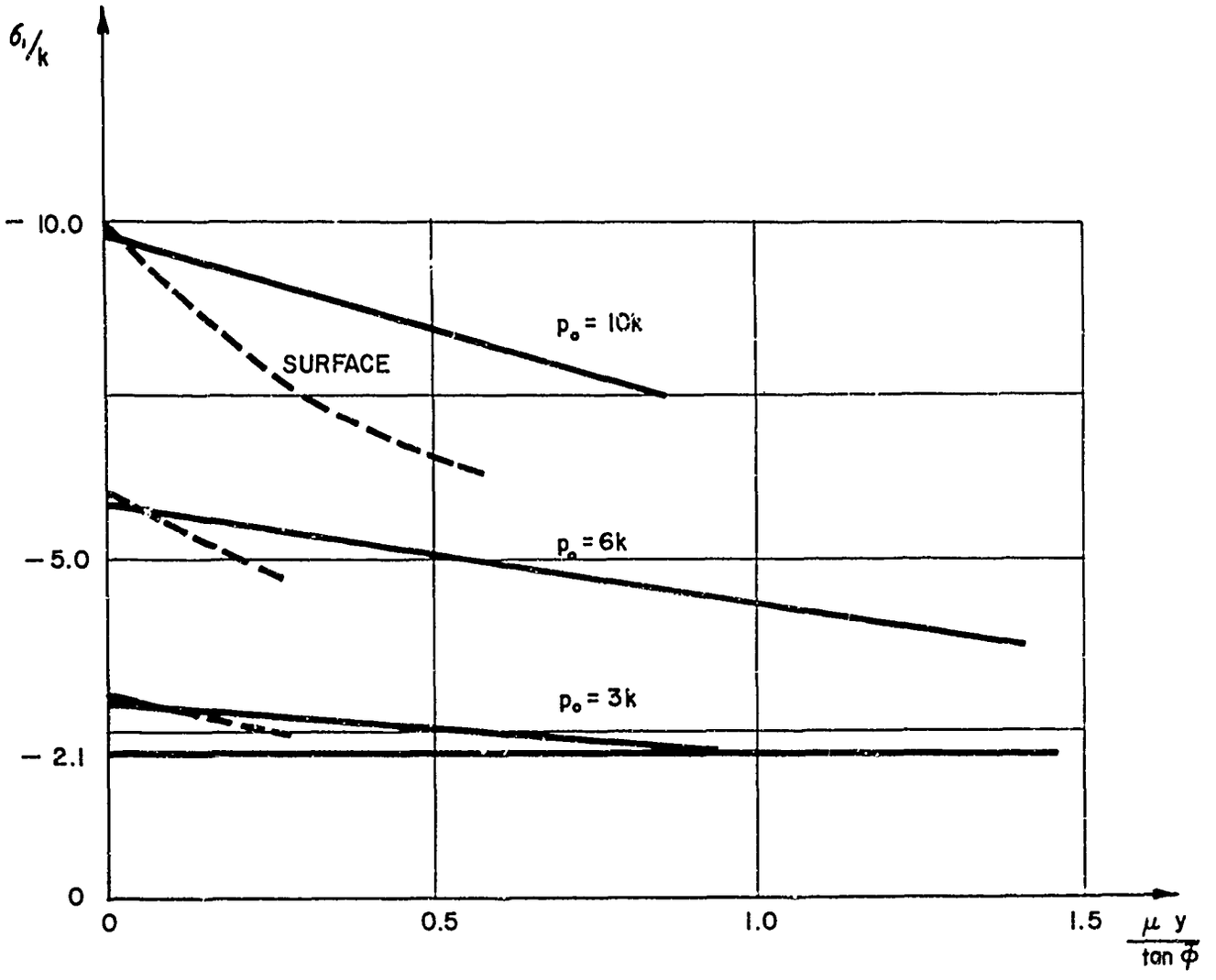

PRINCIPAL STRESS σ_1/k AT $\bar{\phi}$
FOR $\nu = 0.15$ $V/c_p = 2.0$

FIG. 11

TABLE V

RESULTS FOR $\nu = 0.150$, $V/c_p = 2.0$, $p_o = 3.0k$

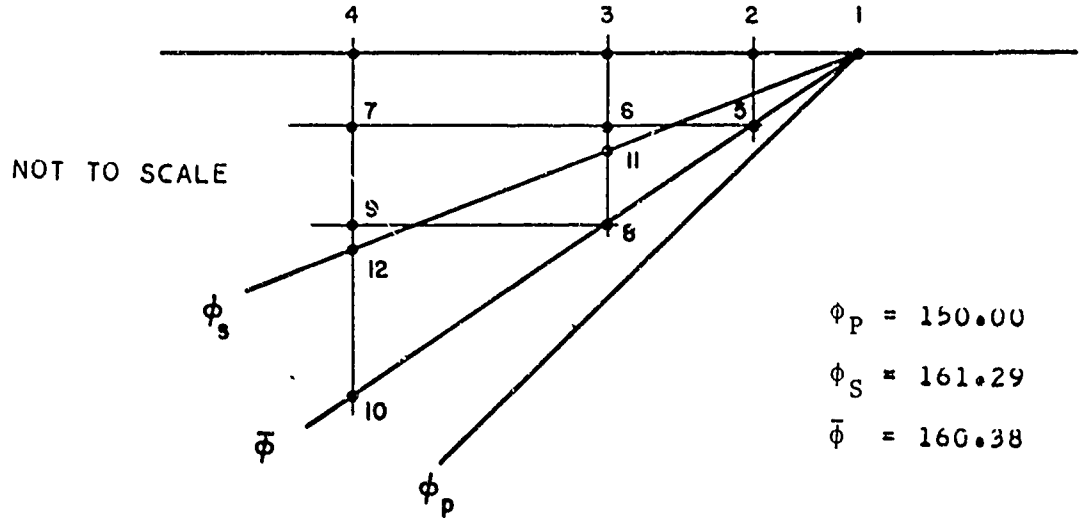

Pt.	$\mu\xi$	μy	σ_1/k	σ_2/k	σ_3/k	θ^o	n
1*	0.000	0.000	-2.103	-0.371	-0.371	60.000	1.000
1**	0.000	0.000	-2.859	-1.127	-1.127	60.000	1.000
1***	0.000	0.000	-3.000	-0.986	-1.127	60.000	1.124
2	-0.281	0.000	-2.266	-0.783	-0.986	90.000	0.804
3	-0.561	0.000	-1.712	-0.605	-0.877	90.000	0.577
4	-0.842	0.000	-1.293	-0.448	-0.790	90.000	0.425
5	-0.281	0.100	-2.600	-0.868	-0.868	60.000	1.000
6	-0.561	0.100	-2.048	-0.576	-0.742	91.690	0.806
7	-0.842	0.100	-1.540	-0.425	-0.643	92.970	0.591
8	-0.561	0.200	-2.367	-0.635	-0.635	60.000	1.000
9	-0.842	0.200	-1.855	-0.387	-0.521	93.180	0.812
10	-0.842	0.300	-2.157	-0.425	-0.425	60.000	1.000
11****	-0.561	0.190	-2.430	-0.531	-0.644	91.330	1.065
12****	-0.842	0.285	-2.190	-0.337	-0.438	92.000	1.042

* For $\phi_p < \phi < \bar{\phi}$

** For $\bar{\phi} < \phi < \phi_S$

*** For $\phi_S < \phi \leq \pi$

**** At ϕ_S^+

$\Delta\tau = 0.944k$

TABLE VI

RESULTS FOR $\nu = 0.150$, $V/c_p = 2.0$, $p_o = 6.0k$

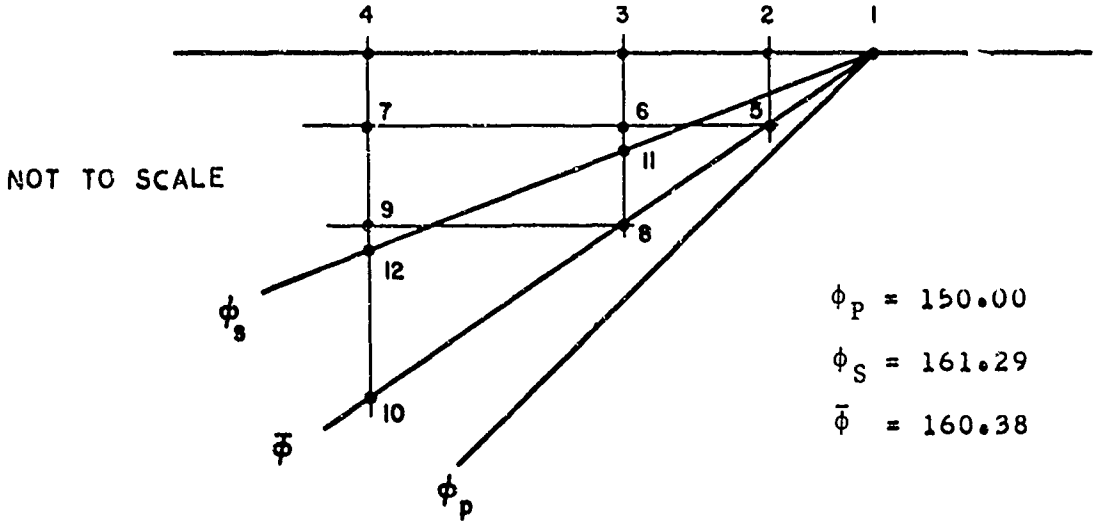

Pt.	$\mu\xi$	μy	σ_1/k	σ_2/k	σ_3/k	θ^o	n
1*	0.000	0.000	-2.103	-0.371	-0.371	60.000	1.000
1**	0.000	0.000	-5.859	-4.127	-4.127	60.000	1.000
1***	0.000	0.000	-6.000	-3.986	-4.127	90.000	1.124
2	-1.122	0.000	-1.953	-2.630	-3.317	90.000	0.682
3	-1.403	0.000	-1.474	-2.377	-3.20,	90.000	0.867
4	-1.683	0.000	-1.107	-2.148	-3.117	90.000	1 006
5	-1.122	0.400	-4.078	-2.345	-2.345	60.000	1.000
6	-1.403	0.400	-3.118	-2.071	-2.160	106.660	0.580
7	-1.683	0.400	-2.516	-1.707	-2.016	127.040	0.408
8	-1.403	0.500	-3.736	-2.005	-2.005	60.000	1.000
9	-1.683	0.500	-2.865	-1.766	-1.838	108.970	0.615
10	-1.683	0.600	-3.430	-1.698	-1.698	60.000	1.000
11****	-1.403	0.475	-3.584	-2.010	-2.040	97.520	0.900
12****	-1.683	0.570	-3.249	-1.720	-1.736	99.080	0.879

* For $\phi_p < \phi < \bar{\phi}$

** For $\bar{\phi} < \phi < \phi_S$

*** For $\phi_S < \phi \leq \pi$

**** At ϕ_S^+

$\Delta\tau = 0.944k$

TABLE VII

RESULTS FOR $\nu = 0.150$, $V/c_p = 2.0$, $p_o = 10.0k$

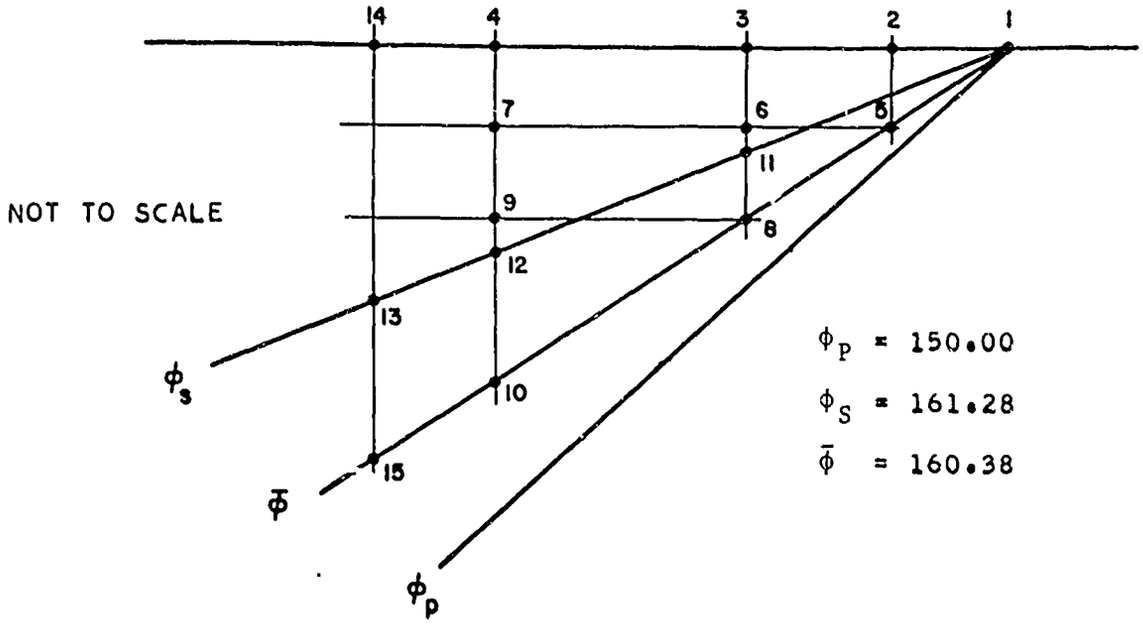

Pt.	$\mu\xi$	μy	σ_1/k	σ_2/k	σ_3/k	θ^o	n
1*	0.000	0.000	-2.193	-0.371	-0.371	60.000	1.000
1**	0.000	0.000	-9.859	-8.127	-8.127	60.000	1.000
1***	0.000	0.000	-10.000	-7.986	-8.127	90.000	1.124
2	-0.280	0.000	-7.553	-7.308	-7.658	90.000	0.179
3	-0.561	0.000	-6.716	-5.705	-7.292	90.000	0.803
4	-0.701	0.000	-6.447	-4.958	-7.140	90.000	1.114
5	-0.280	0.100	-8.996	-7.264	-7.264	60.000	1.000
6	-0.561	0.100	-6.899	-6.548	-6.842	117.688	0.188
7	-0.701	0.100	-6.425	-5.856	-6.667	71.592	0.416
8	-0.561	0.200	-8.218	-6.487	-6.487	59.989	0.999
9	-0.701	0.200	-7.183	-6.177	-6.285	102.388	0.552
10	-0.701	0.250	-7.859	-6.128	-6.128	59.989	0.999
11****	-0.561	0.190	-8.108	-6.460	-6.518	95.150	0.935
12****	-0.701	0.237	-7.703	-6.122	-6.165	96.651	0.900
13****	-1.500	0.508	-5.824	-4.466	-4.466	106.026	0.784
14	-1.500	0.000	-5.168	-2.225	-6.538	90.000	2.203

* For $\phi_p < \phi < \bar{\phi}$

** For $\bar{\phi} < \phi < \phi_S$

*** For $\phi_S < \phi \leq \pi$

**** At ϕ_S^+

$\Delta\tau = 0.944k$

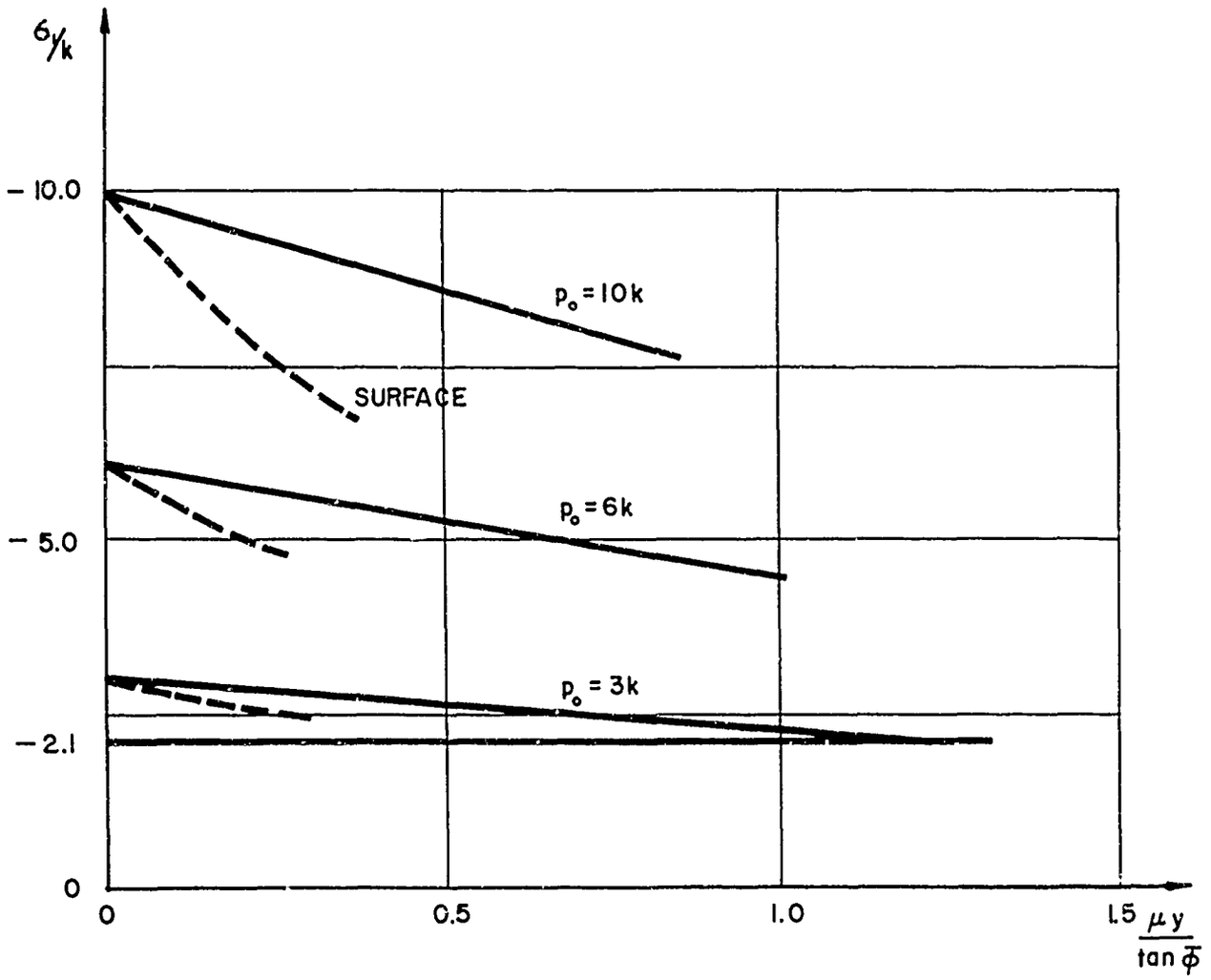

PRINCIPAL STRESS σ_{y}/k AT $\bar{\phi}$

FOR $\nu = 0.15$ $V/C_p = 4.0$

FIG. 12

TABLE VIII

RESULTS FOR $\nu = 0.150$, $V/c_p = 4.0$, $p_o = 3.0k$

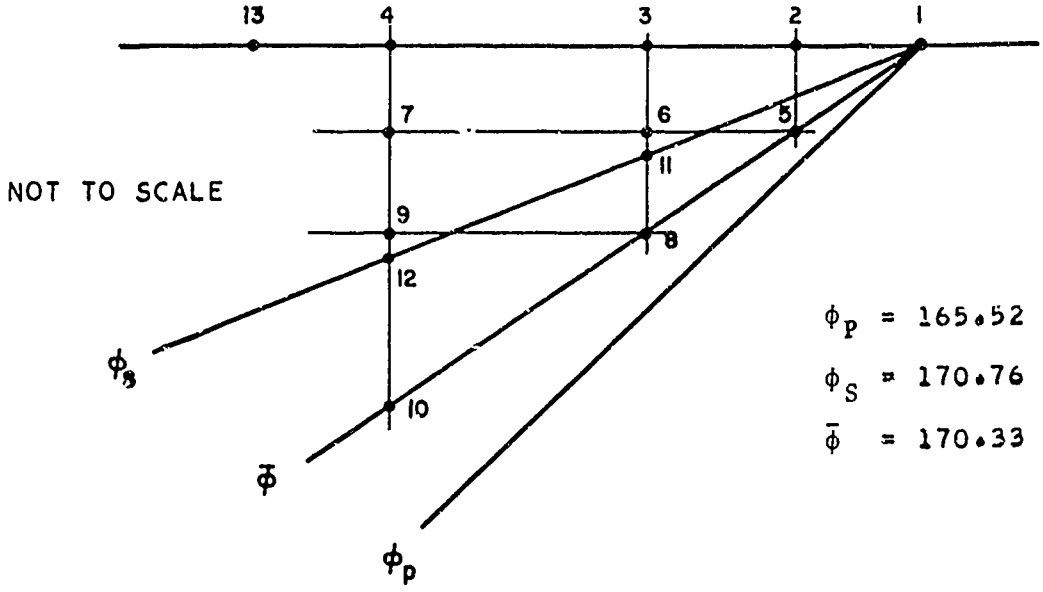

Pt.	$\mu\xi$	μy	σ_1/k	σ_2/k	σ_3/k	θ^o	n
1*	0.000	0.000	-2.103	-0.371	-0.371	75.522	1.000
1**	0.000	0.000	-2.968	-1.236	-1.236	75.522	1.000
1***	0.000	0.000	-3.000	-1.204	-1.236	90.000	1.027
2	-0.587	0.000	-1.667	-0.783	-0.973	90.000	0.465
3	-0.798	0.000	-1.349	-0.661	-0.907	90.000	0.348
4	-1.174	0.000	-0.926	-0.475	-0.815	90.000	0.235
5	-0.587	0.100	-2.493	-0.761	-0.761	75.522	1.000
6	-0.798	0.100	-2.046	-0.600	-0.670	107.294	0.815
7	-1.174	0.100	-1.471	-0.343	-0.545	113.343	0.601
8	-0.798	0.136	-2.342	-0.612	-0.612	75.549	0.998
9	-1.174	0.136	-1.724	-0.294	-0.472	114.592	0.779
10	-1.174	0.200	-2.102	-0.372	-0.372	75.546	0.999
11****	-0.798	0.129	-2.314	-0.584	-0.620	108.183	0.988
12****	-1.174	0.190	-2.146	-0.255	-0.383	114.461	1.056
13	-1.500	0.000	-0.667	-0.336	-0.756	90.000	0.221

* For $\phi_p < \phi < \bar{\phi}$

** For $\bar{\phi} < \phi < \phi_S$

*** For $\phi_S < \phi \leq \pi$

**** At ϕ_S^+

$\Delta\tau = 0.442k$

TABLE IX

RESULTS FOR $\nu = 0.150$, $V/c_p = 4.0$, $p_o = 6.0k$

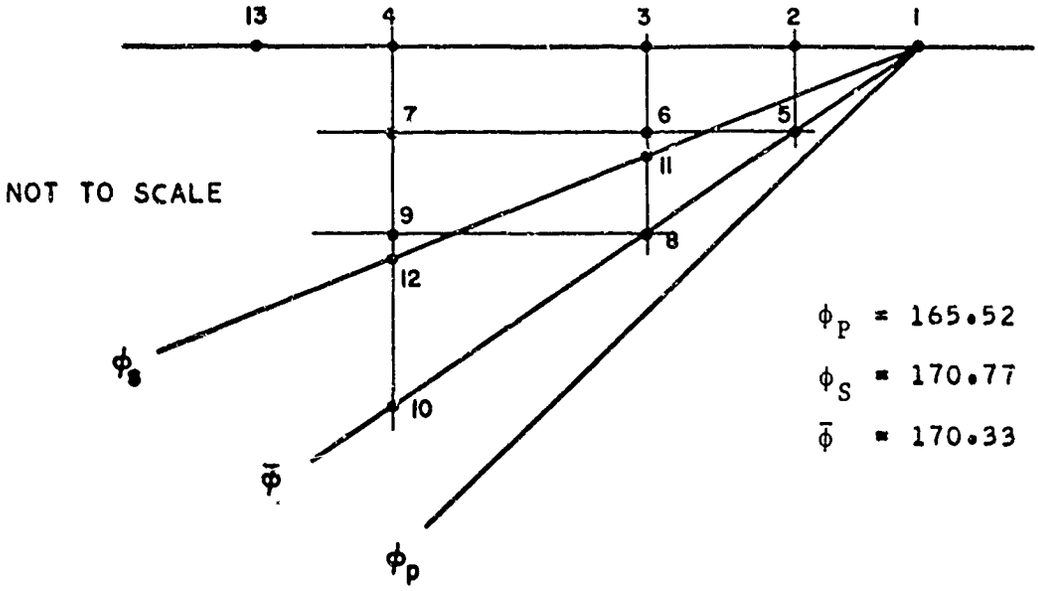

Pt.	$\mu\xi$	μy	σ_1/k	σ_2/k	σ_3/k	θ°	n
1*	0.000	0.000	-2.103	-0.371	-0.371	75.520	1.000
1**	0.000	0.000	-5.968	-4.236	-4.236	75.520	1.000
1***	0.000	0.000	-6.000	-4.204	-4.236	90.000	1.028
2	-0.294	0.000	-4.473	-3.747	-3.939	90.000	0.377
3	-0.587	0.000	-3.361	-3.335	-3.710	90.000	0.209
4	-0.881	0.000	-3.302	-2.486	-3.533	90.000	0.524
5	-0.294	0.050	-5.470	-3.738	-3.738	75.520	1.000
6	-0.587	0.050	-4.214	-3.196	-3.468	119.020	0.527
7	-0.881	0.050	-3.451	-2.578	-3.261	49.700	0.459
8	-0.587	0.100	-5.016	-3.288	-3.288	75.520	1.000
9	-0.881	0.100	-4.181	-2.495	-3.044	128.680	0.860
10	-0.881	0.150	-4.607	-2.879	-2.879	75.520	1.000
11****	-0.587	0.095	-5.085	-3.129	-3.300	116.430	1.083
12****	-0.881	0.143	-4.891	-2.473	-2.896	123.800	1.291
13	-1.500	0.000	-1.335	-2.469	-3.276	90.000	0.975

* For $\phi_p < \phi < \bar{\phi}$

** For $\bar{\phi} < \phi < \phi_S$

*** For $\phi_S < \phi \leq \pi$

**** At ϕ_S^+

$\Delta\tau = 0.442k$

TABLE X

RESULTS FOR $\nu = 0.150$ $V/c_p = 4.0$ $p_o = 10.0k$

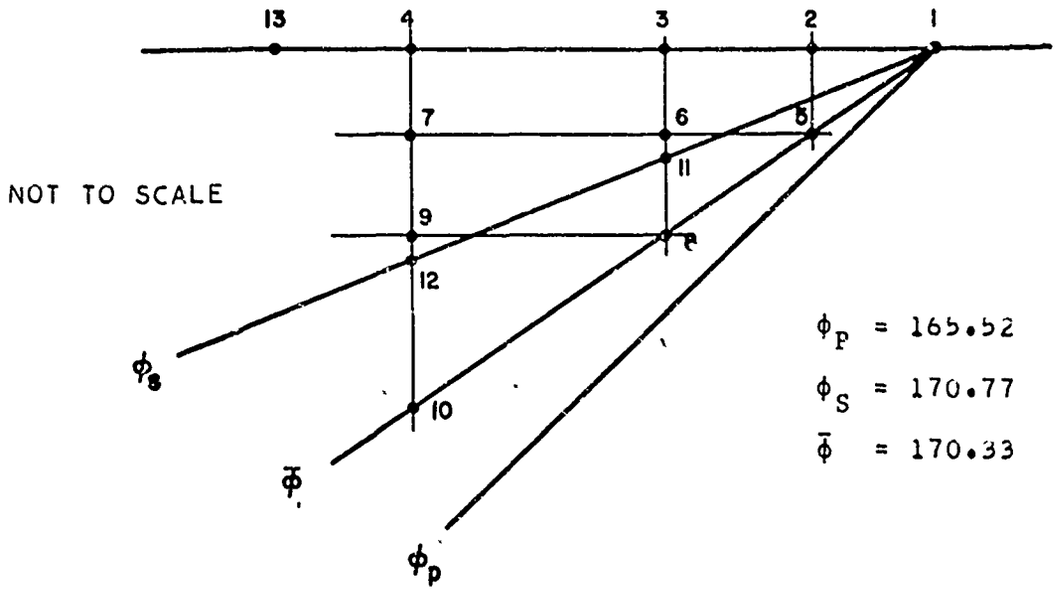

Pt.	$\mu\xi$	μy	σ_1/k	σ_2/k	σ_3/k	θ^o	n
1*	0.000	0.000	-2.103	-0.371	-0.371	75.520	1.000
1**	0.000	0.000	-9.968	-8.236	-8.236	90.000	1.000
1***	0.000	0.000	-10.000	-8.204	-8.236	90.000	1.028
2	-0.117	0.000	-8.892	-7.883	-8.022	90.000	0.547
3	-0.235	0.000	-7.906	-7.584	-7.829	90.000	0.168
4	-0.352	0.000	-7.305	-7.030	-7.656	90.000	0.314
5	-0.117	0.020	-9.626	-7.894	-7.894	75.520	1.000
6	-0.235	0.020	-8.586	-7.558	-7.688	107.500	0.560
7	-0.352	0.020	-7.765	-7.145	-7.503	126.460	0.311
8	-0.235	0.040	-9.292	-7.568	-7.568	75.520	1.000
9	-0.352	0.040	-8.441	-7.099	-7.370	119.720	0.710
10	-0.352	0.060	-8.976	-7.252	-7.252	75.520	1.000
11****	-0.235	0.038	-9.269	-7.523	-7.575	109.480	0.993
12****	-0.352	0.057	-9.058	-7.072	-7.264	117.250	1.095
13	-0.650	0.000	-6.675	-5.220	-7.290	90.000	1.065

* For $\phi_p < \phi < \bar{\phi}$

** For $\bar{\phi} < \phi < \phi_S$

*** For $\phi_S < \phi \leq \pi$

**** At ϕ_S^+

$\Delta\tau = 0.442k$

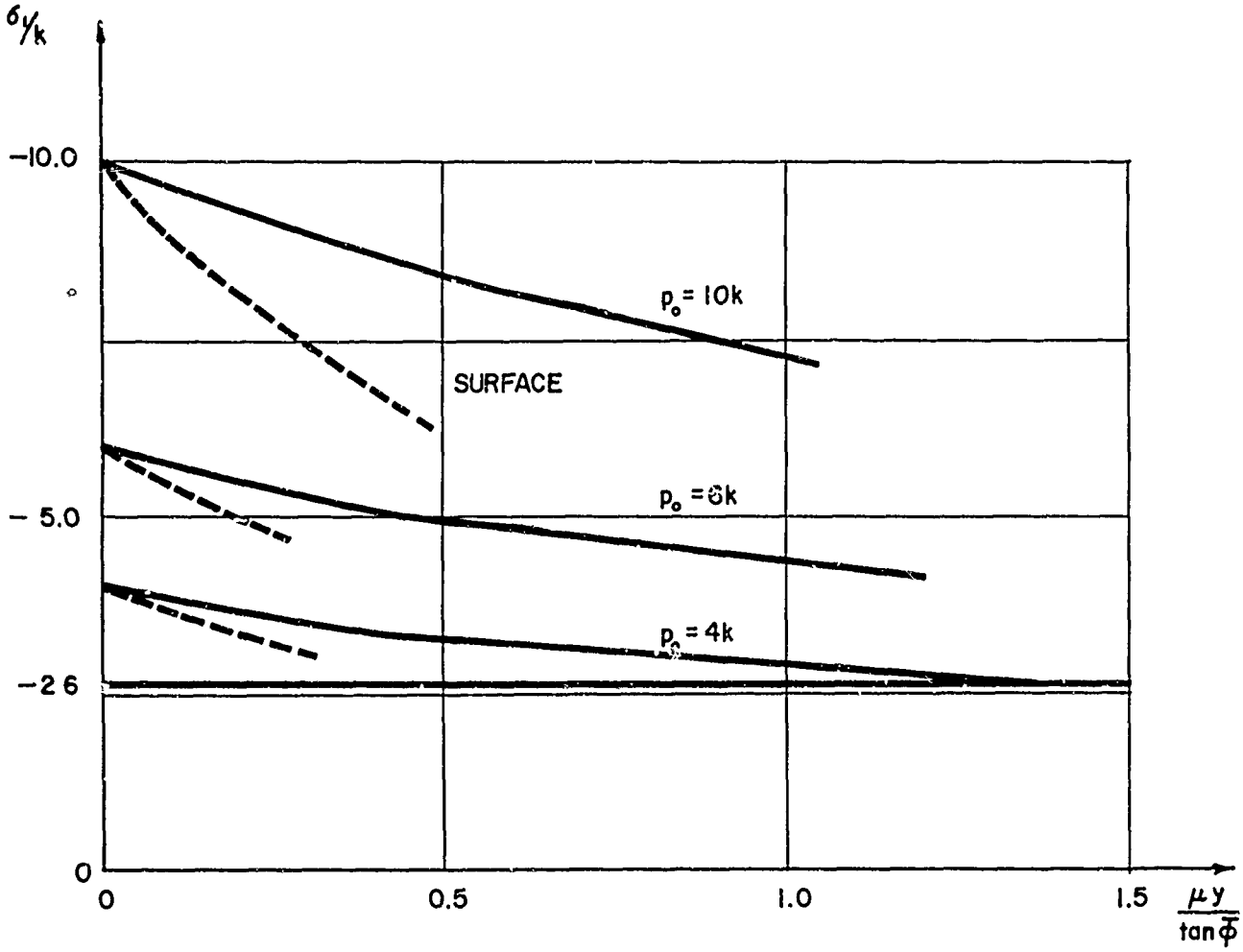

PRINCIPAL STRESS σ_1/k AT $\bar{\phi}$
FOR ν=0.25 V/C_p = 1.5

FIG. 13

TABLE XI

RESULTS FOR $\nu = 0.250$, $V/c_p = 1.5$, $p_o = 4.0k$

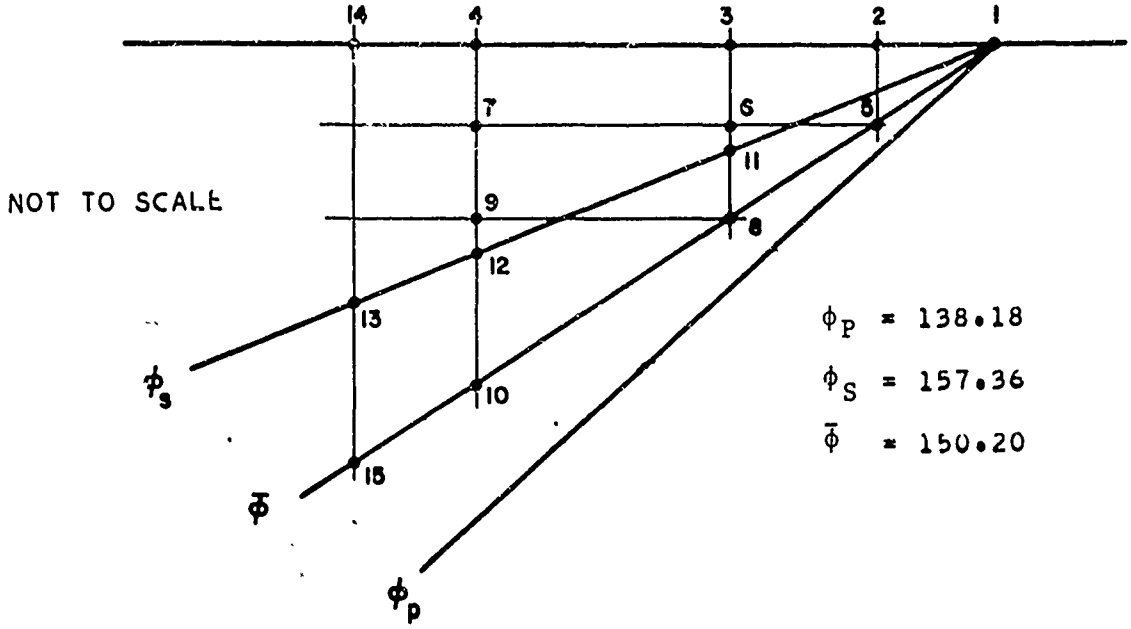

Pt.	$\mu\xi$	μy	σ_1/k	σ_2/k	σ_3/k	θ^o	n
1*	0.000	0.000	-2.598	-0.866	-0.866	48.189	1.000
1**	0.000	0.000	-3.900	-2.168	-2.168	48.189	1.000
1***	0.000	0.000	-4.000	-2.069	-2.168	90.000	1.087
2	-0.174	0.000	-3.359	-1.802	-1.941	90.000	0.861
3	-0.349	0.000	-2.820	-1.567	-1.748	90.000	0.677
4	-0.524	0.000	-2.368	-1.360	-1.583	90.000	0.529
5	-0.174	0.100	-3.677	-1.945	-1.945	48.189	1.000
6	-0.349	0.100	-3.243	-1.526	-1.732	87.788	0.937
7	-0.524	0.100	-2.717	-1.326	-1.550	88.079	0.746
8	-0.349	0.200	-3.467	-1.735	-1.735	48.189	1.000
9	-0.524	0.200	-3.149	-1.252	-1.535	85.850	1.023
10	-0.524	0.300	-3.270	-1.538	-1.538	48.189	1.000
11****	-0.349	0.145	-3.468	-1.491	-1.731	86.718	1.079
12****	-0.524	0.218	-3.239	-1.233	-1.534	85.430	1.082
13****	-1.500	0.625	-2.281	-0.107	-0.652	81.240	1.131
14	-1.500	0.000	-0.890	-0.543	-1.009	90.000	0.242
15	-1.500	0.858	-2.369	-0.637	-0.637	48.189	1.000

* For $\phi_p < \phi < \bar{\phi}$

** For $\bar{\phi} < \phi < \phi_S$

*** For $\phi_S < \phi \leq \pi$

**** At ϕ_S^+

$\Delta\tau = 1.223k$

TABLE XII

RESULTS FOR $\nu = 0.250$, $V/c_p = 1.5$, $p_o = 6.0k$

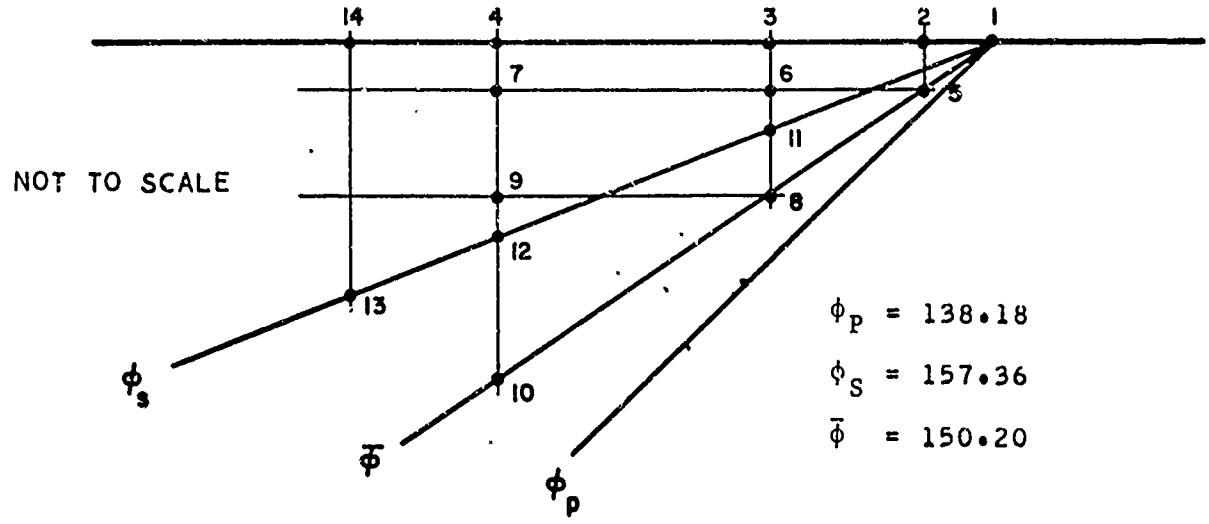

Pt.	$\mu\xi$	μy	σ_1/k	σ_2/k	σ_3/k	θ^o	n
1*	0.000	0.000	-2.598	-0.866	-0.866	48.189	1.000
1**	0.000	0.000	-5.900	-4.168	-4.168	48.189	1.000
1***	0.000	0.000	-6.000	-4.069	-4.168	90.000	1.087
2	-0.174	0.000	-5.038	-3.669	-3.828	90.000	0.748
3	-0.349	0.000	-4.230	-3.316	-3.538	90.000	0.476
4	-0.524	0.000	-3.552	-3.005	-3.290	90.000	0.273
5	-0.174	0.100	-5.565	-3.833	-3.833	48.189	1.000
6	-0.349	0.100	-4.867	-3.251	-3.513	86.467	0.867
7	-0.524	0.100	-4.077	-2.952	-3.241	86.432	0.584
8	-0.349	0.200	-5.251	-3.518	-3.518	48.189	1.000
9	-0.524	0.200	-4.731	-2.836	-3.218	83.742	1.002
10	-0.524	0.300	-4.955	-3.223	-3.223	48.189	1.000
11****	-0.349	0.145	-5.208	-3.198	-3.512	85.145	1.081
12****	-0.524	0.218	-4.868	-2.806	-3.217	83.299	1.091
13****	-1.200	0.500	-3.817	-1.542	-2.248	78.788	1.164
14	-1.200	0.000	-2.085	-1.806	-2.624	90.000	0.415

* For $\phi_P < \phi < \bar{\phi}$

** For $\bar{\phi} < \phi < \phi_S$

*** For $\phi_S < \phi \leq \pi$

**** At ϕ_S^+

$\Delta\tau = 1.223k$

TABLE XIII

RESULTS FOR $\nu = 0.250$, $V/c_p = 1.5$, $p_o = 10.0k$

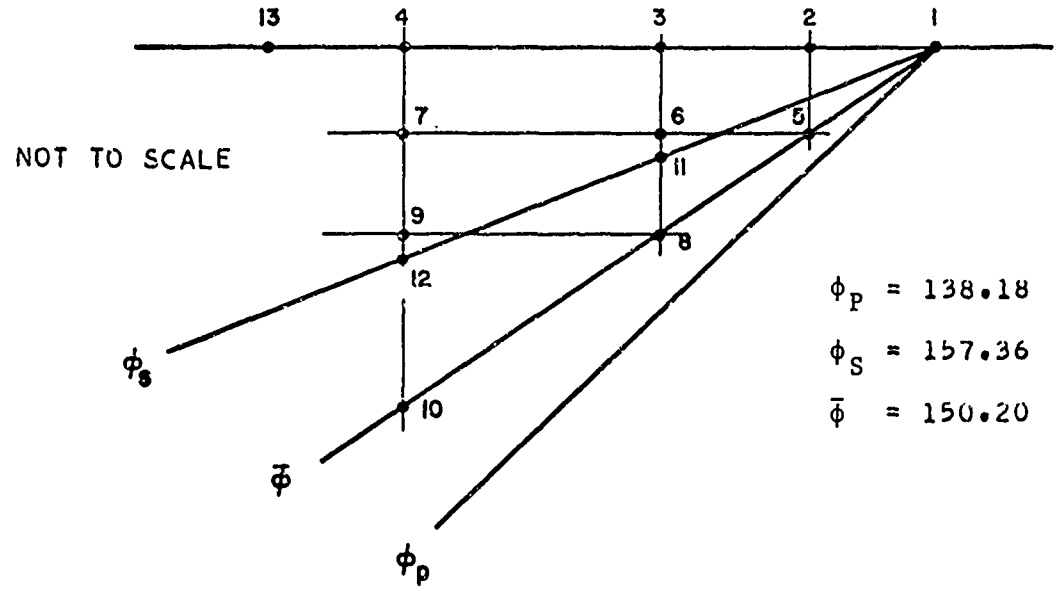

Pt.	$\mu\xi$	μy	σ_1/k	σ_2/k	σ_3/k	θ^o	n
1*	0.000	0.000	-2.598	-0.866	-0.866	48.189	1.000
1**	0.000	0.000	-9.900	-8.168	-8.168	48.189	1.000
1***	0.000	0.000	-10.000	-8.069	-8.168	90.000	1.087
2	-0.174	0.000	-8.397	-7.402	-7.601	90.000	0.526
3	-0.349	0.000	-7.051	-6.814	-7.117	90.000	0.159
4	-0.524	0.000	-6.295	-5.921	-6.705	90.000	0.392
5	-0.174	0.100	-9.342	-7.610	-7.610	48.189	1.000
6	-0.349	0.100	-8.122	-6.697	-7.077	83.278	0.737
7	-0.524	0.100	-6.811	-6.192	-6.623	78.957	0.317
8	-0.349	0.200	-8.817	-7.085	-7.085	48.189	1.000
9	-0.524	0.200	-7.910	-5.989	-6.584	79.569	0.983
10	-0.524	0.300	-8.325	-6.592	-6.592	48.189	1.000
11****	-0.349	0.145	-8.694	-6.602	-7.074	82.168	1.097
12****	-0.524	0.218	-8.142	-5.936	-6.583	79.413	1.134
13	-1.060	0.000	-5.029	-3.463	-5.774	90.000	1.179

* For $\phi_p < \phi < \bar{\phi}$

** For $\bar{\phi} < \phi < \phi_S$

*** For $\phi_S < \phi \leq \pi$

**** At ϕ_S^+

$\Delta\tau = 1.223k$

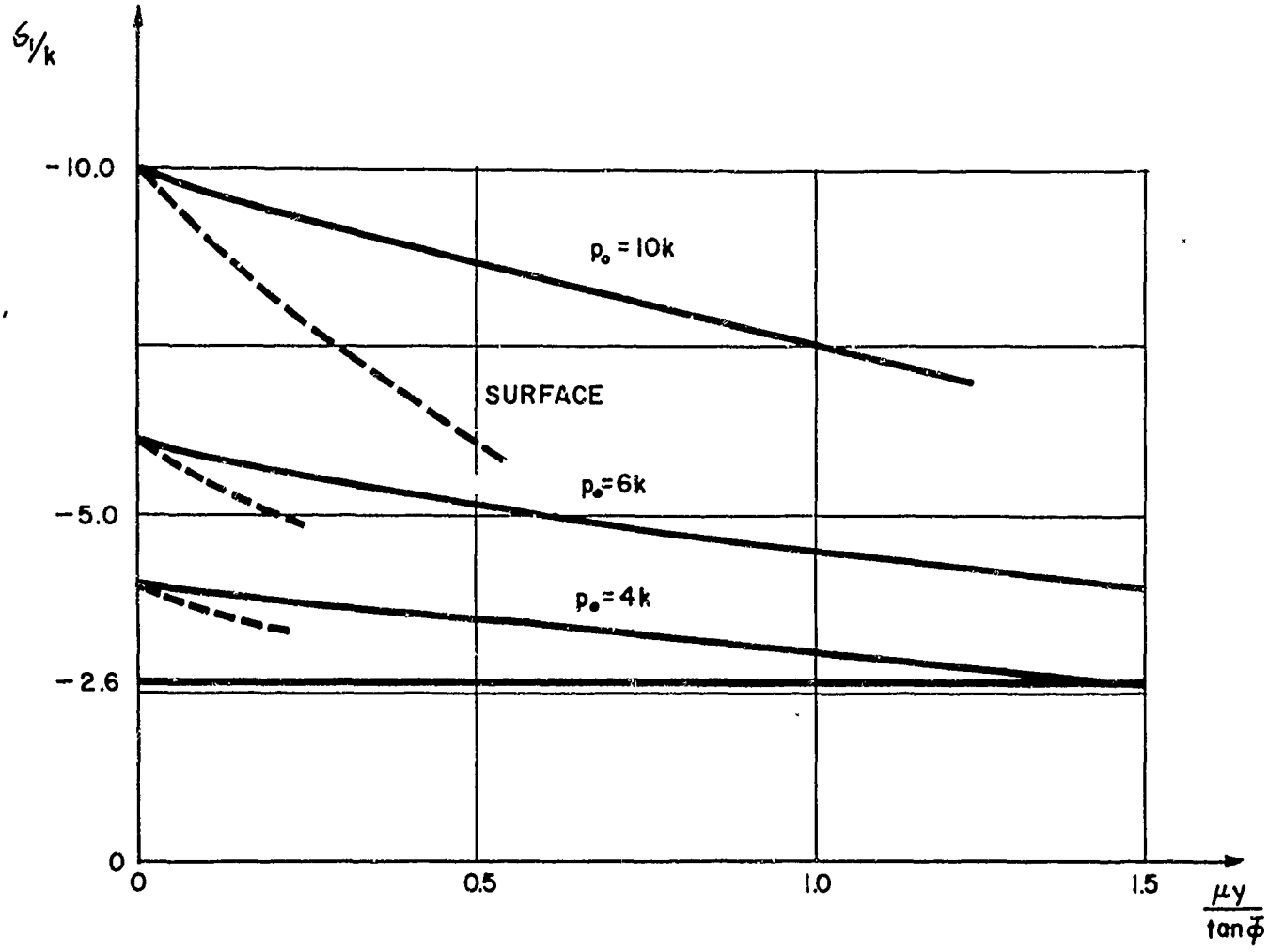

PRINCIPAL STRESS σ_1/k AT $\bar{\phi}$
FOR $\nu = 0.25$ $V/C_p = 2.0$
FIG. 14

TABLE XIV

RESULTS FOR $\nu = 0.250$, $V/c_p = 2.0$, $p_o = 4.0k$

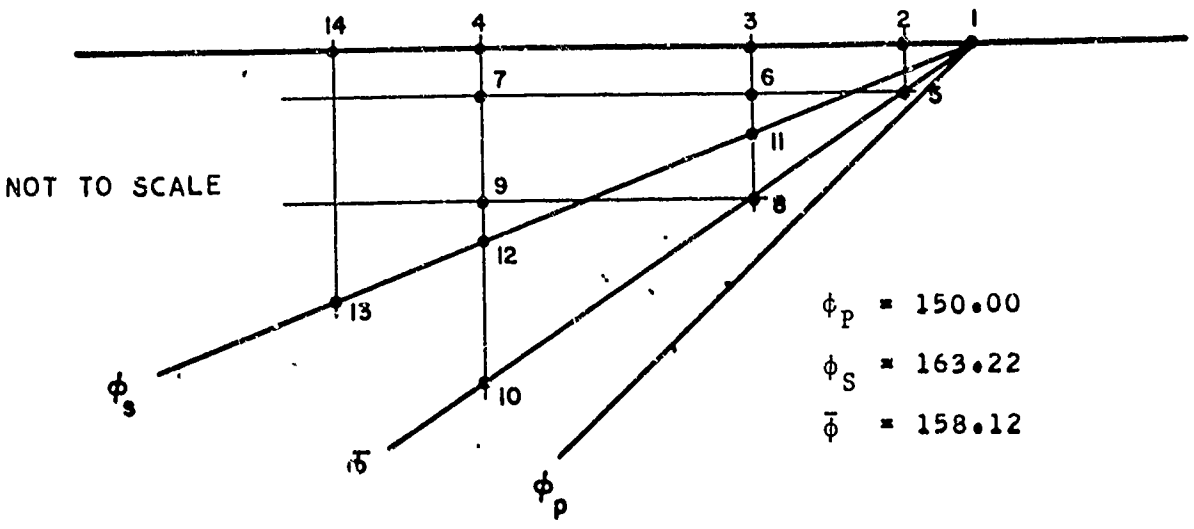

Pt.	$\mu\xi$	μy	σ_1/k	σ_2/k	σ_3/k	θ^o	n
1*	0.000	0.000	-2.598	-0.866	-0.866	60.000	1.000
1**	0.000	0.000	-3.936	2.203	-2.203	60.000	1.000
1***	0.000	0.000	-4.000	-2.139	-2.203	90.000	1.056
2	-0.996	0.000	-1.477	-1.026	-1.294	90.000	0.227
3	-1.245	0.000	-1.151	-0.847	-1.168	90.000	0.181
4	-1.494	0.000	-0.896	-0.693	-1.066	90.000	0.187
5	-0.996	0.400	-2.960	-1.228	-1.228	60.000	1.000
6	-1.245	0.400	-2.502	-0.769	-0.999	54.610	0.941
7	-1.494	0.400	-1.871	-0.674	-0.817	89.640	0.654
8	-1.245	0.500	-2.758	-1.026	-1.026	60.000	1.000
9	-1.494	0.500	-2.334	-0.603	-0.814	55.000	0.944
10	-1.494	0.600	-2.572	-0.840	-0.840	60.000	1.000
11****	-1.245	0.375	-2.329	-0.831	-0.997	87.040	0.821
12****	-1.494	0.450	-2.093	-0.640	-0.812	86.950	0.794
13****	-1.700	0.513	-1.916	-0.496	-0.671	86.990	0.774
14	-1.700	0.000	-0.725	-0.579	-0.995	90.000	0.211

* For $\phi_p < \phi < \bar{\phi}$

** For $\bar{\phi} < \phi < \phi_S$

*** For $\phi_S < \phi \leq \pi$

**** At ϕ_S^+

$\Delta\tau = 0.900k$

TABLE XV

RESULTS FOR $\nu = 0.250$, $V/c_p = 2.0$, $p_o = 6.0k$

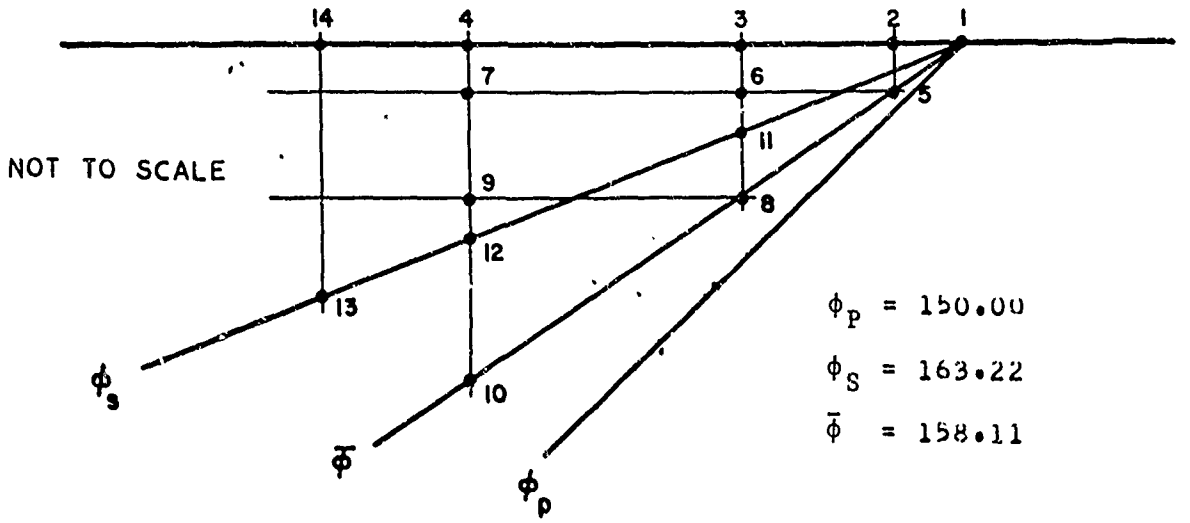

Pt.	$\mu\xi$	μy	σ_1/k	σ_2/k	σ_3/k	θ^o	n
1*	0.000	0.000	-2.598	-0.866	-0.866	60.000	1.000
1**	0.000	0.000	-5.935	-4.203	-4.203	60.000	1.000
1***	0.000	0.000	-6.000	-4.139	-4.203	90.000	1.056
2	-0.996	0.000	-2.469	-2.216	-2.840	90.000	0.313
3	-1.245	0.000	-2.201	-1.726	-2.650	90.000	0.462
4	-1.494	0.000	-1.969	-1.343	-2.497	90.000	0.577
5	-0.996	0.400	-4.471	-2.739	-2.739	60.000	1.000
6	-1.245	0.400	-3.796	-2.040	-2.396	51.966	0.928
7	-1.494	0.400	-2.806	-1.941	-2.123	89.261	0.456
8	-1.245	0.500	-4.169	-2.437	-2.437	59.996	1.000
9	-1.494	0.500	-3.542	-1.792	-2.119	52.540	0.930
10	-1.494	0.600	-3.890	-2.158	-2.158	59.996	1.000
11****	-1.245	0.375	-3.497	-2.172	-2.393	84.958	0.709
12****	-1.494	0.450	-3.143	-1.886	-2.116	84.693	0.669
13****	-1.700	0.512	-2.878	-1.670	-1.905	84.666	0.640
14	-1.700	0.000	-1.799	-1.087	-2.390	90.000	0.652

* For $\phi_P < \phi < \bar{\phi}$

** For $\bar{\phi} < \phi < \phi_S$

*** For $\phi_S < \phi \leq \pi$

**** At ϕ_S^+

$\Delta\tau = 0.900k$

TABLE XVI

RESULTS FOR $\nu = 0.250$, $V/c_p = 2.0$, $p_o = 10.0k$

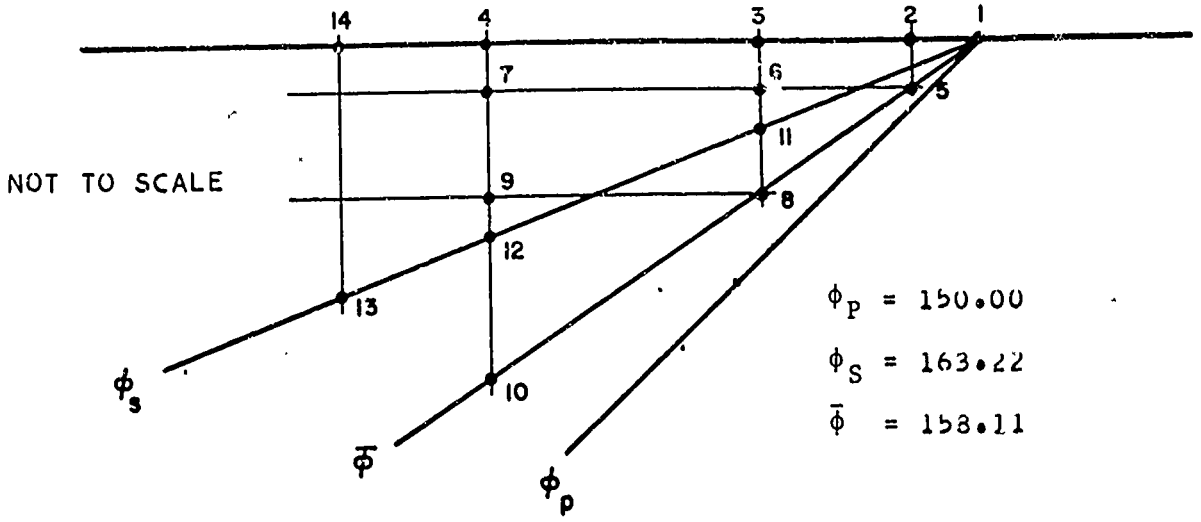

Pt.	$\mu\xi$	μy	σ_1/k	σ_2/k	σ_3/k	θ^o	n
1*	0.000	0.000	-2.598	-0.866	-0.866	60.000	1.000
1**	0.000	0.000	-9.935	-8.203	-8.203	60.000	1.000
1***	0.000	0.000	-10.000	-8.139	-8.203	90.000	1.056
2	-0.249	0.000	-7.795	-7.241	-7.428	90.000	0.281
3	-0.498	0.000	-6.499	-6.076	-6.812	90.000	0.369
4	-0.747	0.000	-5.879	-4.737	-6.322	90.000	0.817
5	-0.249	0.100	-9.254	-7.522	-7.522	60.000	1.000
6	-0.498	0.100	-7.301	-6.599	-6.803	86.970	0.361
7	-0.747	0.100	-5.959	-5.661	-6.233	84.499	0.286
8	-0.498	0.200	-8.622	-6.890	-6.890	59.992	1.000
9	-0.747	0.200	-6.869	-5.979	-6.224	83.656	0.459
10	-0.747	0.300	-8.037	-6.305	-6.305	59.993	1.000
11****	-0.498	0.150	-8.048	-6.622	-6.834	84.925	0.769
12****	-0.747	0.225	-7.231	-5.967	-6.236	82.589	0.666
13****	-1.000	0.301	-6.491	-5.365	-5.680	80.473	0.580
14	-1.000	0.000	-5.347	-3.678	-5.925	90.000	1.166

* For $\phi_P < \phi < \bar{\phi}$

** For $\bar{\phi} < \phi < \phi_S$

*** For $\phi_S < \phi \leq \pi$

**** At ϕ_S^+

$\Delta\tau = 0.900k$

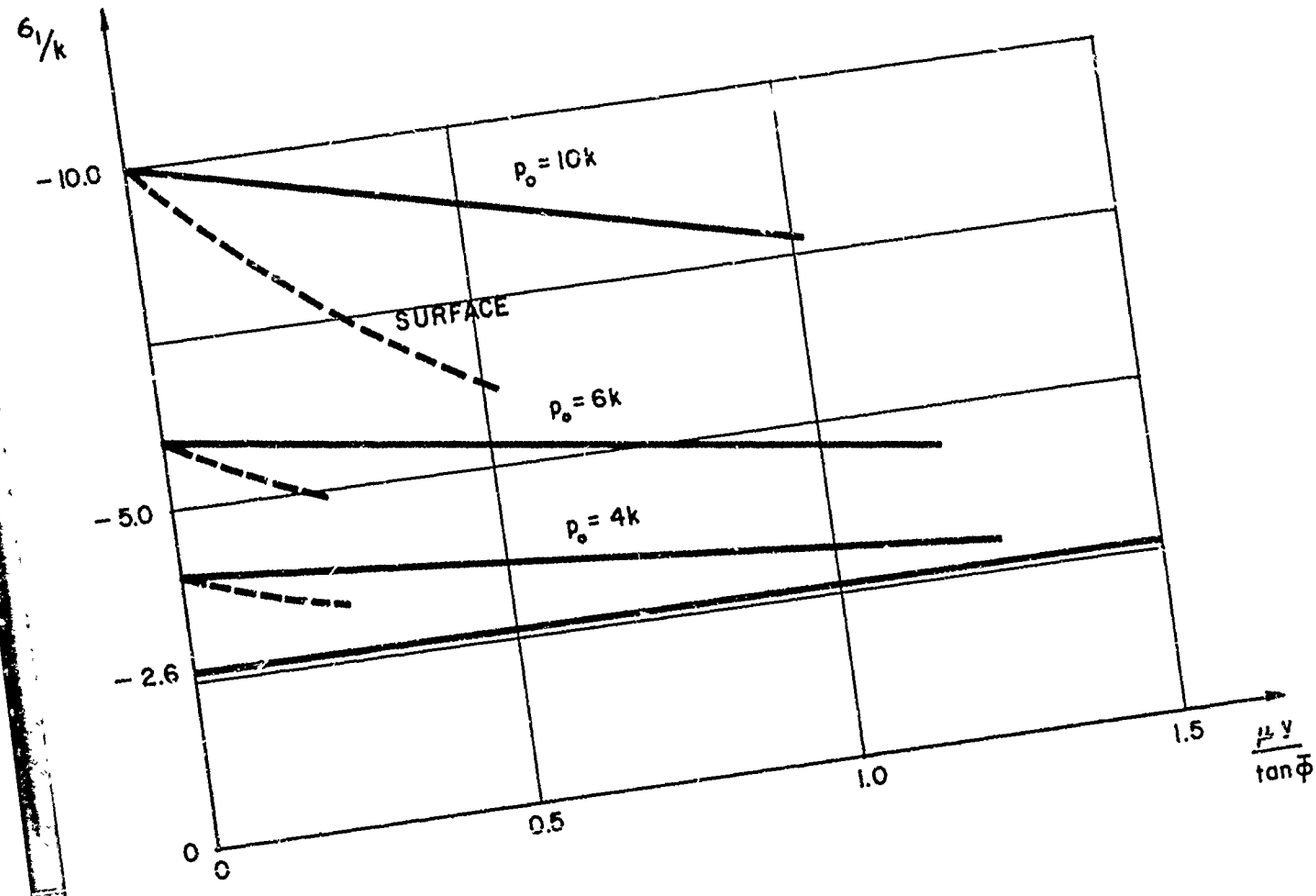

PRINCIPAL STRESS σ_1/k AT $\bar{\Phi}$
FOR $\nu = 0.25$ $V/C_p = 4.0$

FIG. 15

TABLE XVII

RESULTS FOR $\nu = 0.250$, $V/c_p = 4.0$, $p_o = 4.0k$

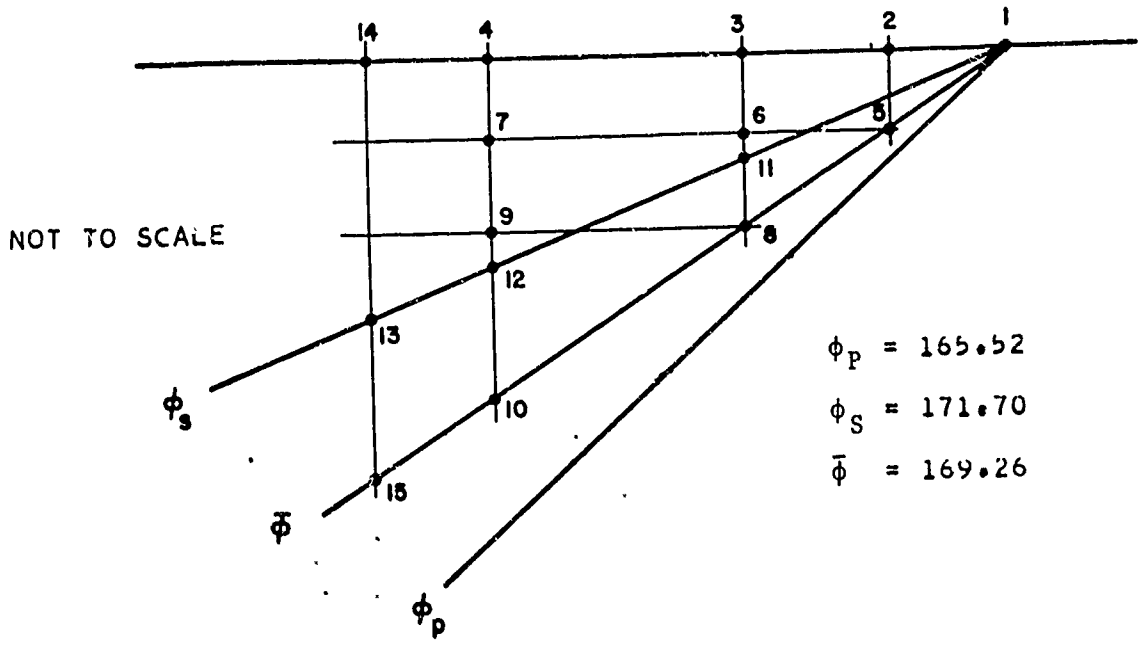

Pt.	$\mu\xi$	μy	σ_1/k	σ_2/k	σ_3/k	θ°	n
1*	0.000	0.000	-2.598	-0.866	-0.866	75.522	1.000
1**	0.000	0.000	-3.983	-2.251	-2.251	75.522	1.000
1***	0.000	0.000	-4.000	-2.234	-2.251	90.000	1.014
2	-0.527	0.000	-2.360	-1.546	-1.669	90.000	0.439
3	-1.054	0.000	-1.393	-1.085	-1.312	90.000	0.159
4	-1.581	0.000	-0.819	-0.761	-1.087	90.000	0.174
5	-0.527	0.100	-3.485	-1.753	-1.753	75.522	1.000
6	-1.054	0.100	-2.112	-1.105	-1.248	111.589	0.545
7	-1.581	0.100	-1.379	-0.599	-0.938	124.339	0.390
8	-1.054	0.200	-3.053	-1.322	-1.322	75.524	0.999
9	-1.581	0.200	-2.027	-0.594	-0.883	121.034	0.757
10	-1.581	0.300	-2.678	-0.946	-0.946	75.524	0.999
11****	-1.054	0.153	-2.604	-1.174	-1.268	110.672	0.799
12****	-1.581	0.230	-2.244	-0.640	-0.888	119.195	0.863
13****	-1.750	0.255	-2.159	-0.476	-0.780	121.233	0.897
14	-1.750	0.000	-0.687	-0.676	-1.033	90.002	0.203
15	-1.750	0.331	-2.569	-0.838	-0.838	75.524	0.999

* For $\phi_P < \phi < \bar{\phi}$

** For $\bar{\phi} < \phi < \phi_S$

*** For $\phi_S < \phi \leq \pi$

**** At ϕ_S^+

$\Delta\tau = 0.043k$

TABLE XVIII

RESULTS FOR $\nu = 0.250$, $V/c_p = 4.0$, $p_o = 6.0k$

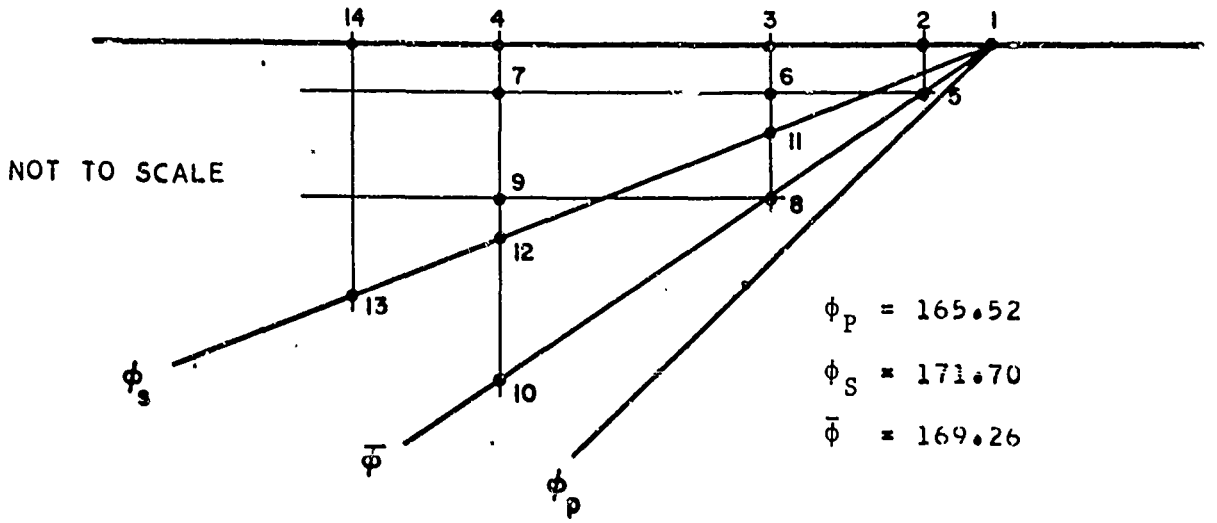

Pt.	$\mu\xi$	μy	σ_1/k	σ_2/k	σ_3/k	θ°	p
1*	0.000	0.000	-2.598	-0.866	-0.866	75.522	1.000
1**	0.000	0.000	-5.983	-4.251	-4.251	75.522	1.000
1***	0.000	0.000	-6.000	-4.234	-4.251	90.000	1.014
2	-0.527	0.000	-3.541	-3.201	-3.378	90.000	0.169
3	-1.054	0.000	-2.510	-2.089	-2.842	89.999	0.377
4	-1.581	0.000	-2.024	-1.225	-2.506	90.000	0.645
5	-0.527	0.100	-5.237	-3.505	-3.505	75.522	1.000
6	-1.054	0.100	-3.383	-2.326	-2.747	129.020	0.532
7	-1.581	0.100	-2.516	-1.334	-2.282	56.390	0.625
8	-1.054	0.200	-4.588	-2.857	-2.857	75.526	0.999
9	-1.581	0.200	-3.358	-1.455	-2.199	133.128	0.959
10	-1.581	0.300	-4.026	-2.294	-2.294	75.525	0.999
11****	-1.054	0.153	-4.071	-2.479	-2.777	121.415	0.846
12****	-1.581	0.230	-3.646	-1.563	-2.207	129.772	1.066
13****	-1.700	0.248	-3.575	-1.369	-2.092	130.937	1.124
14	-1.700	0.000	-1.934	-1.087	-2.448	90.000	0.687

* For $\phi_p < \phi < \bar{\phi}$

** For $\bar{\phi} < \phi < \phi_S$

*** For $\phi_S < \phi \leq \pi$

**** At ϕ_S^+

$\Delta\tau = 0.043k$

TABLE XIX

RESULTS FOR $\nu = 0.250$, $V/c_p = 4.0$, $P_o = 10.0k$

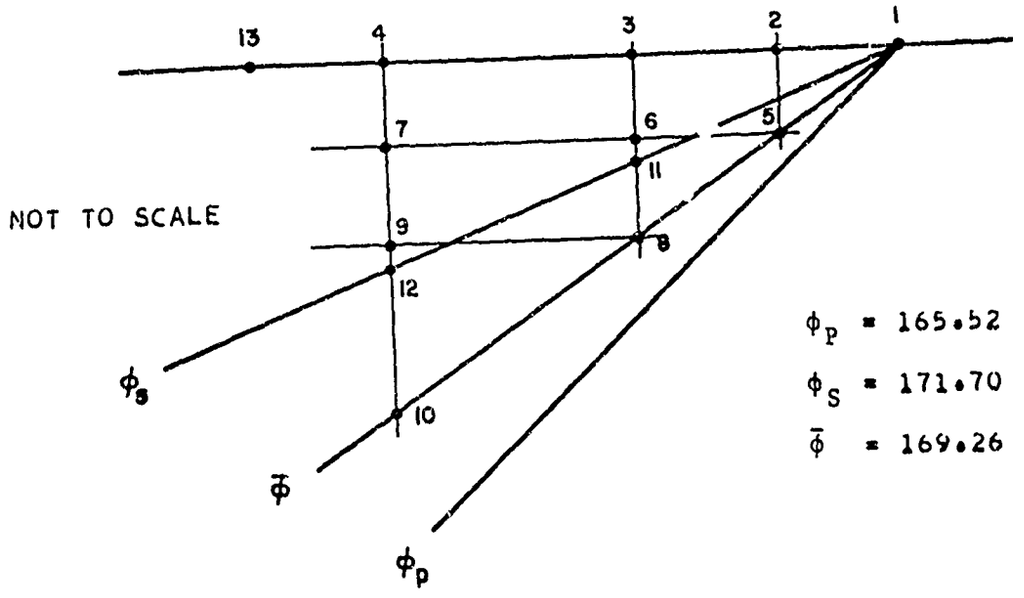

Pt.	$\mu\xi$	μy	σ_1/k	σ_2/k	σ_3/k	θ^o	n
1*	0.000	0.000	-2.598	-0.866	-0.866	75.522	1.000
1**	0.000	0.000	-9.983	-8.251	-8.251	75.522	1.000
1***	0.000	0.000	-10.000	-8.234	-8.251	90.000	1.014
2	-0.263	0.000	-7.682	-7.283	-7.434	90.000	0.201
3	-0.527	0.000	-6.513	-5.901	-6.796	89.999	0.457
4	-0.791	0.000	-5.883	-4.533	-6.296	90.000	0.921
5	-0.263	0.050	-9.339	-7.607	-7.607	75.522	1.000
6	-0.527	0.050	-7.392	-6.508	-6.846	127.183	0.445
7	-0.791	0.050	-6.336	-5.187	-6.251	64.304	0.640
8	-0.527	0.100	-8.738	-7.007	-7.007	75.529	0.999
9	-0.791	0.100	-7.268	-5.640	-6.298	133.341	0.818
10	-0.791	0.150	-8.179	-6.448	-6.448	75.528	0.999
11****	-0.527	0.076	-8.149	-6.695	-6.918	118.565	0.783
12****	-0.791	0.115	-7.620	-5.777	-6.332	128.929	0.945
13	-0.930	0.000	-5.596	-3.945	-6.077	90.000	1.118

* For $\phi_p < \phi < \bar{\phi}$

** For $\bar{\phi} < \phi < \phi_S$

*** For $\phi_S < \phi \leq \pi$

**** At ϕ_S^+

$\Delta\tau = 0.043k$

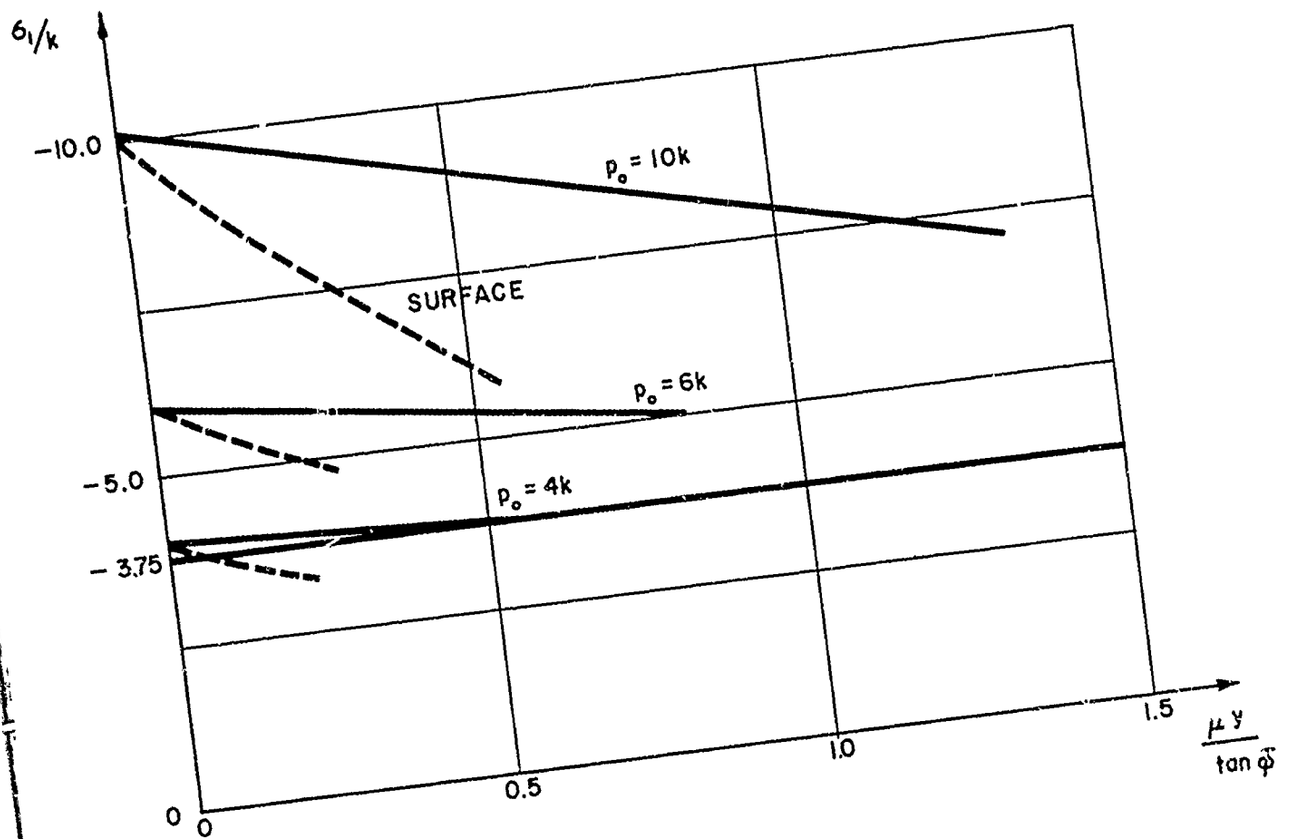

PRINCIPAL STRESS σ_1/k AT $\bar{\phi}$
FOR $\nu = 0.35$ $V/c_p = 1.5$

FIG. 16

TABLE XX

RESULTS FOR $\nu = 0.350$, $V/c_p = 1.5$, $p_o = 4.0k$

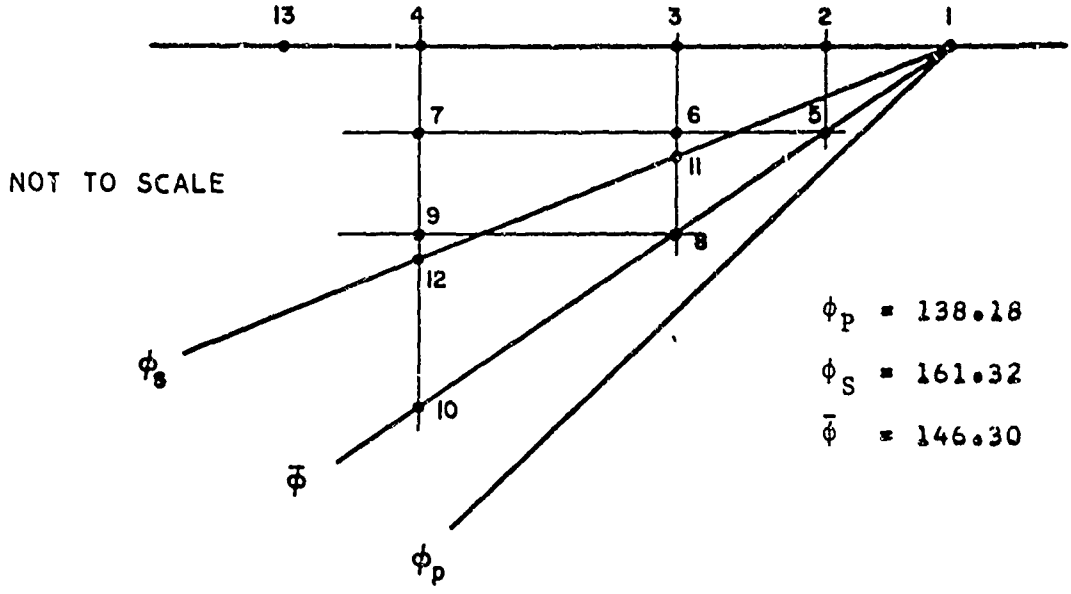

Pt.	$\mu\xi$	μy	σ_1/k	σ_2/k	σ_3/k	θ^o	n
1*	0.000	0.000	-3.752	-2.020	-2.020	48.189	1.000
1**	0.000	0.000	-4.112	-2.380	-2.380	48.189	1.000
1***	0.000	0.000	-4.000	-2.493	-2.380	90.000	0.904
2	-0.150	0.000	-3.442	-2.139	-2.061	90.000	0.775
3	-0.300	0.000	-2.963	-1.830	-1.785	90.000	0.667
4	-0.450	0.000	-2.650	-1.562	-1.547	90.000	0.574
5	-0.150	0.100	-3.960	-2.227	-2.227	48.189	1.000
6	-0.300	0.100	-3.411	-1.899	-1.920	85.469	0.866
7	-0.450	0.100	-2.933	-1.621	-1.655	85.712	0.746
8	-0.300	0.200	-3.812	-2.080	-2.080	48.189	1.000
9	-0.450	0.200	-3.508	-1.541	-1.785	47.700	1.072
10	-0.450	0.300	-3.671	-1.939	-1.939	48.189	1.000
11****	-0.300	0.101	-3.418	-1.900	-1.923	85.407	0.870
12****	-0.450	0.152	-3.170	-1.634	-1.720	83.528	0.862
13	-1.600	0.000	-0.803	-0.349	-0.511	90.000	0.230

* For $\phi_P < \phi < \bar{\phi}$

** For $\bar{\phi} < \phi < \phi_S$

*** For $\phi_S < \phi \leq \pi$

**** At ϕ_S^+

$\Delta\tau = 1.082k$

TABLE XXI

RESULTS FOR $\nu = 0.350$, $V/c_p = 1.5$, $p_o = 6.0k$

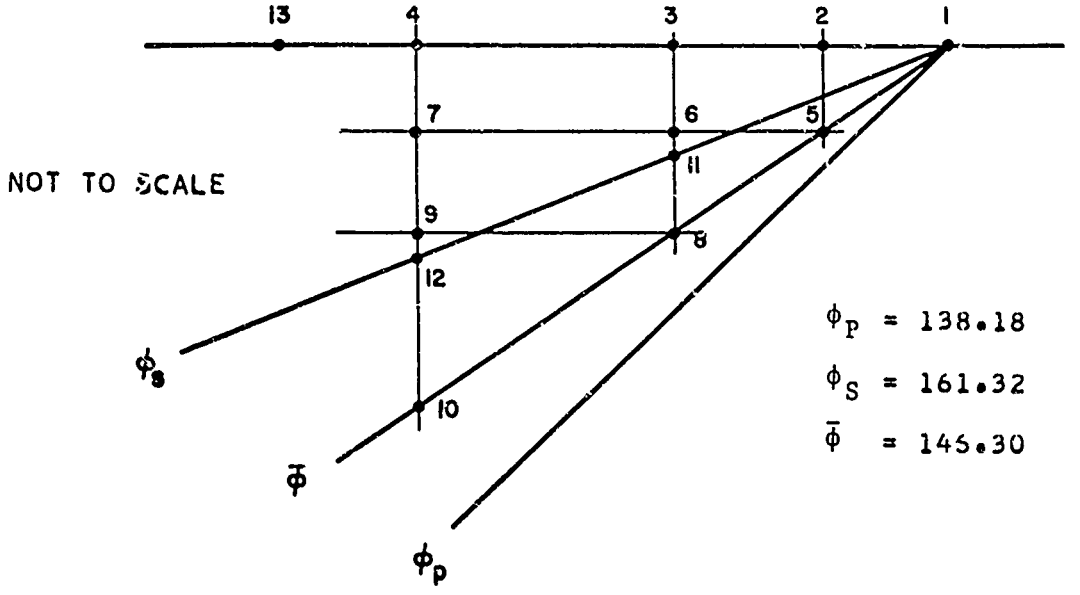

Pt.	$\mu\xi$	μy	σ_1/k	σ_2/k	σ_3/k	θ^o	n
1*	0.000	0.000	-3.752	-2.020	-2.020	48.189	1.000
1**	0.000	0.000	-6.112	-4.380	-4.380	48.189	1.000
1***	0.000	0.000	-6.000	-4.493	-4.380	90.000	0.904
2	-0.150	0.000	-5.164	-3.962	-3.902	90.000	0.711
3	-0.300	0.000	-4.444	-3.499	-3.488	90.000	0.548
4	-0.450	0.000	-3.825	-3.096	-3.130	90.000	0.411
5	-0.150	0.100	-5.883	-4.151	-4.151	48.189	1.000
6	-0.300	0.100	-5.123	-3.595	-3.690	83.244	0.856
7	-0.450	0.100	-4.403	-3.178	-3.293	83.082	0.676
8	-0.300	0.200	-5.662	-3.930	-3.930	48.189	1.000
9	-0.450	0.200	-5.206	-3.122	-3.487	47.497	1.112
10	-0.450	0.300	-5.450	-3.718	-3.718	48.189	1.000
11****	-0.300	0.101	-5.134	-3.596	-3.694	83.165	0.861
12****	-0.450	0.152	-4.769	-3.190	-3.390	80.461	0.859
13	-1.500	0.000	-1.376	-1.335	-1.657	90.000	0.175

* For $\phi_p < \phi < \bar{\phi}$

** For $\bar{\phi} < \phi < \phi_S$

*** For $\phi_S < \phi \leq \pi$

**** At ϕ_S^+

$\Delta\tau = 1.082k$

TABLE XXII

RESULTS FOR $\nu = 0.350$, $V/c_p = 1.5$, $p_o = 10.0k$

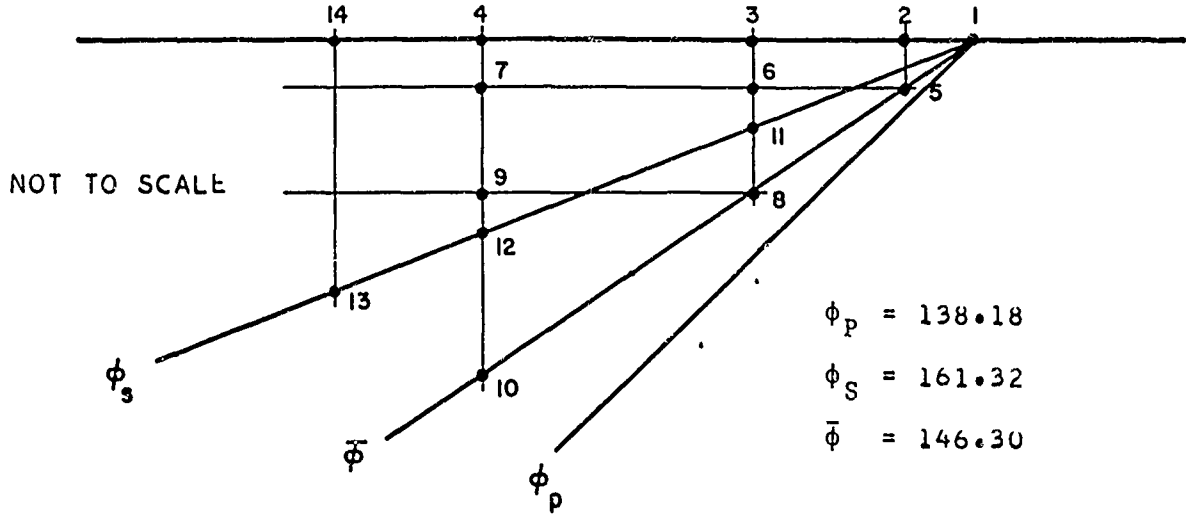

Pt.	$\mu\xi$	μy	σ_1/k	σ_2/k	σ_3/k	θ°	n
1*	0.000	0.000	-3.752	-2.020	-2.020	48.189	1.000
1**	0.000	0.000	-10.112	-8.380	-8.380	48.189	1.000
1***	0.000	0.000	-10.000	-8.493	-8.380	90.000	0.904
2	-0.075	0.000	-9.277	-8.035	-7.967	90.000	0.737
3	-0.150	0.000	-8.606	-7.607	-7.582	90.000	0.583
4	-0.225	0.000	-7.984	-7.208	-7.225	90.000	0.443
5	-0.075	0.050	-9.920	-8.187	-8.187	48.189	1.000
6	-0.150	0.050	-9.234	-7.713	-7.782	84.016	0.858
7	-0.225	0.050	-8.565	-7.305	-7.405	83.435	0.700
8	-0.150	0.100	-9.730	-7.997	-7.997	48.188	1.000
9	-0.225	0.100	-9.320	-7.271	-7.600	47.540	1.100
10	-0.225	0.150	-9.544	-7.812	-7.812	48.188	1.000
11****	-0.150	0.050	-9.243	-7.715	-7.785	83.952	0.863
12****	-0.225	0.076	-8.902	-7.339	-7.505	81.298	0.858
13****	-0.300	0.101	-8.580	-6.974	-7.236	78.918	0.851
14	-0.300	0.000	-7.407	-6.836	-6.893	90.000	0.314

* For $\phi_p < \phi < \bar{\phi}$

** For $\bar{\phi} < \phi < \phi_S$

*** For $\phi_S < \phi \leq \pi$

**** At ϕ_S^+

$\Delta\tau = 1.082k$

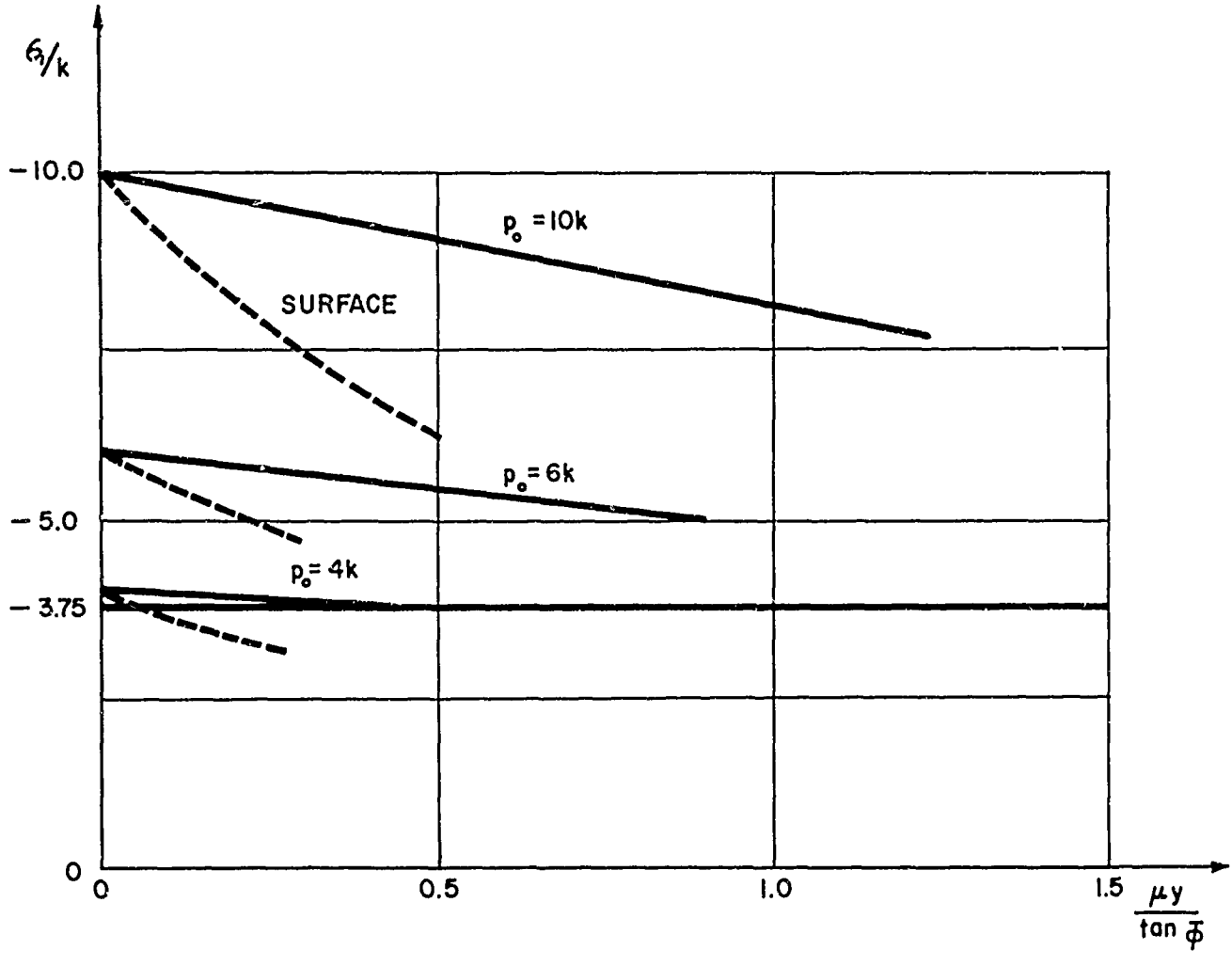

PRINCIPAL STRESS σ_1/k AT $\bar{\Phi}$
FOR $\nu = 0.35$ $V/C_p = 2.0$
FIG. 17

TABLE XXIII

RESULTS FOR $\nu = 0.350$, $V/c_p = 2.0$, $p_o = 4.0k$

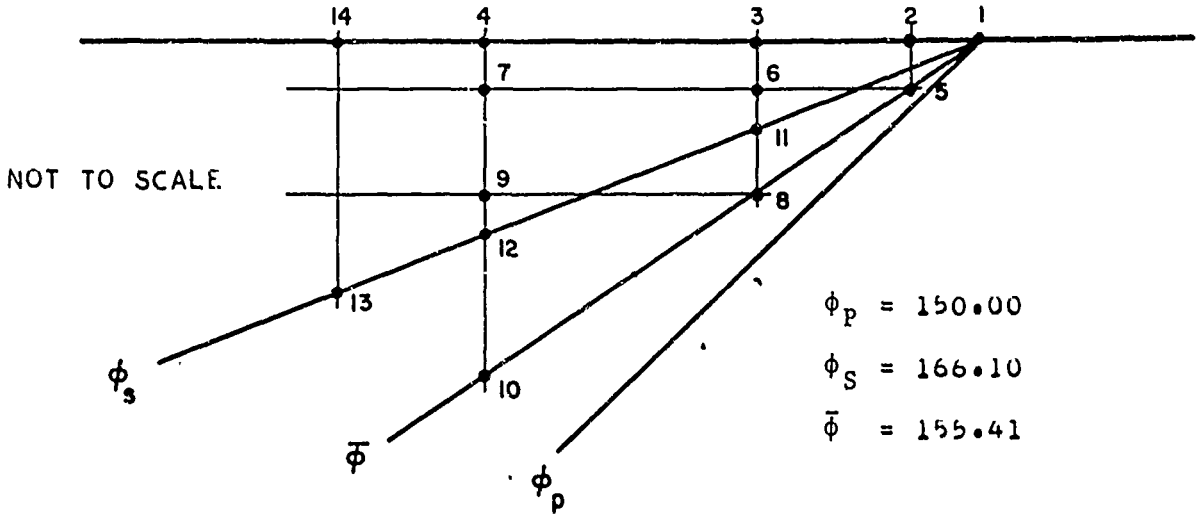

Pt.	$\mu\xi$	μy	σ_1/k	σ_2/k	σ_3/k	θ°	n
1*	0.000	0.000	-3.752	-2.020	-2.020	60.000	1.000
1**	0.000	0.000	-4.037	-2.305	-2.305	60.000	1.000
1***	0.000	0.000	-4.000	-2.343	-2.305	90.000	0.967
2	-0.109	0.000	-3.585	-2.096	-2.074	90.000	0.866
3	-0.218	0.000	-3.214	-1.874	-1.866	90.000	0.776
4	-0.299	0.000	-2.964	-1.723	-1.726	90.000	0.715
5	-0.109	0.050	-3.944	-2.212	-2.212	60.000	1.000
6	-0.218	0.050	-3.530	-1.980	-1.986	88.108	0.893
7	-0.299	0.050	-3.254	-1.820	-1.833	88.213	0.823
8	-0.218	0.100	-3.852	-2.120	-2.120	89.997	1.000
9	-0.299	0.100	-3.638	-1.861	-1.954	88.253	1.000
10	-0.299	0.137	-3.786	-2.054	-2.054	89.997	1.000
11****	-0.218	0.054	-3.557	-1.988	-1.996	87.938	0.903
12****	-0.299	0.074	-3.408	-1.866	-1.890	87.218	0.883
13****	-1.500	0.371	-1.836	-0.522	-0.717	79.975	0.708
14	-1.500	0.000	-0.890	-0.401	-0.537	90.000	0.252

* For $\phi_p < \phi < \bar{\phi}$

** For $\bar{\phi} < \phi < \phi_S$

*** For $\phi_S < \phi \leq \pi$

**** At ϕ_S^+

$\Delta\tau = 0.847\,k$

TABLE XXIV

RESULTS FOR $\nu = 0.350$, $V/c_p = 2.0$, $p_o = 6.0k$

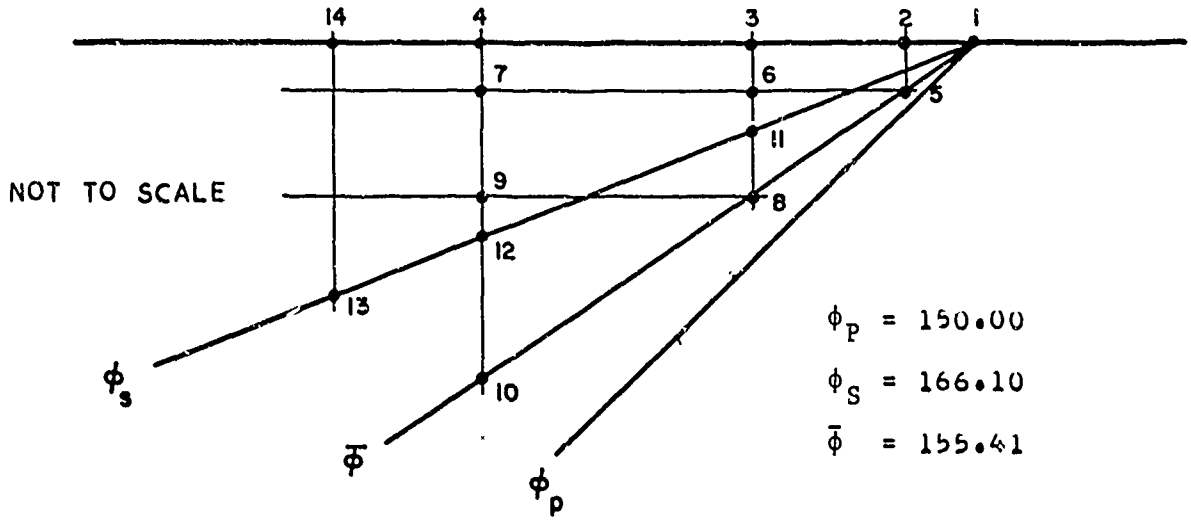

Pt.	$\mu\xi$	μy	σ_1/k	σ_2/k	σ_3/k	θ^o	n
1*	0.000	0.000	-3.752	-2.020	-2.020	60.000	1.000
1**	0.000	0.000	-6.037	-4.305	-4.305	60.000	1.000
1***	0.000	0.000	-6.000	-4.343	-4.305	90.000	0.967
2	-0.437	0.000	-3.875	-3.065	-3.114	90.000	0.453
3	-0.765	0.000	-2.791	-2.392	-2.500	90.000	0.206
4	-1.311	0.000	-1.624	-1.615	-1.819	89.999	0.115
5	-0.437	0.200	-5.495	-3.763	-3.763	60.000	1.000
6	-0.765	0.200	-4.408	-2.404	-2.907	52.029	1.042
7	-1.311	0.200	-2.321	-1.804	-1.966	81.448	0.264
8	-0.765	0.350	-5.120	-3.388	-3.388	59.996	1.000
9	-1.311	0.350	-3.592	-1.470	-2.182	49.447	1.080
10	-1.311	0.600	-4.550	-2.818	-2.818	59.997	1.000
11****	-0.765	0.189	-4.023	-2.685	-2.879	79.699	0.723
12****	-1.311	0.324	-3.065	-1.818	-2.138	74.556	0.647
13****	-1.550	0.383	-2.728	-1.508	-1.869	72.975	0.626
14	-1.550	0.000	-1.383	-1.269	-1.614	90.000	0.175

* For $\phi_p < \phi < \bar{\phi}$

** For $\bar{\phi} < \phi < \phi_S$

*** For $\phi_S < \phi \leq \pi$

**** At ϕ_S^+

$\Delta\tau = 0.847\ k$

TABLE XXV

RESULTS FOR $\nu = 0.350$, $V/c_p = 2.0$, $p_o = 10.0k$

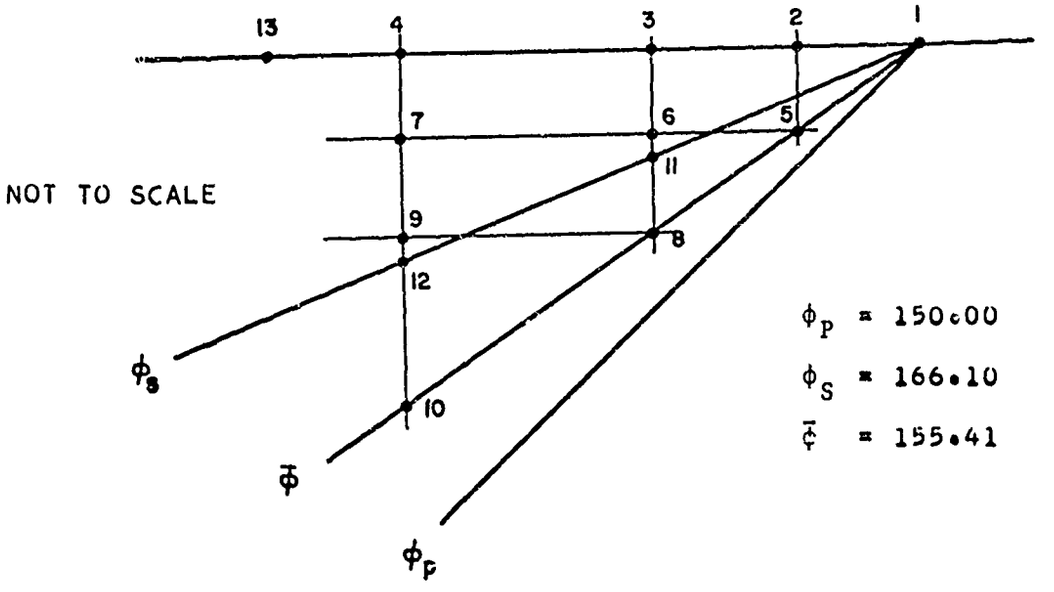

Pt.	$\mu\xi$	μy	σ_1/k	σ_2/k	σ_3/k	θ^o	n
1*	0.000	0.000	-3.752	-2.020	-2.020	60.000	1.000
1**	0.000	0.000	-10.037	-8.305	-8.305	60.000	1.000
1***	0.000	0.000	-10.000	-8.343	-8.305	90.000	0.967
2	-0.218	0.000	-8.036	-7.171	-7.208	90.000	0.489
3	-0.437	0.000	-6.458	-6.213	-6.320	90.000	0.122
4	-0.655	0.000	-5.430	-5.190	-5.602	90.000	0.207
5	-0.218	0.100	-9.575	-7.843	-7.843	60.000	1.000
6	-0.437	0.100	-7.826	-6.597	-6.795	79.099	0.660
7	-0.655	0.100	-6.281	-5.722	-5.948	73.468	0.281
8	-0.437	0.200	-9.133	-7.401	-7.401	59.994	1.000
9	-0.655	0.200	-7.875	-5.800	-6.400	50.897	1.067
10	-0.655	0.300	-8.712	-6.980	-6.980	59.994	1.000
11****	-0.437	0.108	-7.957	-6.624	-6.839	78.643	0.715
12****	-0.655	0.162	-7.139	-5.867	-6.216	73.189	0.657
13	-1.500	0.000	-3.489	-2.225	-3.885	90.000	0.866

* For $\phi_p < \phi < \bar{\phi}$

** For $\bar{\phi} < \phi < \phi_S$

*** For $\phi_S < \phi \leq \pi$

**** At ϕ_S^+

$\Delta\tau = 0.847k$

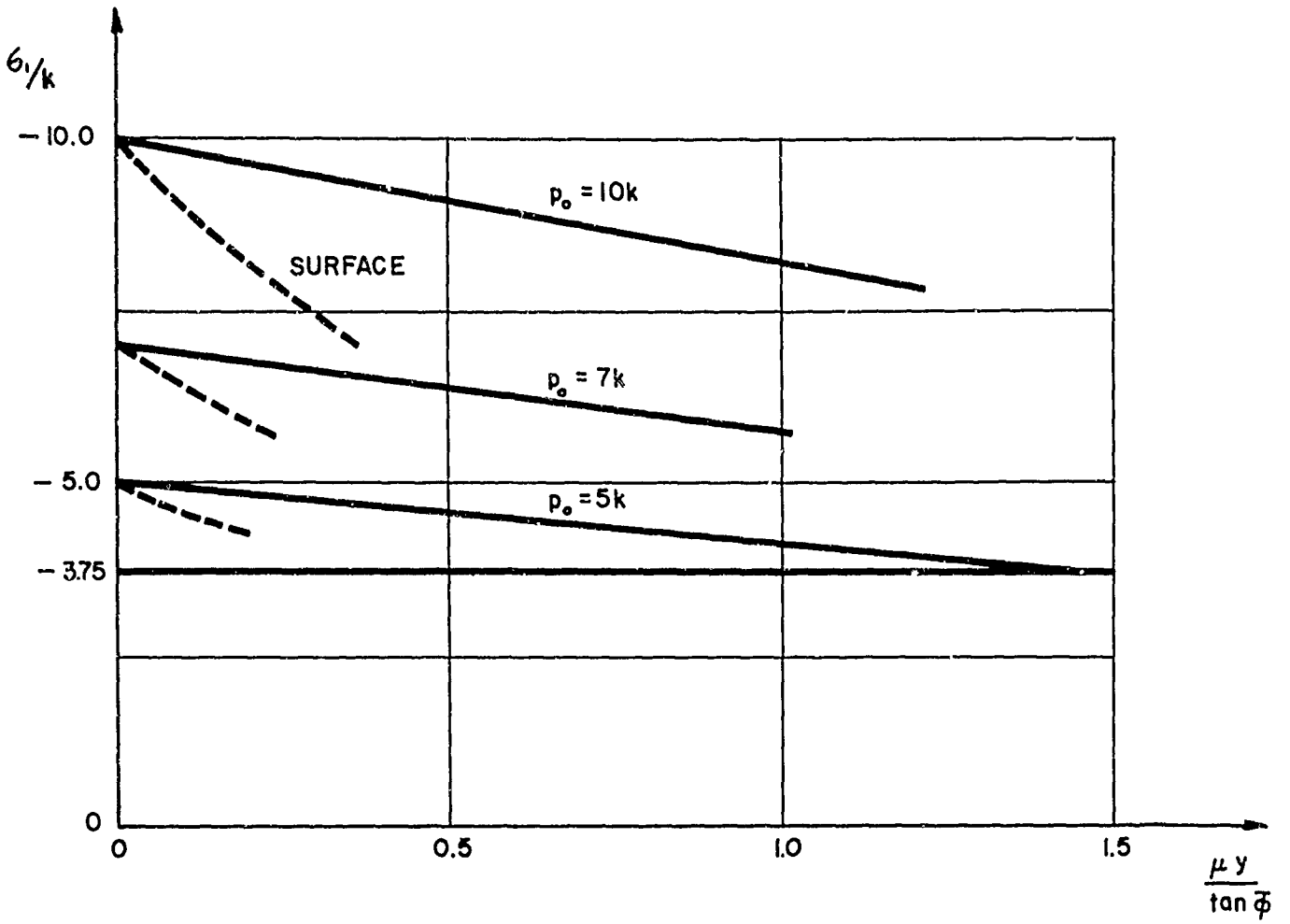

PRINCIPAL STRESS σ_1/k AT $\bar{\Phi}$
FOR $V = 0.35$ $V/C_p = 4.0$

FIG. 18

TABLE XXVI

RESULTS FOR $\nu = 0.350$, $V/c_p = 4.0$, $p_o = 5.0k$

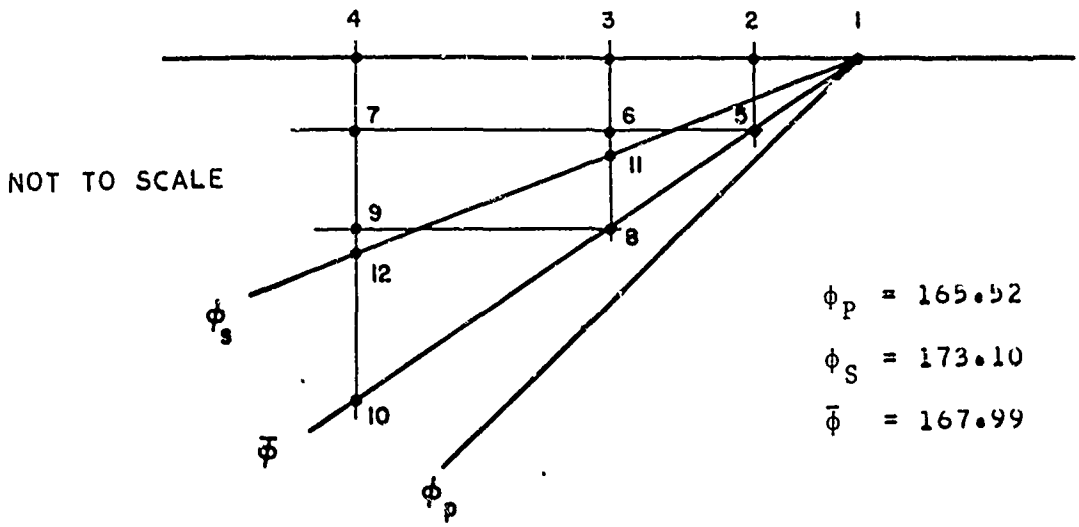

Pt.	$\mu\xi$	μy	σ_1/k	σ_2/k	σ_3/k	θ°	n
1*	0.000	0.000	-3.752	-2.020	-2.020	75.522	1.000
1**	0.000	0.000	-5.005	-3.273	-3.273	75.522	1.000
1***	0.000	0.000	-5.000	-3.278	-3.273	90.000	0.995
2	-0.470	0.000	-3.124	-2.189	-2.235	90.000	0.526
3	-0.940	0.000	-1.952	-1.483	-1.578	90.000	0.247
4	-1.410	0.000	-1.218	-1.016	-1.158	90.000	0.103
5	-0.470	0.100	-4.583	-2.851	-2.851	75.522	1.000
6	-0.940	0.100	-2.840	-1.869	-1.897	98.950	0.553
7	-1.410	0.100	-1.804	-1.180	-1.294	110.612	0.332
8	-0.940	0.200	-4.194	-2.463	-2.463	75.521	0.999
9	-1.410	0.200	-2.534	-1.620	-1.587	73.550	0.537
10	-1.410	0.300	-3.838	-2.106	-2.106	75.521	0.999
11****	-0.940	0.113	-2.993	-1.938	-1.958	98.376	0.603
12****	-1.410	0.170	-2.339	-1.418	-1.481	106.188	0.514

* For $\phi_p < \phi < \bar{\phi}$

** For $\bar{\phi} < \phi < \phi_S$

*** For $\phi_S < \phi \leq \pi$

**** At ϕ_S^+

$\Delta\tau = 0.431k$

TABLE XXVII

RESULTS FOR $\nu = 0.350$, $V/c_P = 4.0$, $p_o = 7.0k$

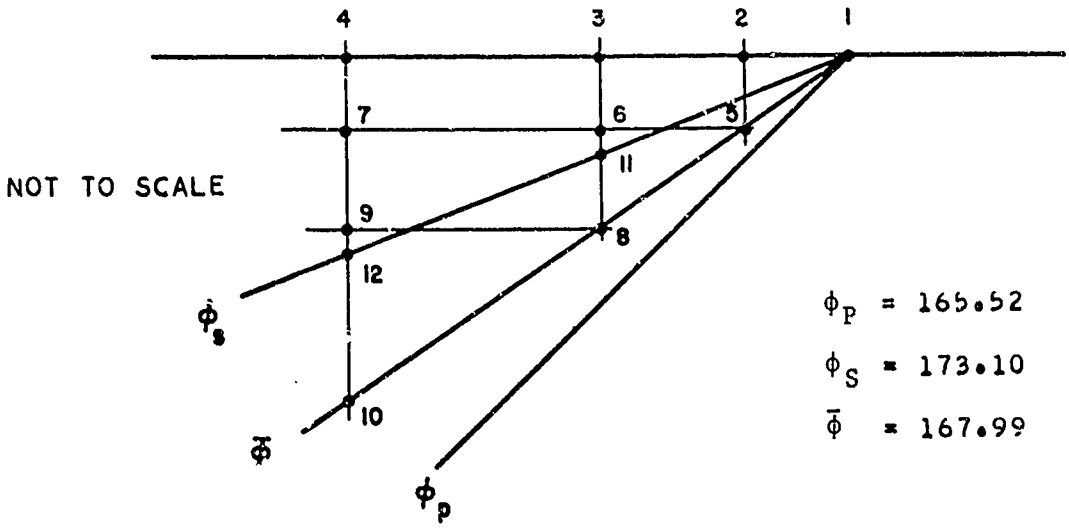

$\phi_P = 165.52$

$\phi_S = 173.10$

$\bar{\phi} = 167.99$

Pt.	$\mu\xi$	μy	σ_1/k	σ_2/k	σ_3/k	θ°	n
1*	0.000	0.000	-3.752	-2.020	-2.020	75.522	1.000
1**	0.000	0.000	-7.005	-5.273	-5.273	75.522	1.000
1***	0.000	0.000	-7.000	-5.278	-5.273	90.000	0.995
2	-0.470	0.000	-4.374	-3.754	-3.820	90.000	0.340
3	-0.940	0.000	-2.765	-2.732	-2.900	89.999	0.088
4	-1.410	0.000	-2.112	-1.705	-2.311	89.999	0.309
5	-0.470	0.100	-6.414	-4.682	-4.682	75.522	1.000
6	-0.940	0.100	-4.009	-3.273	-3.347	107.300	0.405
7	-1.410	0.100	-2.722	-2.145	-2.502	46.569	0.290
8	-0.940	0.200	-5.870	-4.139	-4.139	75.521	0.999
9	-1.410	0.200	-3.547	-2.958	-2.912	71.232	0.354
10	-1.410	0.300	-5.371	-3.639	-3.639	75.521	0.999
11****	-0.940	0.113	-4.217	-3.376	-3.433	105.202	0.470
12****	-1.410	0.170	-3.373	-2.575	-2.764	119.950	0.417

* For $\phi_P < \phi < \bar{\phi}$

** For $\bar{\phi} < \phi < \phi_S$

*** For $\phi_S < \phi \leq \pi$

**** At ϕ_S^+

$\Delta\tau = 0.431k$

TABLE XXVIII

RESULTS FOR $\nu = 0.350$, $V/c_p = 4.0$, $p_o = 10.0k$

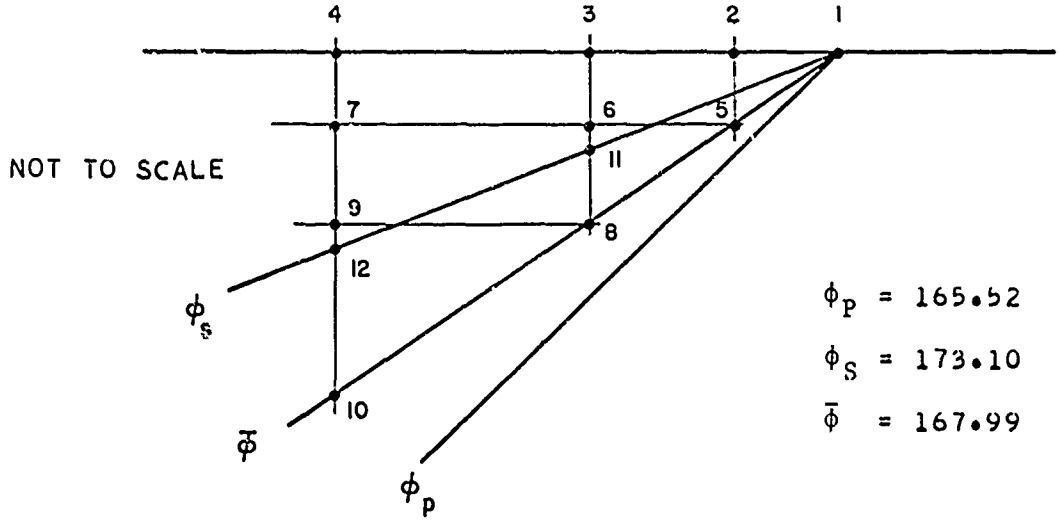

Pt.	$\mu\xi$	μy	σ_1/k	σ_2/k	σ_3/k	θ^o	n
1*	0.000	0.000	-3.752	-2.020	-2.020	75.522	1.000
1**	0.000	0.000	-10.005	-8.273	-8.273	75.522	1.000
1***	0.000	0.000	-10.000	-8.278	-8.273	90.000	0.995
2	-0.470	0.000	-6.248	-6.101	-6.198	90.000	0.675
3	-0.940	0.000	-4.688	-3.904	-4.883	90.000	0.538
4	-1.500	0.000	-3.615	-2.225	3.920	90.000	0.903
5	-0.470	0.100	-9.161	-7.429	7.429	75.522	1.000
6	-0.940	0.100	-5.876	-5.265	-5.521	126.944	0.306
7	-1.500	0.100	-4.219	-2.975	-4.140	68.375	0.696
8	-0.940	0.200	-8.384	-6.652	-6.652	75.520	0.999
9	-1.500	0.200	-4.761	-4.552	-4.649	86.927	0.104
10	-1.500	0.319	-7.542	-5.811	-5.811	75.521	0.999
11****	-0.940	0.113	-6.131	-5.454	-5.644	121.934	0.349
12****	-1.500	0.181	-4.968	-3.880	-4.528	51.378	0.547

* For $\phi_p < \phi < \bar{\phi}$

** For $\bar{\phi} < \phi <$ $_S$

*** For $\phi_S < \phi \leq \pi$

**** At ϕ_S^+

$\Delta\tau = 0.431k$

case the value θ stays at 60.00° for $\phi_p < \phi < \phi_s$ and at 90.00° for $\phi_s < \phi < \pi$.

Looking at results for other grid points it is seen that at point 10 in Table XIV the plastic shock has reached a small tensile value, indicating that the requirement of compressive shocks is violated from there on.

For the higher loads $p_o/k = 6.0$ and 10.0, Tables XV, XVI, the shock remains compressive in the entire range of the tables. Table XV for $p_o/k = 6.0$ is limited only by the condition $\mu\xi \geq -1.7$ due to the truncation of the expansions. For the highest load $p_o/k = 10.0$, the validity is limited to $\mu\xi \geq -1.0$ because the yield condition on the surface, beyond point 14 would be violated excessively.

For other values of ν and V/c_p the situation is generally similar. Violation of the yield condition for low values of p_o/k occurs first on the S-front, while for higher values of p_o/k the violation appears first on the surface.

2. Range of depth for which results apply

The previous discussions considered the validity of results with respect to a nondimensional depth μy. It is appropriate to consider values of μ of physical interest to find out for what actual depth y results have been obtained.

Let t_o = 0.2 sec, V = 4000 ft/sec, then $\frac{1}{\mu} = Vt_o$ = 800 ft. For the typical values ν = 0.25 and V/c_p = 2.0 discussed above, information on peak pressures for values of the surface load p_o = 4.0k and 6.0k are contained in Tables XIV and XV up to about μy = 0.6 or for a depth of 480 feet. A time history can be plotted using interpolation for the depths μy = 0.5 or 400 feet. For the same values of ν and V/c_p , but p_o/k = 10.0, the limit of applicability is μy = 0.3, or about 240 feet.

In general, for larger values of V/c_p and for larger values of p_o/k the depth for which the results apply decreases.

SECTION V

CONCLUSIONS

An analytical approach has been presented to describe the effect of a decaying pressure moving with superseismic velocity $V \geq 1.5\ c_p$ on the surface of a half-space of an elastic-plastic material subject to the von Mises yield condition. Numerical results have been obtained for a wide range of surface pressure and material properties. Due to simplifications in the analysis the results obtained are approximate and restricted to target points of limited depth, as discussed in Section IV.

Information on the stress field for exponential decay of the applied load is contained in Tables II - XXVIII and in the accompanying figures. Comparing the effects of step loads given in Ref. [1] with the new results for decaying loads, it is found that in the latter case the peak and subsequent pressures decrease with depth, which is not the case for a step load. However, the decrease found at any depth y is smaller than the decrease of the applied pressure at the point on the surface directly above the target point, i.e., at a distance equal to $(-y/\mathrm{tg}\ \bar{\phi})$ behind the shock front. This is graphically shown in Figs. 10 to 18. While the attenuation is therefore less important than one might expect, it is still greater than found in a similar analysis, Ref. [3], for an elastic-plastic material of the Coulomb type.

APPENDIX I - Special Case, m = 0

Although an approach analogous to that used in the text for $m > 0$ may be used for $m = 0$, it is considerably simpler to derive expressions for a step pressure using the simple configuration shown in Fig. 8, consisting of three shock fronts only.

For $\phi_P \leq \phi < \bar{\phi}$

$$\frac{\sigma_1}{k} = \frac{\Delta\sigma^P}{k} \tag{86}$$

$$\frac{\sigma_2}{k} = \frac{\sigma_3}{k} = \frac{\nu}{1-\nu}\,\frac{\Delta\sigma^P}{k} \tag{87}$$

where

$$\frac{\Delta\sigma^P}{k} = -\frac{\sqrt{3}(1-\nu)}{1-2\nu} \tag{88}$$

For $\bar{\phi} < \phi < \phi_S$

$$\frac{\sigma_1}{k} = \frac{\Delta\sigma^P}{k} + \frac{\overline{\Delta\sigma}}{k} \tag{89}$$

$$\frac{\sigma_2}{k} = \frac{\sigma_3}{k} = \frac{\Delta\sigma^P}{k}\left(\frac{\nu}{1-\nu}\right) + \frac{\overline{\Delta\sigma}}{k} \tag{90}$$

where

$$\frac{\overline{\Delta\sigma}}{k} = -\frac{p_o}{k} + \frac{\sqrt{3}}{2}\left[\frac{2(1-\nu)}{1-2\nu}\cos 2\phi_S + \frac{\sin 2\phi_p \sin 2\phi_S}{\cos 2\phi_S}\right] \tag{91}$$

For $\phi_s < \phi < \pi$

$$\frac{\sigma_1}{k} = -\frac{p_o}{k} \tag{92}$$

$$\frac{\sigma_2}{k} = -\sqrt{3}\left[\cos^2\phi_p + \left(\frac{1-\nu}{1-2\nu}\right)\right] + \sqrt{3}\,\frac{\tan 2\phi_s \sin 2\phi_p}{2\cos 2\phi_s} + \frac{\overline{\Delta\sigma}}{k} \tag{93}$$

$$\frac{\sigma_3}{k} = \frac{\sqrt{3}}{2}\left(\frac{\nu}{1-2\nu}\right) + \frac{\overline{\Delta\sigma}}{k} \tag{94}$$

APPENDIX II - Elastic Solutions

The exrressions for the stresses in a purely elastic material subjected to a step pressure may be found in Ref. [1]. The equivalent expressions for a decaying surface pressure are:

For $\phi_p \leq \phi < \phi_s$

$$\frac{\sigma_y}{k} = \frac{\Delta\sigma^p}{k} \cos 2\phi_s \, e^{\mu(\xi-\xi_p)} \tag{95}$$

$$\frac{\sigma_x}{k} = \frac{\Delta\sigma'}{k} [1 - 2 \sin^2\phi_s \cot^2\phi_p] \, e^{\mu(\xi-\xi_p)} \tag{96}$$

$$\frac{\sigma_z}{k} = \frac{\Delta\sigma^p}{k} [\frac{1}{2} (\frac{1-2\nu}{1-\nu}) \sin 2\phi_p] \, e^{\mu(\xi-\xi_p)} \tag{97}$$

$$\frac{\tau}{k} = - \frac{\Delta\sigma^p}{k} [2 \sin^2\phi_s \cot \phi_p] \, e^{\mu(\xi-\xi_p)} \tag{98}$$

$$\frac{\Delta\sigma^p}{k} = - \frac{p_o}{k} \frac{(1-\nu) \cos 2\phi_s}{[\cos^2\phi_s + (1-2\nu) \cos^2(\phi_s - \phi_p) - (1-\nu)]} \tag{99}$$

$$\xi_p = \frac{y \cos \phi_p}{\sin \phi_p} \tag{100}$$

For $\phi_s < \phi < \pi$

$$\frac{\sigma_y}{k} = - \frac{p_o}{k} e^{\mu\xi} \tag{101}$$

$$\frac{\sigma_x}{k} = \frac{\Delta\sigma^P}{k}\left[1 - 2\sin^2\phi_S \cot^2\phi_P\right]e^{\mu(\xi-\xi_P)} - \frac{\Delta\tau^S}{k}\sin 2\phi_S\, e^{\mu(\xi-\xi_S)} \tag{102}$$

$$\frac{\sigma_z}{k} = \frac{\Delta\sigma^P}{k}\frac{(1-2\nu)}{2(1-\nu)}\sin 2\phi_P\, e^{\mu(\xi-\xi_P)} \tag{103}$$

$$\frac{\tau}{k} = -\frac{\Delta\sigma^P}{k}\left[2\sin^2\phi_S \cot\phi_P\right]e^{\mu(\xi-\xi_P)} + \frac{\Delta\tau^S}{k}\cos 2\phi_S\, e^{\mu(\xi-\xi_S)} \tag{104}$$

$$\frac{\Delta\tau^S}{k} = \frac{1-2\nu}{2(1-\nu)}\frac{\sin 2\phi_P}{\cos 2\phi_S}\frac{\Delta\sigma^P}{k} \tag{105}$$

$$\xi_S = \frac{y\cos\phi_S}{\sin\phi_S} \tag{106}$$

UNCLASSIFIED

Security Classification

DOCUMENT CONTROL DATA - R & D

(Security classification of title, body of abstract and indexing annotation must be entered when the overall report is classified)

1 ORIGINATING ACTIVITY (Corporate author)	2a. REPORT SECURITY CLASSIFICATION
Paul Weidlinger, Consulting Engineer New York, New York 10017	UNCLASSIFIED 2b. GROUP

3 REPORT TITLE

EXPONENTIALLY DECAYING PRESSURE PULSE MOVING WITH SUPERSEISMIC VELOCITY ON THE SURFACE OF A HALF-SPACE OF VON MISES ELASTO-PLASTIC MATERIAL

4 DESCRIPTIVE NOTES (Type of report and inclusive dates)

October 1967 to May 1968

5 AUTHOR(S) (First name, middle initial, last name)

Bleich, Hans H.
Matthews, Alva

6 REPORT DATE	7a. TOTAL NO. OF PAGES	7b. NO. OF REFS
August 1968	98	3

8a. CONTRACT OR GRANT NO	9a. ORIGINATOR'S REPORT NUMBER(S)
F29601-67-C-0091 b. PROJECT NO 5710 c. Subtask No RSS2144 d.	AFWL-TR-68-46 9b. OTHER REPORT NO(S) (Any other numbers that may be assigned this report)

10 DISTRIBUTION STATEMENT This document is subject to special export controls and each transmittal to foreign governments or foreign nationals may be made only with prior approval of AFWL (WLDC), Kirtland AFB, NMex 87117. Distribution is limited because of the technology discussed in the report.

11 SUPPLEMENTARY NOTES	12. SPONSORING MILITARY ACTIVITY
	DASA

13 ABSTRACT

(Distribution Limitation Statement No. 2)

An approximate solution is given for the effect of an exponentially decaying pressure pulse traveling with superseismic velocity on the surface of a half-space. The half-space is an elastic-plastic material of the von Mises type. The effect of a step wave for this geometry and medium was treated previously. For that case, the peak pressures do not decrease with increase in depth, while such a decrease is obtained for a decaying surface load. The prime purpose of this investigation is to determine the magnitude of this attenuation. The approximate solutions obtained are valid for a limited distance behind the wave front, and are tabulated for different sets of parameters pertaining to the material and velocity. The tabulated results show that the peak pressures in the case of the decaying surface load do decrease with depth, but that the decrease is less that one might intuitively expect. On the other hand the attenuation is in general larger than that encountered in the similar problem of an elasto-plastic material of the Coulomb type.

DD FORM 1 NOV 65 1473

UNCLASSIFIED

Security Classification

14. KEY WORDS	LINK A		LINK B		LINK C	
	ROLE	WT	ROLE	WT	ROLE	WT
Elastic-Plastic						
Wave Propagation						
Ground Motion						
Decaying Pressure Pulse						